Understanding the Cellular Response to Cytosolic Cytochrome *c*

by

Carrie Elizabeth Johnson

Department of Pharmacology and Cancer Biology
Duke University

Date:_____

Approved:

_____
Sally Kornbluth, Supervisor

_____
Donald McDonnell

_____
Robert Wechsler-Reya

_____
Gerard Blobe

_____
Salvatore Pizzo

Dissertation submitted in partial fulfillment of
the requirements for the degree of Doctor
of Philosophy in the Department of
Pharmacology and Cancer Biology in the Graduate School
of Duke University

2009

ABSTRACT

Understanding the Cellular Response to Cytosolic Cytochrome *c*

by

Carrie Elizabeth Johnson

Department of Pharmacology and Cancer Biology
Duke University

Date:_____

Approved:

_____
Sally Kornbluth, Supervisor

_____
Donald McDonnell

_____
Robert Wechsler-Reya

_____
Gerard Blobe

_____
Salvatore Pizzo

An abstract of a dissertation submitted in partial
fulfillment of the requirements for the degree
of Doctor of Philosophy in the Department of
Pharmacology and Cancer Biology in the Graduate School
of Duke University

2009

# Abstract

Cytosolic cytochrome *c* promotes apoptosis by triggering caspase activation. In healthy cells cytochrome *c* localizes to mitochondria, where it participates in the electron transport chain. Apoptotic stimuli induce permeabilization of the outer mitochondrial membrane and release of cytochrome *c.* Once cytosolic, cytochrome *c* binds Apaf-1, inducing the formation of a protein complex that recruits and activates caspases, which serve to dismantle the dying cell. Although the steps of this signaling pathway have been described, many of the regulatory mechanisms influencing the cellular response to cytosolic cytochrome *c* remain unclear. Using apoptosis assays and microinjection techniques, we investigated the response of several cell-types to cytosolic cytochrome *c.*

First, we demonstrate that cytosolic cytochrome *c* kills brain tumor cells but not normal brain tissue. This differential sensitivity to cytochrome *c* is attributed to high Apaf-1 levels in brain tumors compared with negligible Apaf-1 in brain tissue. These differences in Apaf-1 abundance correlate with differences in E2F1, a previously identified activator of Apaf-1 transcription. Chromatin immunoprecipitation assays reveal that E2F1 binds the Apaf-1 promoter specifically in tumor tissue, suggesting that E2F1 contributes to Apaf-1 expression in brain tumors. These results demonstrate an unexpected sensitivity of brain tumors to cytochrome *c* and raise the possibility that this phenomenon could be exploited therapeutically to selectively kill brain cancers.

Secondly, we develop a method for monitoring caspase activity in *Xenopus laevis* oocytes and early embryos. The approach, utilizing microinjection of a near-infrared dye

that emits fluorescence only after its cleavage by active caspases, has enabled the elucidation of subtleties in the apoptotic program. We demonstrate that brief caspase activation is sufficient to cause death. We illustrate the presence of a cytochrome *c* dose threshold, which is lowered by neutralization of inhibitor of apoptosis proteins. We show that meiotic oocytes develop resistance to cytochrome *c,* and that eventual death of these oocytes is caspase-independent. Imaging caspase activity in the embryo suggests that apoptosis in early development is not cell-autonomous. Finally, we believe this method presents a useful screening modality for identifying novel apoptotic regulators as well as pro-apoptotic small-molecules that could be useful in treating brain tumors.

# Dedication

For my late father, whose battle with pancreatic cancer inspired me to pursue physician scientist training.

# Contents

# List of Figures

# List of Abbreviations

| | |
|---|---|
| Apaf-1 | Apoptotic protease activating factor-1 |
| BBB | Blood-brain-barrier |
| BIR | Baculovirus IAP repeat |
| CARD | Caspase recruitment domain |
| Caspase | Cysteine-dependent aspartate-directed protease |
| CGN | Cerebellar granule neurons |
| ChIP | Chromatin immunoprecipitation |
| CNS | Central nervous system |
| DISC | Death inducing stimulus complex |
| DRG | Dorsal root ganglion |
| E15 | Embryonic day 15 |
| EGFR | Epidermal growth factor receptor |
| FADD | Fas-associated death domain |
| FRET | Fluorescence resonance energy transfer |
| GVBD | Germinal vesicle breakdown |
| IAP | Inhibitor of apoptosis protein |
| IGF | Insulin-like growth factor |
| $IP_3R$ | Inositol 1,4,5-triphosphate receptor |
| IRDye | IRDye® 800CW/QC-1 CSP-3 substrate |

| | |
|---|---|
| IRES | Internal ribosomal entry segment |
| MS | Mass spectrometry |
| NIR | Near-infrared |
| NOD | Nucleotide-binding and oligomerization domain |
| $O^6$-BG | $O^6$-benzylguanine |
| OT | $O^6$-BG- and temozolomide |
| P2 | Postnatal day 2 |
| PARP | Poly (ADP-ribose) polymerase |
| PDGF | Platelet-derived growth factor |
| PHAPI | Putative HLA class II associated protein I |
| PI3K | Phosphoinositide-3 kinase |
| RT-PCR | Reverse transcriptase polymerase chain reaction |
| Shh | Sonic hedgehog |
| tBid | Truncated Bid |
| TOM | Transporter outer membrane |
| TRAIL | Tumor necrosis factor (TNF)-related apoptosis-inducing ligand |
| TR | Temozolomide-resistant |
| XIAP | X-linked IAP |

# Acknowledgements

We thank the laboratory of Mohanish Deshmukh (University of North Carolina at Chapel Hill) for their collaboration with us on the brain tumor project and providing the recombinant Smac protein; the laboratory of Robert Wechsler-Reya (Duke University), with special thanks to Jessica Kessler, Tracy-Ann Read, and Jack Dutton for mouse medulloblastoma dissections and Shirley Markant for her help with the CD15+/- medulloblastoma gene profiling data analysis; the Duke Proteomics Facility, with particular thanks to Erik Soderblom for performing the mass spectrometry analysis; the laboratory of Francis Ali-Osman (Duke University), with special thanks to Simendra Singh for help with optimization and running of the small-molecule screen and providing us with glioblastoma cell lines; Darrell Bigner, Michael Graner, Roger McLendon, Diane Satterfield, Steve Keir, Shelley Davis, and Ian Cummings from the Preston Robert Tisch Brain Tumor Center (Duke University) for the xenograft tumors, human tissues, and brain tumor cell lines; the laboratory of Henry Friedman for providing the temozolomide-resistant glioblastoma cell lines; the Duke Light Microscopy Core Facility for their technical training and support; the laboratory of Jeremy Rich (Cleveland Clinic), with special thanks to Anita Hjelmeland for providing the CD133+/- glioma mRNA samples; Daniel Sanchis (Universitat de Llieda, Lleida, Spain) for providing the SH-SY5Y neuroblastoma cells; John Silber (University of Washington, Seattle) for providing the medulloblastoma UW228 cell line; William Freed (National Institute of Health, Bethesda) for providing the medulloblastoma cell line MCD1; Xiaodong Wang

(University of Texas Southwestern, Dallas) for providing recombinant human Apaf-1; Bruce Kaplan for synthesizing the cytochrome *c* peptides (Beckman Research Insitutue of the City of Hope, Duarte); Jean Gautier (Columbia University, New York) for providing the XLX serum; Shigeru Yamashita (Toho University, Tokyo) for providing the purified xXIAP antibody; and the NIBB *Xenopus laevis* project for the Bok EST clone.

A special thanks to the members of the Kornbluth laboratory, for generously sharing laboratory space, reagents and scientific ideas; to Robert Wechsler-Reya, Salvatore Pizzo, Donald McDonnell and Gerard Blobe, who have graciously served as members of my thesis committee; and to my thesis advisor, Sally Kornbluth, for her invaluable scientific guidance and support throughout my PhD training. Finally, the work presented in this dissertation was supported by the Medical Scientist Training Program and the Pediatric Brain Tumor Foundation.

# 1. Introduction

## 1.1 Apoptosis

Apoptosis is a form of programmed cell death in which individual cells are removed from an organism without disturbing tissue architecture. In contrast to necrosis, or traumatic cell death, programmed cell death is a normal process initiated by and conferring advantage to an organism. The phenomenon of programmed cell death was first reported by the German scientist Carl Vogt in 1842 (Peter *et al.,* 1997). However, coining of the term "apoptosis" to describe this process did not occur until 1972, when John Kerr, Alastair Currie and Andrew Wyllie published a seminal article on the topic (Kerr *et al.,* 1965). In the report they credit their colleague James Cormack, a Greek professor, for suggesting the term. Indeed, the word apoptosis is of Greek origin meaning "dropping off" or "falling off," as in leaves falling from a tree. Notably, as there is often debate among researchers studying apoptosis, the scientists suggested the second half of the word be pronounced like ptosis, with a silent "p."

Apoptosis is a critical process in both development and homeostasis (Cotran *et al.,* 1999). During development, extensive cellular proliferation and differentiation generate organs and tissues, which are then pruned into their appropriate form by apoptosis. For example, digits of the hands and feet begin as webbed structures at the ends of limb buds. During development, the webs are lost through apoptosis, resulting in individual digits (Mirkes, 2001). The role of apoptosis in development of the central

nervous system highlights the essential nature of this process, as a lack of apoptosis in the developing brain results in death of the entire organism (Cecconi *et al.,* 1998). Apoptosis continues to play an important role in adult organisms, by ridding the body of autoreactive or damaged cells. This homeostatic mechanism ensures a constant number of cells in the organism and also prevents the accumulation of malfunctioning or potentially self-harmful cells (Cotran *et al.,* 1999).

Cells undergoing apoptosis display characteristic morphological features, regardless of the cell type, tissue type, timing, or apoptotic stimulus (Wride and Sanders, 1995). First the cell shrinks and begins to round up, producing a dense cytoplasm and tightly packed organelles. The chromatin condenses, forming a pyknotic nucleus, which is followed by nuclear envelope breakdown and fragmentation of the DNA. The cell membrane then forms numerous blebs, and ultimately the cellular material is parceled into individual vesicles, known as apoptotic bodies (Figure 1.1). These cell remnants are recognized and phagocytosed by nearby phagocytic cells, allowing for tidy removal of the cell without release of intracellular contents that otherwise would trigger inflammation and tissue damage (Li *et al.,* 2003).

On a biochemical level it is the activity of *c*ysteine-dependent *asp*artate-directed prote*ases*, called caspases, which underlies this characteristic morphological death (Earnshaw *et al.,* 1999). Although a variety of signals, both internal and external, can trigger apoptosis in a cell, the common mechanism that defines an apoptotic death is caspase activation. It is the proteolytic activity of these caspases that results in the

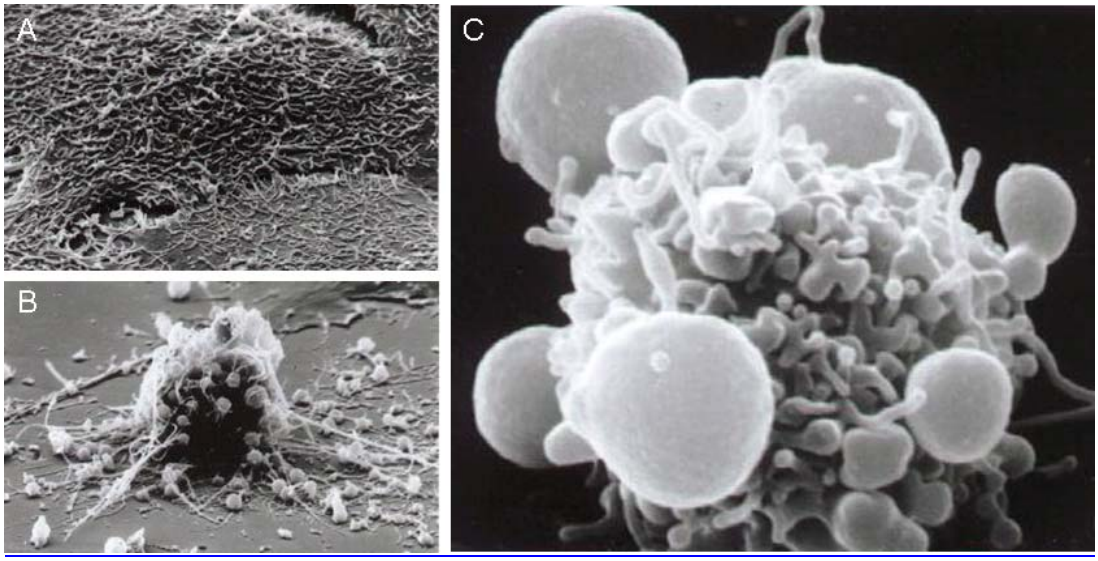


**Figure 1.1: Morphological features of apoptosis.**

**Figure 1.1:** Scanning electron micrographs of epithelial cells illustrate the process of apoptotic death, with a flat cell, **A**, undergoing different forms of rounding, surface blebbing and cell retraction, **B**, preceding the typical apoptotic figure, **C**. Images from W. Malorni, published in: The Purdue Cytometry CD-ROM Volume 4, J. Watson, Guest Ed., J.Paul Robinson, Publisher. Purdue University Cytometry Laboratories, West Lafayette, IN 1997, ISBN 1-890473-03-0.

precisely timed and efficiently-executed process of cell dismantling. The apoptotic program, with the potential to activate caspases, exists in virtually all cells of the body. Inappropriate regulation of caspase activity contributes to the pathophysiology of many human disease states, including cancer, autoimmunity and neurodegeneration. Thus, it is the process by which caspases get activated (and its potential for manipulation) that has attracted much scientific inquiry, and over the past two decades we have greatly expanded our understanding of the signaling pathways leading to caspase activation.

### 1.1.1 Apoptosis signaling pathways

Apoptotic signaling can occur along two principle pathways: 1) an intrinsic pathway in which intracellular signals promote cell death in response to stress or developmental cues and 2) an extrinsic pathway initiated by extracellular signals engaging cell surface receptors (e.g. FasL binding Fas) (Schultz and Harrington, 2003; Bellamy *et al.,* 1995). Although distinct in their upstream events, the two pathways converge at the level of effector caspase activation (Figure 1.2).

Initiation of the intrinsic cell death program is governed by the Bcl-2 family of proteins. Bcl-2 proteins can be either pro- or anti-apoptotic, and they function to regulate the permeability of the outer mitochondrial membrane (Brunelle and Letai, 2009). Apoptotic stimuli, such as irreparable DNA damage, developmental cues or hypoxic stress, lead to alterations in the complex interactions of pro-apoptotic (e.g., Bax, Bak) and anti-apoptotic (e.g., Bcl-2, Bcl- $X_L$) Bcl-2 family members, resulting in the assembly of pore-forming channels in the outer membrane of the mitochondria (Ow *et al.,* 2008). The

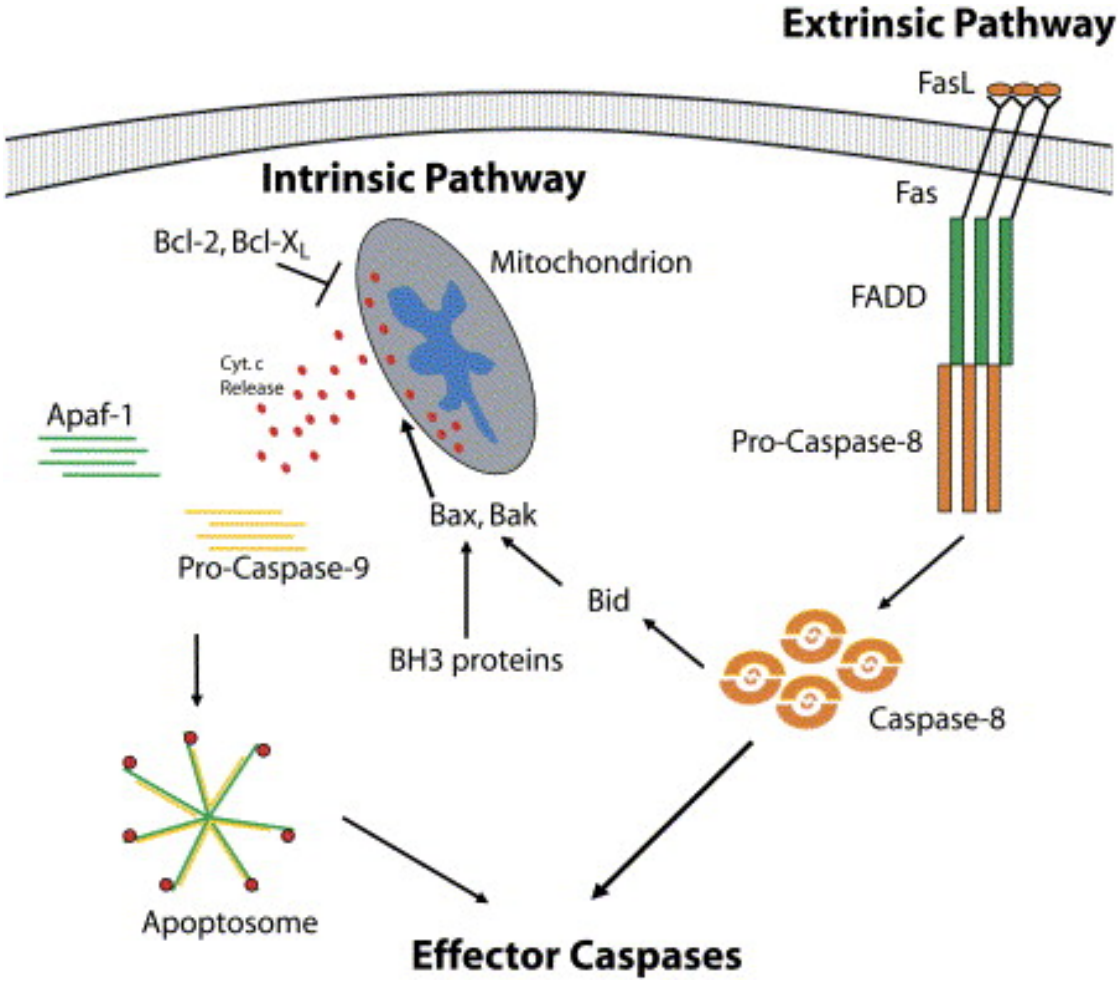


**Figure 1.2: Caspase activation via the intrinsic and extrinsic pathways of apoptosis.**

**Figure 1.2:** The activation of caspases during apoptosis proceeds through two distinct mechanisms. Activation of caspases through the extrinsic pathway involves the binding of extracellular ligands (e.g., FasL) to their cognate receptors (e.g., Fas) and the recruitment of intracellular adaptor proteins (e.g., FADD) to activate caspase-8 and subsequent downstream effector caspases. The intrinsic pathway involves the release of cytochrome c from the mitochondria into the cytosol. This leads to the formation of the apoptosome, the activation of caspase-9, and the cleavage of effector caspases. Adapted from Schafer and Kornbluth (2006), with permission from Elsevier.

resulting mitochondrial permeabilization allows the release of sequestered macromolecules, including the electron transfer protein cytochrome *c*, from the mitochondrial intermembrane space to the cytosol (Green and Amarante-Mendes, 1998; Green and Reed, 1998). Once cytosolic, cytochrome *c* induces the assembly of a caspase-activating complex termed the apoptosome (Cain *et al.,* 1999). Formation of this complex begins when cytochrome *c* interacts with the ATP-binding protein Apoptotic protease activating factor-1 (Apaf-1), thereby exposing Apaf-1's caspase recruitment domain (CARD). The altered conformation of Apaf-1 promotes Apaf-1 oligomerization and yields recruitment of procaspase-9 to the assembling complex, promoting dimerization-induced activation of caspase-9 within the mature apoptosome (Li *et al.,* 1997). Apoptosome-bound caspase-9 serves as an initiator caspase that activates downstream effector caspases-3 and -7 (Cain *et al.,* 2002). These "workhorses" of apoptosis cleave a host of cytoplasmic and nuclear target proteins, ultimately resulting in the cell shrinkage, chromatin condensation and membrane blebbing characteristic of apoptotic cell death (Cotran *et al.,* 1999).

The extrinsic pathway is triggered by the binding of a specific extracellular ligand, FasL, to the Fas transmembrane death receptor (Kischkel *et al.,* 1995). This interaction leads to the recruitment of the Fas-associated death domain (FADD), which then leads to further recruitment of an initiator caspase, procaspase-8. This complex of Fas, FADD and caspase-8 is referred to as the death inducing stimulus complex (DISC) (Peter and Krammer, 2003). The DISC functions to activate caspase-8, which it achieves

by bringing together multiple caspase-8 molecules, facilitating its auto-activation (Shi, 2005). Similarly to caspase-9, caspase-8 functions to cleave and thereby activate downstream effector caspases. However, caspase-8 can also trigger the intrinsic pathway by cleaving a protein Bid; the resulting truncated Bid (tBid) induces activation of the pro-apoptotic Bcl-2 protein Bax and subsequent mitochondrial permeabilization and release of cytochrome *c* (Li *et al.,* 1998). In this regard, caspase-8 activity functions as part of a positive-feedback loop to enhance the activation of effector caspases. Therefore, both intrinsic and extrinsic pathway stimulation can result in mitochondrial release of cytochrome *c.*

## 1.2 Post-mitochondrial apoptosis signaling

### 1.2.1 Cytochrome *c:* structure and function

Cytochrome *c* is a multifunctional protein primarily known for its role in the mitochondria shuttling electrons between complexes III (cytochrome $bc_1$) and IV (cytochrome *c* oxidase) of the electron transport chain (Skulachev, 1998). The redox activity of cytochrome *c* is engendered by its prosthetic heme group, which is covalently attached at two cysteine residues by the enzyme cytochrome *c* heme lyase (Tong and Margoliash, 1998). Heme modification occurs in concert with the transport of cytochrome *c* into the intermembrane space of the mitochondria, which will be described here below.

Like many mitochondrial proteins, cytochrome *c* is encoded by a nuclear gene, translated in the cytosol and transported into the mitochondria. However, unlike many mitochondrial proteins, cytochrome *c* does not contain a cleavable N-terminal targeting sequence and its transport does not require ATP hydrolysis or the outer membrane components of the mitochondrial transporter outer membrane (TOM) complex (Dumont *et al.,* 1998; Dumont *et al.,* 1991; Mayer *et al.,* 1995). Although the details of its transport through the outer mitochondrial membrane are not completely understood, a general model has been proposed (Diekert *et al.,* 2001). In this model, the translated precursor to cytochrome *c,* known as apocytochrome *c,* interacts with negatively charged phospholipids at the mitochondrial surface, resulting in its partial insertion in the outer mitochondrial membrane. This insertion is stabilized by apocytochrome *c* binding to Tom40, a protease-resistant component of the TOM complex. Although this interaction begins to drive apocytochrome *c* across the outer mitochondrial membrane, full membrane translocation requires cytochrome *c* heme lyase, which itself is located in the intermembrane space. In this step, cytochrome *c* heme lyase not only acts as an internal receptor for apocytochrome *c,* but also simultaneously catalyzes the addition of the heme moiety to the protein, resulting in properly-localized holocytochrome *c.*

Holocytochrome *c* (referred to as cytochrome *c)* assumes a compact, globular structure, with the heme group located centrally and many surface-exposed lysine residues (Figure 1.3). This small protein (roughly 100 amino acids) has a molecular weight of about 12,000 daltons, and its structure has been extensively characterized. For

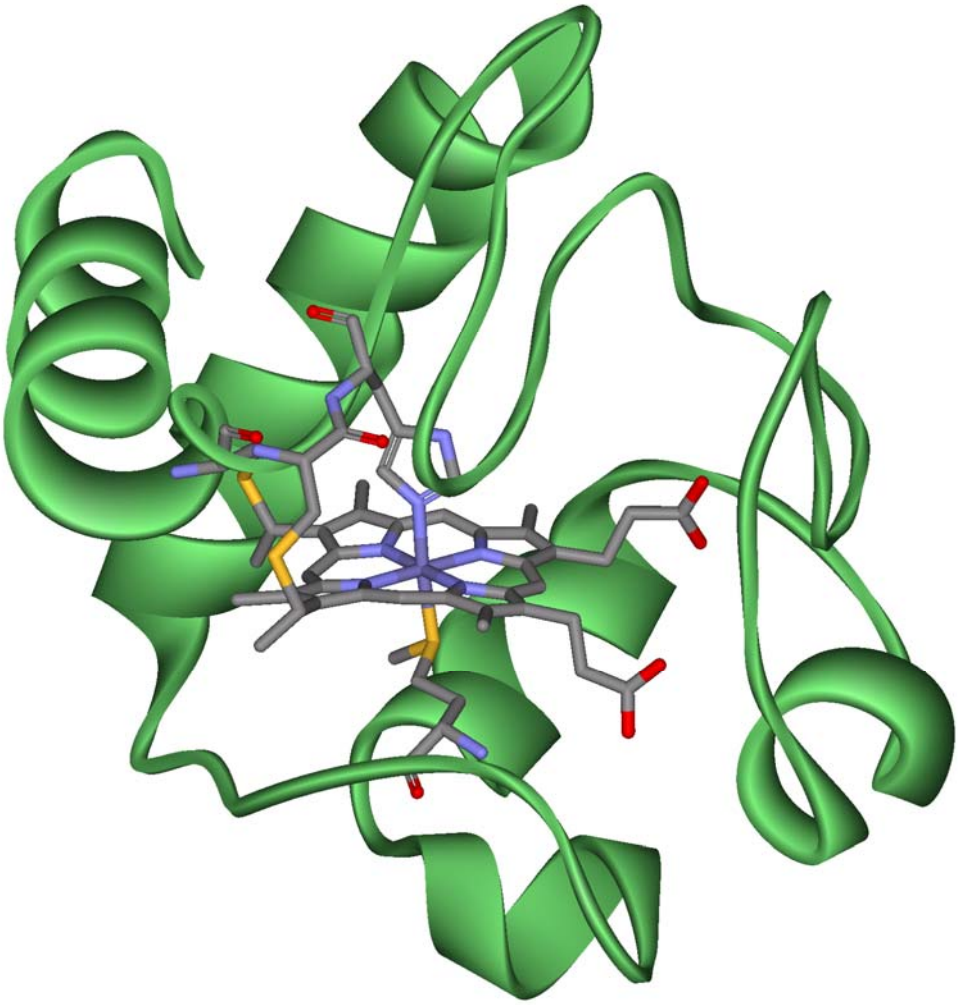

**Figure 1.3: Structure of cytochrome *c*.**

**Figure 1.3:** The image of the crystal structure of bovine heart cytochrome *c* (2b4z) was generated using KiNG, with the ribbon structure in green and the internal heme molecule in gray, yellow, blue and red.

example, the first crystal structures from horse and tuna cytochromes *c* were reported in 1971 (Dickerson *et al.,* 1971). Cytochrome *c* is highly-conserved across species, from yeast to mammals. The conserved structural elements enable cytochrome *c* to perform its function as a mobile electron carrier (Mauk *et al.,* 1995).

It turns out that the particular three-dimensional structure of cytochrome *c* is also critical for its role in mediating apoptosis (Yu *et al.,* 2001). As was discussed in the previous section, apoptotic stimuli induce permeabilization of the outer mitochondrial membrane, which results in the release of cytochrome *c* into the cytosol. The primary function of cytosolic cytochrome *c* is to bind the adaptor protein Apaf-1, triggering apoptosome formation and activation of effector caspases. The specific manner in which cytochrome *c* binds Apaf-1 is critical for initiating this process and will be discussed in detail below. However, it must be pointed out that cytochrome *c* has also been reported to interact with inositol 1,4,5-triphosphate receptors ($IP_3R$) in the endoplasmic reticulum (Boehning *et al.,* 2003). This binding is proposed to facilitate calcium exit from the endoplasmic reticulum, which then enters the mitochondria, promoting further (and complete) release of mitochondrial cytochrome *c* (Goldstein *et al.,* 2000).

### 1.2.2 Cytochrome *c* binding to Apaf-1 and apoptosome formation

Apaf-1 is a large protein (120 kDa) containing an N-terminal CARD, a central nucleotide-binding and oligomerization domain (NOD), and 13 WD40 repeats (Figure 1.4A) (Riedl *et al.,* 2005). Apaf-1 exists in the cytosol in a closed conformation, in which the WD40 repeats interact with the CARD domain (Hu *et al.,* 1998). Although a structure

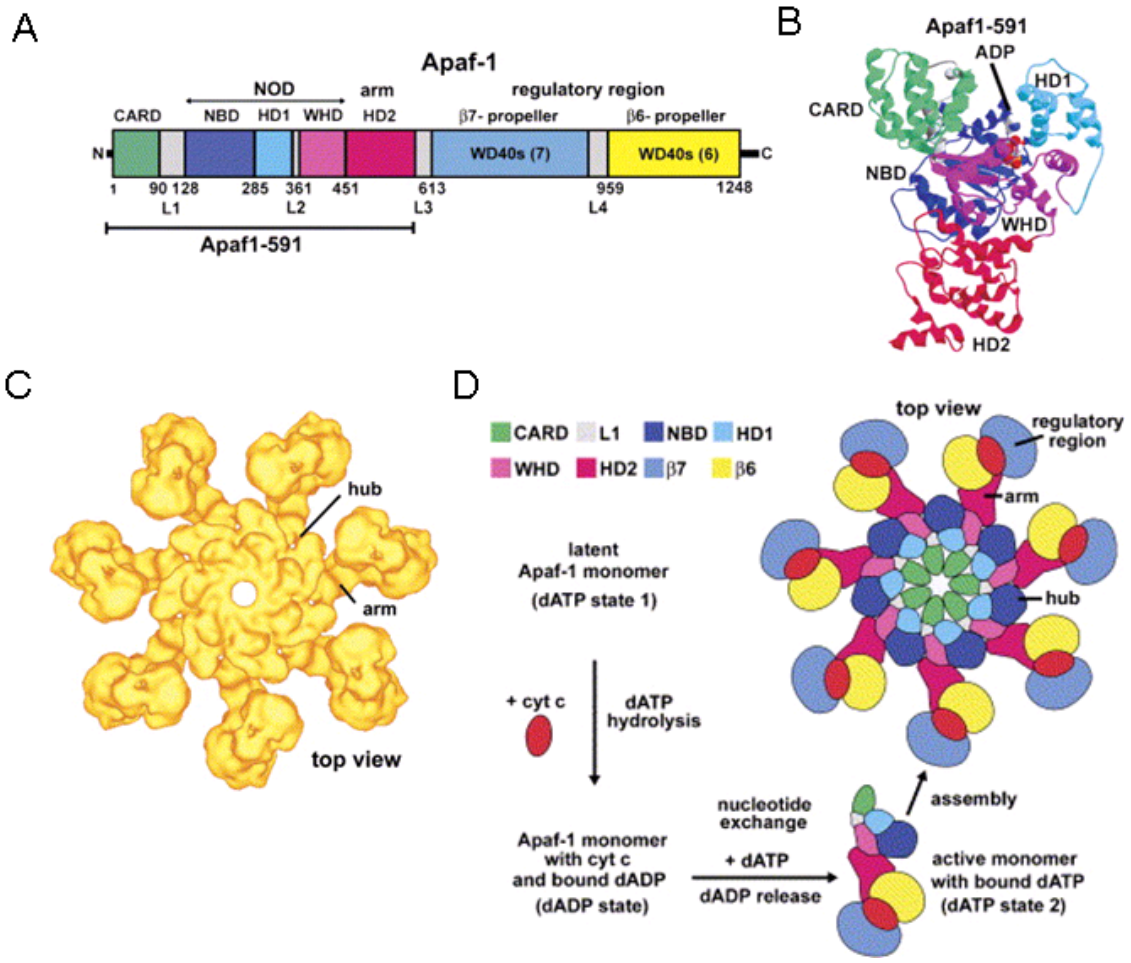


**Figure 1.4: Apaf-1 and apoptosome formation.**

**Figure 1.4:** **A**, Linear diagram of Apaf-1 is shown with color-coded domains. Linkers are shown in gray. **B**, Crystal structure of Apaf1-591 is shown with color-coded ribbons. **C**, The apoptosome is viewed down the 7-fold axis. In this top view, features of the wheel-like particle, including the central hub and arms, are revealed. **D**, An assembly model for the human apoptosome (described in text). From Yu *et al.* (2005), with permission from Elsevier.

of full-length Apaf-1 is not known, Apaf-1 lacking the WD40 repeats has been crystallized (Figure 1.4B) (Riedl *et al.,* 2005).

This Apaf-1 deletion mutant demonstrates constitutive activity in promoting caspase activation (Srinivasula *et al.,* 1998). Thus, presumably it is the CARD—WD40 interaction that maintains Apaf-1 inactivity, preventing it from interacting with its primary binding partners, procaspase-9 and other Apaf-1 monomers. Functionally, the presence of cytochrome *c* in the cytosol mimics the deletion of the WD40 repeats, promoting rapid Apaf-1 activity.

On a biochemical level, it remains unclear exactly how cytochrome *c* binds Apaf-1 in order to achieve this feat. However, research over the last decade, probing the nature of the cytochrome *c*—Apaf-1 interaction has provided some interesting hints. For example, one required feature of the binding event is the particular three-dimensional structure of cytochrome *c*. This is perhaps best demonstrated by the observation that cytochrome *c* from the yeast *Saccharomyces cervisaie,* despite being highly homologous to mammalian cytochrome *c,* is unable to bind Apaf-1 due to the presence of a trimethylation on lysine 72 (Yu *et al.,* 2001). Mutational analysis of mammalian cytochrome *c* identified several additional surface-exposed lysine residues as being critical for Apaf-1 binding; these residues are not localized in one region of the protein but rather exist on opposite faces of the globular structure (Yu *et al.,* 2001). Further, apocytochrome *c,* which lacks the structural components conferred by the heme group, is incapable of triggering apoptosis (Yang *et al.,* 1997). One group reported that despite

apocytochrome *c* lacking apoptosome-inducing activity, it retains the ability to bind Apaf-1 (Martin and Fearnhead, 2002). However, the determinants of that purported binding interaction (and confirmation of the interaction by other researchers) have not been reported.

The importance of the cytochrome *c* structure in mediating its binding to Apaf-1 is further supported by studies identifying variants of cytochrome *c* that demonstrate enhanced apoptosis-inducing ability. One such study characterized the testicular form of cytochrome *c,* and found that although it is almost 90% identical to the somatic form, it is significantly more potent in its ability to induce caspase activation (Liu *et al.,* 2006). Another group identified a mutation in the cytochrome *c* in a family with autosomal dominant thrombocytopenia. The mutation results in a single base pair substitution within cytochrome *c*, from a glycine at residue 41 to a serine. This small change yields a cytochrome *c* mutant protein with enhanced apoptotic activity (Morison *et al.,* 2008). Together, these results suggest that very small changes in cytochrome *c* structure influence the ability of the protein to interact with Apaf-1. It is important to note that neither of these groups determined specific Apaf-1 binding affinities of the cytochrome *c* variants. Therefore it is possible that these alterations in caspase activation result from changes in activity of the formed apoptosome rather than in the cytochrome *c*—Apaf-1 binding. However, given that cytochrome *c* has been reported to be dispensable for the function of the fully-formed apoptosome (Hill *et al.,* 2004), it is likely that these changes

in caspase activation do reflect changes in the initial interaction of cytochrome *c* with Apaf-1.

In terms of which region of Apaf-1 is involved in the binding of cytochrome *c,* it has been proposed that cytochrome *c* interacts with the WD40 repeats because WD40-deleted Apaf-1 mimics cytochrome *c*-bound Apaf-1 (Srinivasula *et al.,* 1998; Hu *et al.,* 1998). However, this presumption remains to be demonstrated experimentally. Although much remains unknown about cytochrome *c*—Apaf-1 binding, we do understand a lot about the consequences of this interaction: apoptosome formation.

In 2005 a group of researchers led by Christopher Akey determined a structure of the apoptosome using electron cryomicroscopy (Figure 1.4C) (Yu *et al.,* 2005). Synthesis of relevant biochemical analyses with the structural information enabled the group to propose a model for apoptosome assembly (Figure 1.4D). Although the structure is limited by low resolution and alternative assembly models with slight variations have been proposed (Shi, 2006; Riedl and Salvesen, 2007), it does provide a reasonable framework for understanding the establishment of this important death platform. Once cytochrome *c* binds Apaf-1, the auto-inhibited form of Apaf-1 is unlocked and Apaf-1 unfolds. This event triggers hydrolysis of the dATP bound within the nucleotide-binding domain of Apaf-1. Hydrolyzed dADP then exchanges for a new molecule of dATP (given sufficient cytosolic levels of dATP) (Kim *et al.,* 2005). This dATP exchange is thought to confer an additional conformational change in Apaf-1 such that it spontaneously oligomerizes with six other primed Apaf-1 molecules. Oligomerization occurs between

NOD domains, bringing neighboring Apaf-1 molecules together to form a heptameric wheel-like structure. Importantly, the CARD domains are located centrally in this structure, with the WD40 repeats extending outwards, like spokes on a wheel. This structure is the Apaf-1 apoptosome, an oligomeric adaptor complex that functions to regulate the catalytic activity of the initiator caspase, caspase-9 (Shi, 2008).

### 1.2.3 Recruitment of caspase-9 and activation of effector caspases

The Apaf-1 apoptosome functions as a platform for the recruitment and activation of caspase-9. Monomeric procaspase-9 is recruited to the apoptosome via interactions between its own N-terminal CARD domain with a CARD domain of Apaf-1 (Zhou *et al.,* 1999). Interestingly, unlike most caspases, caspase-9 does not require cleavage in order to become active (Stennicke *et al.,* 1999). Rather the prevailing model for caspase-9 activation is one of proximity-driven dimerization (Boatright and Salvesen, 2003). It has long been postulated that initiator caspases, including caspase-9, autoprocess when brought into close proximity of each other (Salvesen and Dixit, 1999). Usually caspase-9 exists as a monomer in the cytosol, but the high local concentration of caspase-9 at the apoptosome is thought to favor dimerization and subsequent activation (Acehan *et al.,* 2002). Indeed, engineered caspase-9 dimers exhibit catalytic activity, providing evidence that dimerization may be sufficient for activation (Yin *et al.,* 2006). However, these types of forced caspase-9 dimers demonstrate significantly less activity than apoptosome-bound caspase-9 (Chao *et al.,* 2005). These data suggest that although dimerization is important for caspase-9 activation, there may be additional factors (e.g., induced

conformation of caspase-9 or enhanced affinity for effector caspases) conferred by the apoptosome that enables maximal caspase-9 activity (Chao *et al.,* 2005; Shi, 2008).

The active caspase-9-bound apoptosome can be thought of as a holoenzyme for activating effector caspases (Rodriguez and Lazebnik, 1999). Effector caspase zymogens (procaspase-3, -6 and -7) exist as constitutive dimers and require intrachain cleavage to become active (Chai *et al.,* 2001; Fuentes-Prior and Salvesen, 2004). Procaspase-3 and, to a lesser extent, procaspase-7 are cleaved by the caspase-9 holoenzyme while procaspase-6 is cleaved by active caspase-3 (Slee *et al.,* 1999). Procaspase-3 is considered the physiologic substrate of caspase-9 and discussion of "effector caspase activity" is often used interchangeably with "caspase-3 activity" (Yin *et al.,* 2006; Shiozaki *et al.,* 2002). Importantly, cleavage of procaspase zymogens represents an irreversible activation event, meaning that once cleaved, effector caspases exhibit constant catalytic activity, which is thought to enable efficient cell dismantling (Denault *et al.,* 2006; Riedl and Salvesen; 2007.

### 1.2.4 Cell dismantling by activated effector caspases

(This subsection is adapted with permission from Elsevier: Cell, 2008 Sep 5; 134: 720-1.)

Activated effector caspases are the chief executioners of apoptotic cell death, transforming intact cells into parceled remnants suitable for phagocytic ingestion. Although dismantling of cells by caspases could, in theory, result from indiscriminate proteolysis, the packaging of apoptotic cells might also reflect the selective proteolysis of precise cellular substrates. Distinguishing between these possibilities requires a

comprehensive identification and functional analysis of caspase substrates. Many caspase substrates have been identified either through large-scale *in vitro* cleavage of peptide libraries, which provides no information about physiological relevance, or through analysis of individual proteins by gel electrophoresis, which is low throughput and often relies on the availability of specific antibodies to track proteolytic fragments.

Two recent studies (Dix *et al.,* 2008; Mahrus *et al.,* 2008) address deficiencies in these approaches by developing proteomics based platforms that enable large-scale profiling of proteolytic events. Despite using different methodologies, both studies uncovered hundreds of previously unreported caspase substrates. With Dix *et al.* documenting 170 new substrates and Mahrus *et al.* finding 240 new substrates, these data highlight our incomplete knowledge of caspase-mediated proteolysis. Indeed, Lüthi and Martin (2007) recently compiled every caspase substrate published to date in a searchable database (CASBAH), with substrate numbers upwards of 400. Given that the lists generated by CASBAH, Dix *et al*„ and Mahrus *et al.* only have minimal overlap (Figure 1.5A), it is likely that the list of substrates will only continue to grow.

Given the vast number of substrates, are caspases acting indiscriminately, or is there some method to the madness? Certain substrates are known to be crucial for affecting typical apoptotic morphology, such as membrane blebbing induced by cleavage of the Rho-associated kinase ROCK1 and DNA fragmentation induced by cleavage of the endonuclease CAD/DFF40 (Coleman et al., 2001; Woo et al., 2004). But are these examples the exception or the rule? Intriguing data from each study suggest that an active

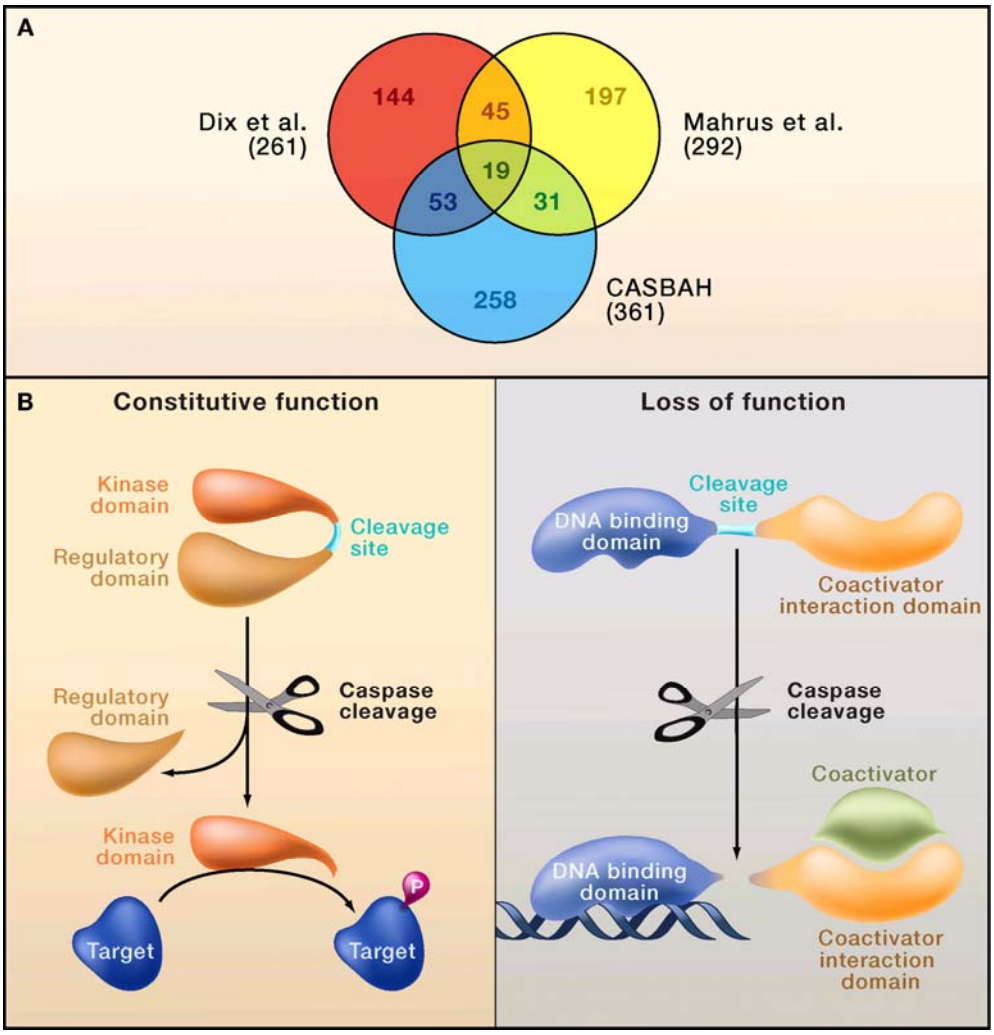


**Figure 1.5: Caspase substrates and potential functions of their cleavage products.**

**Figure 1.5: A,** Depicted is the overlap between the caspase substrates in apoptotic Jurkat T cells identified by Dix *et al.,* 2008, Mahrus *et al.,* 2008, and the previously reported human caspase substrates as compiled in the CASBAH database (Lüthi and Martin, 2007). The total number of substrates reported in each study is indicated in parentheses. **B,** Caspase-mediated cleavage of a cellular substrate resulting in separation of functional domains could lead to either constitutive activity of one of the proteolytic fragments (left) or to loss of function of the substrate (right). Depicted is the separation of a kinase domain from its regulatory domain, which allows for unchecked phosphorylation of target proteins (left). Conversely, separation of a DNA binding domain from a coactivator interaction domain within a transcription factor would prevent coactivator recruitment to the DNA, thereby hindering transcriptional induction (right).

caspase is not a haphazard "Pac-Man" but rather a purposeful and incisive surgeon. Perhaps most surprising is the observation by Mahrus *et al.* that caspases appear to target multiple proteins within single protein complexes or biochemical pathways. Their analysis most strongly implicates proteins involved in the regulation of transcription as caspase targets but also identifies subnetworks of substrates in eleven other pathways, including those that regulate DNA repair and block apoptosis. These data suggest that caspases may coordinately control specific biochemical pathways or signaling networks.

A second surprising result, reported by Dix *et al.*, suggests that more than one-third of proteolytic fragments generated by caspase cleavage are stable for at least four hours (in cells that died within six hours after apoptotic stimulation). This is in contrast to the notion that cleaved caspase substrates are rapidly degraded. For example, Ditzel et al. (2003) reported that caspase-mediated cleavage of DIAP1, a *Drosophila* inhibitor of apoptosis protein (IAP), generates an unstable N-degron that quickly undergoes complete degradation via the N-end rule pathway. Although production of stable fragments may be frequent, caspase cleavage-induced degradation of antiapoptotic proteins (such as DIAP1) makes sense as a means for "releasing the brakes" on apoptosis.

Even more interesting, Dix *et al.* noticed that a number of the persistent peptide fragments mapped to distinct, stably folded protein domains, leading them to speculate that caspase-mediated proteolysis yields a class of effector protein fragments with new activities. As to the purpose of such cleavage events, Mahrus *et al.* speculate that physical separation of functional domains can lead to protein inactivation (or perhaps production

of dominant negative fragments) while Dix *et al.* predict cleavage-induced activation of domain-containing fragments. We believe that perhaps both models are correct, depending on the individual substrate in question (Figure 1.5B). It has long been appreciated that cleavage of kinases can release constitutively active domains (such as cleaved HPK1, a modulator of the JNK pathway), whereas cleavage of other substrates, such as poly (ADP-ribose) polymerase (PARP), is associated with loss of function (Chen et al., 1999; D'Amours et al., 2001).

Collectively, the data suggest that dismantling the apoptotic cell is more akin to folding a tent after careful removal of the pegs than to gathering and disposing of indiscriminately destroyed debris after an explosion. Caspases selectively target certain biochemical pathways, generating a unique set of stable protein fragments possessing new functionality within the dying cell. Given the large number of substrates identified, one of the most daunting but important next steps will be to verify each putative caspase substrate and determine what, if any, functional significance it may have in mediating the execution of apoptosis.

## 1.3 Regulation of post-mitochondrial apoptosis

### 1.3.1 Regulation of apoptosome formation—Apaf-1 down-regulation

The complexities of apoptosome assembly are only beginning to be appreciated, but already a multitude of factors have been reported to regulate this process. Fundamental to our understanding of apoptosome formation, recent work from Xiaodong

Wang's laboratory has identified PHAP1, CAS and Hsp70 as proteins that accelerate nucleotide exchange on Apaf-1, thereby enabling proper apoptosome assembly and preventing the formation of inactive Apaf-1/cytochrome *c* aggregates (Kim *et al.,* 2008). Implied by these data is the notion that apoptosome formation depends on protein factors that do not constitute the core apoptosome machinery. Although PHAP1 and Hsp70 had been previously reported to regulate the apoptosome, their mechanism of action was unknown and Hsp70 had been reported as a negative apoptosome regulator (Jiang *et al.,*2003; Beere *et al.,* 2000; Saleh *et al.,* 2000); a relationship between CAS and the apoptosome had not been described. This work highlights the importance of Apaf-1 nucleotide exchange in apoptosome assembly and will certainly guide future research in the field.

In addition to the described role of these accessory proteins, formation of the apoptosome is thought to depend on ionic conditions, energy status, reducing environment, metabolic status and kinase/phosphatase signaling present within the cell (Bao *et al.,* 2007; Cain *et al.,* 2001; Chandra *et al.,* 2006; Vaughn and Deshmukh, 2008; Martin *et al.,* 2005; Kurokawa *et al.,* 2008). Although a discussion of these factors is beyond the scope of this dissertation, the degree of regulatory complexity suggests that global cellular homeostasis is "evaluated" before a cell commits to death via apoptosome-dependent caspase activation. Finally, apoptosome assembly depends on the presence (or absence) of the core apoptosome proteins. Down-regulation of Apaf-1 occurs in certain

cell types, and employment of this process as a means for preventing apoptosis will be described here.

Observations that children with traumatic brain injury fared worse than adults with comparable injuries led to the fundamental discovery that injury-induced apoptosis is markedly enhanced in the immature brain (Adelson and Kochanek, 1998; Bittigau *et al.,* 1999). Probing for the underlying mechanism, it was demonstrated that during cortical maturation Apaf-1 is down-regulated, leading to decreased cellular susceptibility to cytochrome *c*-induced apoptosis (Yakovlev *et al.,* 2001). Thus, immature neurons, with high Apaf-1 levels, are particularly susceptible to death-inducing stimuli (like trauma) while mature neurons are fairly resistant to similar insults. Decreasing levels of Apaf-1 during neuronal differentiation have also been observed in the retina, in sympathetic neurons and in cultured PC-12 cells (Donovan and Cotter, 2002; Deshmukh *et al.,* 2002; Wright *et al.,* 2002). These observations led to the proposal that Apaf-1 down-regulation occurs during cell differentiation as a mechanism for preventing unwanted apoptosis in long-living cells (Madden *et al.,* 2007). This model has been upheld in examining other types of differentiated cells, such as cardiomyocytes and skeletal muscle, which also have extremely low levels of Apaf-1 (Sanchis *et al.,* 2003; Burgess *et al.,* 1999). Results reported in this dissertation provide additional evidence for this phenomenon, demonstrating that resistance to cytochrome *c*-induced apoptosis develops during maturation of a number of different neuronal sub-types, including neurons from the cortex and cerebellum. In all cases, apoptotic resistance correlates with

decreased Apaf-1 expression while caspase-9 expression remains unchanged. These experiments were contributed by the laboratory of our collaborator, Mohanish Deshmukh, and the results provided a basis for examining the susceptibility of brain cancer cells to cytochrome *c*-induced apoptosis, which will be discussed in detail in sections 1.4 and 1.5.

It appears that Apaf-1 expression dramatically decreases during cellular differentiation, but through what mechanism? As neurons differentiate they exit the cell cycle to become post-mitotic cells, a process mediated, in part, by decreasing the expression of cell cycle promoting transcription factors such as E2F1. Previous work had identified E2F1 as a transcriptional activator of Apaf-1 (Moroni *et al.,* 2001; Furukawa *et al.,* 2002), and thus it was hypothesized that re-expression of E2F1 in mature neurons might induce Apaf-1 expression. However, recent work by the Deshmukh laboratory suggests that mature neurons require both chromatin depression and E2F1 transcriptional activity in order to express Apaf-1 (Wright *et al.,* 2007). These data suggest that at least two levels of regulation on Apaf-1 expression ensure apoptotic resistance in mature neurons. Interestingly, mature neurons are able to restore their apoptotic potential in response to certain types of stress, including irreparable DNA damage. In these cases there is a delayed apoptotic death that occurs only after re-entry into the cell cycle and reactivation of the Apaf-1 gene (Wright *et al.,* 2007).

### 1.3.2 Regulation of caspase activity by inhibitor of apoptosis proteins

Inhibitor of apoptosis proteins (IAPs) are so named for their ability to protect cells from death-inducing stimuli, a characteristic conferred by caspase neutralization. This family of proteins is defined according the presence of a Baculovirus IAP repeat (BIR) domain, which is an approximately 70 amino acid zinc-binding motif important for mediating protein-protein interactions (Deveraux and Reed, 1999). One to three copies of the BIR motif are present in the eight identified human IAPs (Salvesen and Duckett, 2002). The X-linked IAP (XIAP) demonstrates potent anti-apoptotic activity and is the best characterized of the human IAPs. XIAP contains three BIR motifs, with apoptosis-suppressing function attributed to both BIR2 and BIR3, although through distinct mechanisms (Srinivasula and Ashwell, 2008). The BIR2 motif and a small segment immediately amino-terminal to the BIR2 binds strongly to caspases-3 and -7, preventing their interaction with substrates (Huang *et al.,* 2001; Riedl *et al.,* 2001; Chai *et al.,* 2001). Interestingly, although XIAP binding occludes the caspase active site, it binds in the opposite orientation and does not require the substrate-binding residues, suggesting that XIAP simply masks the active site rather than functioning as a pseudosubstrate. The XIAP BIR3 motif selectively inhibits caspase-9. It does so through binding to the dimerization interface of caspase-9, preventing dimerization-induced activation of the caspase (Shiozaki and Shi, 2004). Thus, through these BIR-mediated interactions, XIAP serves to inhibit active effector caspases and to prevent caspase-9 activation.

Given the widespread expression of endogenous IAPs, how do caspases ever become active? IAP inhibitors provide at least a partial answer to this question. Outer mitochondrial membrane permeabilization enables release not only of cytochrome *c* but also of several other mitochondrial proteins, including Smac and Omi. These proteins interact with the BIR2 and BIR3 motifs, sequestering IAPs and therefore enabling caspase activation (Srinivasula *et al.,* 2001). So it would appear that when a cell decides to undergo apoptosis it must release the IAP brake in order to execute the pro-death cytochrome *c* signal. However, in many circumstances this does not appear to be case. XIAP knockout mice are viable and without any morphological defects (Harlin *et al.,* 2001). Moreover, in most cell types cytochrome *c* addition (either to cell lysates or via microinjection) is sufficient to induce caspase activation—no IAP inhibition required (Wright *et al.,* 2004). So the physiological importance of IAPs (and their inhibitors) in apoptosis has been unclear. In fact, mounting evidence suggests that IAPs play a role in a diverse set of processes, ranging from cell division to heavy metal homeostasis, and these functions may prove more important than their role in mediating cell death (Srinivasula and Ashwell, 2008).

Despite this shifting paradigm, studies in differentiating neurons have identified a putative role for endogenous IAPs in regulating apoptosis. Post-mitotic sympathetic neurons demonstrate a remarkable resistance to cytochrome *c,* as was described previously. During differentiation, as levels of Apaf-1 are decreasing, IAP inhibition enables cytochrome *c*-mediated caspase activation (Deshmukh *et al.,* 2002). XIAP has

been identified as the critical IAP for mediating this phenomenon, and XIAP-deficient differentiating sympathetic neurons demonstrate rapid caspase activation in response to cytochrome *c* whereas wild-type differentiating sympathetic neurons are resistant to cytochrome *c* (Potts *et al.,* 2003). Thus, during neuronal differentiation XIAP levels may help to set the apoptotic threshold. Importantly, it seems that Apaf-1 levels essentially determine when IAPs will be important for regulating apoptosis (Wright *et al.,* 2004). In situations of high Apaf-1, an apoptotic stimulus will generate sufficient caspase activity to overcome any IAP-mediated inhibition. In cells with virtually no Apaf-1, cytochrome *c* will be unable to induce caspase activation even in the absence of IAPs. However, in cases of intermediate Apaf-1 levels, such as in differentiating neurons, IAPs are sufficient to prevent cytochrome *c*-induced death and their inhibition allows apoptosis to proceed.

## 1.4 Mechanisms of apoptotic evasion in cancer

In 2000, Douglas Hanahan and Rober Weinberg published a seminal review on the hallmarks of cancer, in which they proposed that all human cancers share a small number of acquired capabilities required for oncogenic transformation. These traits include self-sufficiency in growth signals, insensitivity to anti-growth signals, tissue invasion and metastasis, limitless replicative potential, sustained angiogenesis, and evasion of apoptosis (Hanahan and Weinberg, 2000). In discussing the evasion of apoptosis, they divide the apoptotic machinery into two broad components—sensors and effectors. Any protein that monitors the cellular environment for conditions that influence whether a cell should live or die is a sensor, and proteins that are regulated by the sensors

are the effectors of apoptosis. On a mechanistic level, a variety of anti-apoptotic strategies are employed by cancers, with certain types of cancer inactivating sensors and others deregulating effectors.

The prototypical example of a pro-apoptotic sensor that is lost in cancers is the p53 tumor suppressor gene, in which mutation results in functional inactivation of the protein (Vazquez *et al.,* 2008). Observed in more than half of human cancers, alterations in p53 prevent a cell from being able to sense DNA damage, hypoxia or oncogene activation as necessitating apoptosis (Harris, 1996; Levine, 1997). Aside from loss of p53, aberrant pro-survival signaling through the phosphoinositide-3 kinase (PI3K)-Akt pathway and abrogation of the Fas death signal are two additional illustrations of apoptotic sensor abnormalities found in cancers (Cantley and Neel, 1999; Pitti, 1998).

In terms of apoptotic effectors, Bcl-2 is an anti-apoptotic regulator of mitochondrial membrane permeability whose activity prevents cytochrome *c* release. Cancers that up-regulate Bcl-2, such as follicular lymphomas, become resistant to apoptotic stimuli—not because they do not sense a given death stimulus but rather because transmission of the apoptotic signal is blocked upstream of the mitochondria (Korsmeyer, 1992; Verma *et al.,* 2006). In this manner, dysregulation of apoptotic effectors allows cancer cells to survive in the absence of survival signals, in hostile extracellular environments, and in the presence of DNA damage and oncogene activation.

Moving further downstream, decreasing apoptosome formation or activity is yet another mechanism by which cancer cells could acquire apoptotic resistance. For

example, the oncogenic tyrosine kinase Bcr-Abl has been reported to protect leukemic cells from apoptosis downstream of cytochrome *c* release (Deming *et al.,* 2004). More recently, it has been demonstrated that this protection is mediated by suppression of Hsp90β phosphorylation in cells expressing oncogenic tyrosine kinases. This results in tight binding of the hypophosphorylated Hsp90 β to Apaf-1, preventing cytochrome *c*-induced Apaf-1 oligomerization and caspase-9 recruitment (Kurokawa *et al.,* 2008). Additionally, inactivation and down-regulation of Apaf-1 have been reported in melanoma and ovarian cancer, respectively (Soengas *et al.,* 2001; Wolf *et al.,* 2001; Liu *et al.,* 2002). However, such findings have been disputed, with more recent studies suggesting technical issues limited Apaf-1 detection in melanoma (Allen *et al.,* 2005; Peltenburg *et al.,* 2005). Collectively, dysregulation of apoptotic effectors that act downstream of cytochrome *c* release seems to be the exception rather than the rule in cancers. Perhaps this is not surprising, given that once a cancer cell has released cytochrome *c* from the mitochondria it is likely to have compromised mitochondrial membrane potential and would therefore die via necrosis even if it could suppress apoptosis. In other words, there may be less selective pressure for cancer cells to develop apoptotic resistance downstream of cytochrome *c* release because it offers less survival advantage than developing resistance upstream of the mitochondria.

In accordance with this theory, recent work from our laboratory has demonstrated that breast cancer cells are actually more sensitive to cytochrome *c*-induced apoptosis than normal mammary epithelial cells (Schafer *et al.,* 2006). The data suggest that breast

cancers evade apoptosis by preventing release of cytochrome *c* while the downstream apoptotic machinery remains intact. Further, the observed heightened sensitivity to cytochrome *c* was traced to overexpression of the apoptosome activator Putative HLA class II associated protein I (PHAPI) in breast cancers (Figure 1.6). Although the driving factors underlying PHAPI overexpression remain unknown, the survival of breast cancer cells is unlikely to be compromised by PHAPI since the cells evade apoptosis by blocking apoptotic signaling upstream of the mitochondria. The fundamental principle that some cancers may be more susceptible to cytochrome *c* than their normal counterparts sparked our interest in investigating apoptosis in brain tumors, due to earlier observations that mature neuronal cells display resistance to cytochrome *c*-mediated apoptosis (Wright *et al.,* 2004).

## 1.5 Apoptosis regulation in primary brain cancers

### 1.5.1 Glial cell cancers

Primary brain tumors originate in the central nervous system and include a heterogeneous group of neoplasms. Glial-cell tumors, or gliomas, account for more than 70% of brain tumors (Ohgaki, 2009). The majority of gliomas are astrocytomas, with glioblastoma multiforme (World Health Organization grade IV astrocytoma) being the most frequent sub-type (Lesniak and Brem, 2004). Glioblastoma is a highly-aggressive cancer, with a five-year survival less than 3% (Ohgaki, 2009). The currently recommended treatment regimen includes surgical debulking combined with post-

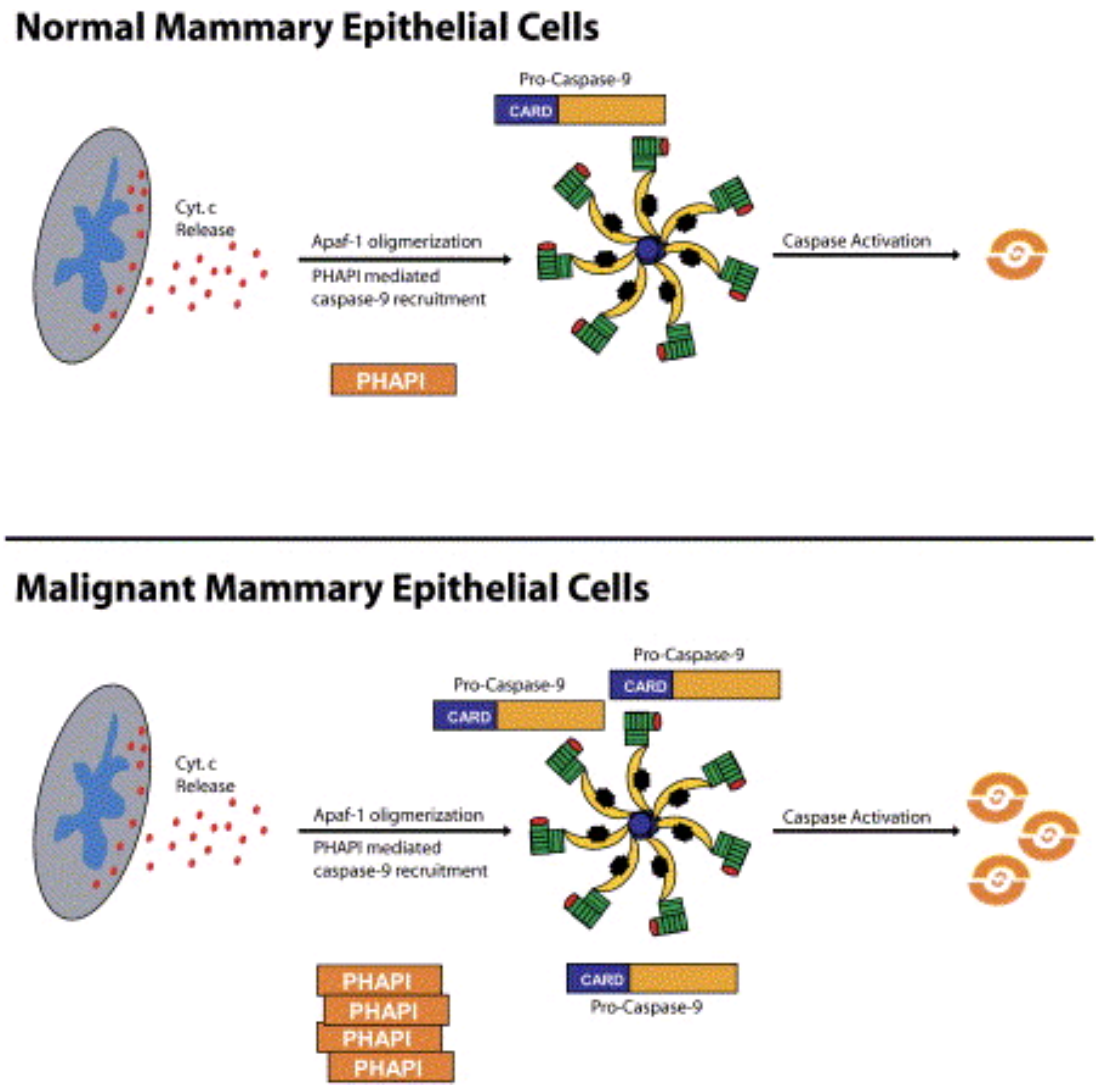


**Figure 1.6: PHAPI-mediated sensitivity to cytochrome *c*-induced apoptosis in breast cancer.**

**Figure 1.6:** Malignant mammary epithelial cells activate caspases more efficiently and robustly after the release of cytochrome c into the cytosol. This is due to the overexpression of PHAPI, which causes enhanced recruitment of caspase-9 to the apoptosome. From Schafer and Kornbluth (2006), with permission from Elsevier.

surgical radiation therapy and administration of temozolomide, an orally administered alkylating chemotherapeutic (Mrugula and Chamberlain, 2008). Even with this intense therapeutic intervention median survival remains less than two years (Hart *et al.,* 2008). Thus, it is imperative that novel therapeutics be developed to improve outcome in patients suffering from aggressive gliomas, such as glioblastoma.

Constitutive activation of growth factor signaling pathways is observed in almost all high-grade gliomas. The epidermal growth factor receptor (EGFR) is overexpressed in 85% of cases, with glioblastomas often expressing a mutant form of the receptor, EGFRvIII, that is constitutively active (Broniscer and Gajjar, 2004; Mellinghoff *et al.,* 2005). Additionally, malignant gliomas often express both platelet-derived growth factor (PDGF) and the PDGF receptor, enabling the tumor cells to fuel their own growth and survival via an autocrine (or paracrine) loop (Hermanson *et al.,* 1992). Activity through both of these growth factor receptors provides strong and continuous stimulatory input to the PI3K/Akt signaling pathway (Knobbe and Reifenberger, 2003). Activation of this pathway stimulates cell proliferation and survival, significantly contributing to their oncogenic potential. Mutations or deletions of the tumor suppressor PTEN are found in over one-third of glioblastomas, and because PTEN plays an important role in regulation of the PI3K pathway, loss of PTEN amplifies PI3K/Akt activity (Broniscer and Gajjar, 2004; Cheng *et al.,* 2009).

The prevalence of aberrant PI3K/Akt signaling in gliomas has important implications for how these cancers evade apoptosis. It is well-recognized that this

pathway plays a critical role in keeping cells alive by blocking apoptotic signaling (Duronio, 2008). Many potential mechanisms to explain how PI3K/Akt activity prevents apoptosis have been reported, including suppression of pro-apoptotic Bcl-2 family members and disruption of p53 activation (Tsuruta *et al.,* 2002; Downward, 2004). Notably, all proposed mechanisms involve either apoptotic sensors or apoptotic effectors that are upstream of cytochrome *c* release. The particular cellular context may determine which process is crucial for mediating the anti-apoptotic effect of PI3K/Akt in a given cell type or cancer. Although it remains unclear which specific mechanism is the driving force in gliomas, it has been demonstrated that inhibition of the PI3K/Akt pathway sensitizes these cancers to apoptotic stimuli (Opel *et al.,* 2008).

Therefore, it is likely that dysregulation of apoptosis in gliomas is due to a blockade of apoptotic signaling upstream of the mitochondria. This is supported by studies demonstrating that expression of the EGFR is sufficient to block cytochrome *c* release in response to strong apoptotic stimuli (Nagane *et al.,* 1998; Stegh *et al.,* 2007). However, two reports in the literature implicate the involvement of factors downstream of cytochrome *c* release. One study reported Apaf-1 inactivation due to loss of heterozygosity at chromosome 12q22-23, the locus of the *Apaf-1* gene (Watanabe *et al.,* 2003). However, since publication of that report a reassessment of the Apaf-1 gene location was made, casting serious doubt on whether *Apaf-1* LOH occurs at all in glioblastoma (Umetanin and Hoon, 2004). A second report characterizes a novel Bcl-2 family member, Bcl2L12, and its role in inhibiting apoptosis in glioblastoma (Stegh *et*

*al.,* 2007). They find expression of Bcl2L12 in the vast majority of these cancers, and show that Bcl2L12 enhances resistance to staurosporine-induced apoptosis, likely through its ability to interact with and neutralize caspase-7. While this factor may decrease the robustness of caspase activation in glioblastoma, their work did not address the functionality of the core apoptotic machinery and whether cytochrome *c* release in these cells could result in apoptosis despite the potential inhibitory effect of Bcl2L12. In summary, the primary mechanism of apoptotic resistance in gliomas is likely to be due to a blockade of upstream signaling that prevents the release of cytochrome *c.* Expression of apoptosome components and sensitivity to cytochrome *c*-induced caspase activation remain to be examined in these cancers.

### 1.5.2 Medulloblastomas

Medulloblastomas occur predominantly in children and develop exclusively within the cerebellum. This tumor accounts for approximately 20% of pediatric brain tumors and is highly malignant (Weir *et al.,* 2003). Although medulloblastomas are generally sensitive to radiation therapy, this treatment modality is quite harmful to the developing central nervous system (CNS). As a result, the majority of patients suffer long-term brain damage with demonstrable drops in overall IQ (Mulhern *et al.,* 2004). Therefore, alternative therapies that would spare the surrounding normal neural tissue while eliminating malignant cells would provide a significant clinical benefit for children with this type of cancer.

Medulloblastomas are believed to arise from cerebellar granule cell precursors (Wechsler-Reya and Scott, 2001). Mitogenesis of these cells is potently stimulated by the morphogen Sonic hedgehog (Shh) and conversely is inhibited by the Shh antagonist Patched. Consistent with the importance of these factors in medulloblastoma development, patients with inherited mutations in *Patched* display an increased propensity to develop medulloblastoma (Pietsch *et al.,* 1997). Moreover, mutations in the Shh/Patched pathway have been observed in spontaneous human medulloblastoma (Raffel *et al.,* 1997; Xie *et al.,* 1997).

The transforming action of Shh stimulation in medulloblastomas is thought to be enhanced by expression of the Myc oncogene and hyperactivation of insulin-like growth factor (IGF) signaling (Ye *et al.,* 1996; Kenney *et al.,* 2004). These factors not only drive proliferation but also must prevent apoptosis in order for full oncogenic transformation. The anti-apoptotic protein Bcl-2 has been identified as a transcriptional target of Shh (Bar *et al.,* 2007), and there is evidence that human medulloblastomas frequently overexpress Bcl-2 (Schuller *et al.,* 2004). However, there is also evidence to suggest that IGF-mediated activation of the PI3K/Akt signaling pathway is essential for preventing apoptosis in Shh-driven medulloblastomas (Rao *et al.,* 2004; McCall *et al.,* 2007). Similarly to evasion of apoptosis in gliomas, this acquired capability in medulloblastomas seems to be fulfilled through modulation of factors that prevent apoptotic signaling upstream of mitochondrial cytochrome *c* release.

### 1.5.3 Sensitivity of brain cancer cells to cytochrome *c*-induced apoptosis

Many of the defined signaling pathway abnormalities in both gliomas and medulloblastomas involve aberrations in apoptotic signaling upstream of the mitochondria. Commonly reported in the literature are examples of inhibition of a growth-signaling pathway increasing the apoptotic response of cancer cells to a given chemotherapeutic. Implied in this is the presence of functional apoptotic machinery, allowing for the cells to undergo apoptosis when the upstream brakes are released. In this dissertation, we directly examine the cellular response to cytochrome *c* in brain cancers. We found that brain cancer cells are capable of activating caspases in response to cytochrome *c.* Importantly, we demonstrate that normal brain tissue, including neuronal and glial cells, is remarkably resistant to cytochrome *c* due to down-regulation of Apaf-1. Thus, these results suggest direct activation of the apoptosome as a potential anti-cancer strategy.

## 1.6 Activation of the apoptosome as an anti-cancer therapy

Since evasion of apoptosis is a requirement for oncogenic transformation, there has been significant interest in developing therapeutic strategies to reverse this apoptotic block in cancer cells. Many of the efforts to date have focused on targeting the death receptors or Bcl-2 family proteins (Fischer *et al.,* 2007). Unfortunately, use of tumor necrosis factor (TNF)-related apoptosis-inducing ligand (TRAIL) or other ligands aimed at inducing apoptosis via death receptors have not met much success. Although often the

reasons for this are unclear, there are examples of cancer cells upregulating decoy death receptors, resulting in sequestration of extracellular death ligands without the typical consequent DISC assembly and subsequent caspase activation (LeBlanc and Ashkenazi, 2003). Targeting Bcl-2 family members has been attempted using antisense technology against Bcl-2 or Bcl-$X_L$, but very little anti-tumor activity was observed in preclinical trials (Bedikian *et al.,* 2006). The complexity of the Bcl-2 proteins (and their interactions) makes it unlikely that targeting just one Bcl-2 family member would overcome a cancer cell's block in apoptosis, and ongoing work aims to develop a number of small molecule inhibitors that could be utilized to simultaneously target multiple anti-apoptotic Bcl-2 proteins (Oltersdorf *et al.,* 2005; Ziegler *et al.,* 2008).

In addition to the pursuit of these strategies, we believe that additional approaches for actively inducing apoptosis in cancer cells should be explored. The differential sensitivity to cytochrome *c*-induced apoptosis that we observed in brain cancers and normal brain tissue raises the interesting possibility of selectively activating the apoptosome in cancer cells while sparing surrounding normal tissue. Thus, we believe that the core apoptosome represents a valid target for anti-cancer therapeutics. By inducing apoptosis downstream of the mitochondria, this approach offers the major advantage of bypassing blockades in upstream apoptotic signaling, which seem to be common in many cancers. Given that there are more than 100 distinct types of cancer employing a variety of anti-apoptosis strategies (Hanahan and Weinberg, 2000), it is likely that many cancers possess functional apoptotic machinery. Profiling cancer cells

relative to their normal counterparts should help determine in which cases the apoptosome would be a valid target. The ability to locally deliver therapeutics to the brain make the development of apoptosome activators particularly attractive—even if such a therapeutic could not be tolerated systemically it could be used for treating tumors of the central nervous system, where the need for novel anti-cancer therapies is critical.

There have been two reports in the literature of direct activation of the apoptosome as an anti-cancer strategy (Nguyen and Wells, 2003; Jiang *et al.,* 2003). These studies used a cell-free system to screen small-molecules for their ability to enhance cytochrome *c*-induced caspase activation. Both groups identified compounds that function to promote apoptosome formation and the activation of effector caspases. However, the requirement of cytochrome *c* in these assays means that they merely augment apoptosome formation rather than possessing the innate ability to trigger apoptosome formation. These types of compounds might be useful in combination with therapeutics that induce apoptosis upstream of the mitochondria, although they would not be expected to elicit apoptosis selectively in cancer cells. Alternative approaches that involve downstream apoptotic signaling include triggering the release of endogenous cytochrome *c* from the mitochondria and upregulating the apoptosome components (Ledgerwood and Morison, 2009). Pursuit of the first approach identified an inhibitor of acyl-CoA-synthase that selectively induces mitochondrial cytochrome *c* release, and pursuit of the second identified a pan-histone deacetylase inhibitor which leads to the induction of Apaf-1 and caspase-9 expression (Mashima *et al.,* 2005; Wang *et al.,* 2006).

Unfortunately, these compounds would not be expected to demonstrate selectivity for cancer cells, and the second approach would merely sensitive cells to apoptotic stimuli but would not induce apoptosis on its own.

We believe the key to a successful anti-cancer drug is its intrinsic ability to selectively induce death of a cancer cell. Further, the ideal therapeutic should not merely sensitive a cancer cell to other apoptosis-inducing drugs, but stimulate death on its own. Based on our work in characterizing apoptosis regulation in brain cancers and normal brain, we strongly believe that a therapeutic that directly activates the apoptosome would fulfill these criteria and provide a promising new approach for treating brain cancers. In this dissertation we aimed to develop a cytochrome *c*-based therapy. Such a drug would be expected to induce caspase activation only in brain cancer cells, since the apoptotic function of cytochrome *c* depends on Apaf-1, which is absent in the surrounding neural tissue. Additionally, a cytochrome *c*-based therapeutic would be sufficient to trigger apoptosis in the cancer cells on its own, without the requirement for additional apoptotic stimulation. We pursued a multi-tiered strategy in the hopes of developing such a therapeutic, in which we attempted to 1) define the molecular contact surfaces between cytochrome *c* and Apaf-1, 2) express a cytosolic form of active cytochrome *c,* and 3) develop a small-molecule screen (and then perform the screen) to identify a cytochrome *c* mimetic.

## 1.7 Studying apoptosis in *Xenopus laevis*

### 1.7.1 The *Xenopus* egg extract system

Eggs laid from the frog *Xenopus laevis* are arrested in metaphase II of meiosis. Crushing of the eggs by centrifugation causes internal release of $Ca^{++}$ stores, mimicking fertilization and leading to cyclical degradation and synthesis of cyclin B in the resultant cell-free extract. Cyclin B expression drives Cdc2 activity and thus, coincident with fluctuations in Cdc2 activity, the extract repeatedly enters and exits mitosis (Murray, 1991). This property has made the cell-free extract an important model system for studying the cell division cycle. In the presence of sperm chromatin, the extracts form nuclei, replicate DNA and then disassemble the nuclei at entry into mitosis.

To study the process of nuclear assembly in the absence of cycling, eggs can be supplemented with cycloheximide (to prevent synthesis of Cyclin B) prior to centrifugation, resulting in an interphase-arrested extract. It was in these interphase-arrested extracts aged on the bench that recapitulation of apoptosis was first observed (Newmeyer *et al.*, 1994). These apoptotic extracts were recognized by the presence of irregular chromatin condensation and nuclear fragmentation. Since these original observations of apoptosis, the egg extract has become a useful system for studying the biochemical properties of apoptosis signaling (Kornbluth and Evans, 2003).

The crude egg extract described above contains cytoplasmic, membrane and nuclear components. Spontaneous induction of apoptosis over time in these extracts reflects a latent phase followed by release of cytochrome *c* from mitochondria and

effector caspase activation. Recent work from our laboratory has elucidated the upstream signaling events responsible for this phenomenon: nutrient depletion over time in the extract results in dephosphorylation of caspase-2, leading to its activation and stimulation of the intrinsic apoptotic pathway (Nutt *et al.,* 2005).

In addition to studying apoptosis in the crude extract, this cell-free lysate can be further separated into cytosolic, light membrane (endoplasmic reticulum), heavy membrane (mitochondria and rough endoplasmic reticulum) and insoluble (glycogen, ribosomes, assembled cytoskeletal proteins, and large protein complexes) fractions by high-speed centrifugation. The cytosolic fraction derived from interphase-arrested crude extract can be supplemented with various pharmacological compounds and recombinant proteins, and depleted of specific proteins using immunoprecipitation. Thus, the cytosolic extract can serve as an *in vitro* system for identifying and characterizing regulators of caspase activity. Since the cytosolic extract lacks mitochondria, addition of cytochrome *c* (in the presence of an energy-regenerating system) yields caspase activation, which can be assayed by immunoblot analysis or quantitated by monitoring the cleavage of a colorimetric (or fluorescent) caspase substrate. Additionally, because the cytosolic extract can also be prepared from mitotic-arrested crude, this system is uniquely poised to address how the regulation of apoptosis changes throughout the cell cycle, which could aid in our understanding of how highly-proliferative cancer cells evade apoptosis.

### 1.7.2 Post-mitochondrial apoptosis in *Xenopus* oocytes

Despite these strengths, the *Xenopus* cell-free system does not allow evaluation of apoptosis at the single cell level. As an alternative to preparing extracts from eggs, *Xenopus* oocytes can be isolated from frog ovaries. Stage VI *Xenopus* oocytes (Figure 1.7A) are arrested at the G2/M transition of meiosis I, and can be induced to mature with progesterone treatment. Progesterone stimulates entry into M phase of meiosis I, which is characterized by breakdown of the germinal vesicle (oocyte nucleus). This germinal vesicle breakdown (GVBD) can be easily monitored by the appearance of a white spot in the animal pole of the oocyte (Figure 1.7B). The oocyte will continue to mature, exiting meiosis I and entering meiosis II, where it arrests in metaphase. At this point the mature oocyte is awaiting fertilization, and is comparable to the egg which is used to prepare cell-free extract.

Oocytes are very large cells, measuring approximately 1 mm in diameter with a volume of about 1 µl. This large size makes oocytes easy to microinject with mRNA, protein or morpholinos (antisense oligonucleotides). Thus, the two systems (cell-extract and oocyte-based) can be used to complement one another, with studies in the oocyte providing an intact cellular system for the study of mitotic entry (Taieb *et al.,* 1997).

To date, very few studies have utilized oocytes for studying apoptosis. However, microinjection of cytochrome *c* into *Xenopus* oocytes has been demonstrated to reliably induce apoptosis. However, detection of apoptotic death has depended on visual observations of changes in oocyte morphology, which take hours to occur (Figure 1.7C).


**Figure 1.7: Morphological features of *Xenopus* oocytes.**

**Figure 1.7:** Reflective light photographs of stage VI oocytes either untreated, **A**, progesterone-treated and demonstrating GVBD, **B**, or microinjected with cytochrome *c* and demonstrating apoptosis, **C**.

Indirect markers of caspase activation, such as plasma membrane depolarization, have also been reported (Bhuyan *et al.,* 2001). Unfortunately, changes in membrane potential are not specific for apoptotic death, lack the sensitivity of the cell-free system, and cannot be recorded for more than one oocyte at a time. In this dissertation work, we develop an assay for *in vivo* detection of caspase activation in the *Xenopus* oocyte and early embryo. We demonstrate that this assay offers an alternative to the cell-extract system, in which regulation of apoptosis downstream of the mitochondria can be readily examined in an intact cell. Using this method, we demonstrate that only a brief period of caspase activity is required to ensure apoptotic death, that inhibitor of apoptosis proteins function as a brake in the oocyte, and that apoptosis in the early embryo is not a cell-autonomous process. These results confirm this method as a valid means for studying apoptosis, and reveal several important subtleties of the apoptotic program. Further, we believe that this assay will be useful as a screening modality for identifying novel regulators of apoptosis as well as apoptosome-activating small-molecules that could ultimately prove useful in the treatment of brain tumors.

# 2. Materials and methods

## 2.1 Cell culture and microinjection of neurons

Primary neurons from the dorsal root ganglion (DRG) and the cerebellum were cultured as described (Molliver *et al.,* 1997; Miller and Johnson, 1996). SH-SY5Y neuroblastoma cells (gift from Daniel Sanchis, Universitat de Lleida, Lleida, Spain) were maintained in a 1:1 mixture of DMEM and Ham's F12 medium supplemented with 10% FBS. Glioblastoma lines, MGR1 and MGR3 (gifts from Francis Ali-Osman, Duke University), were maintained in low glucose DMEM supplemented with 10% FBS. Medulloblastoma lines UW228 (gift from John Silber, University of Washington, Seattle) and MCD1 (gift from William Freed, National Institutes of Health, Bethesda) were maintained in DMEM supplemented with nonessential amino acids, L-glutamine, and 10% FBS. Glioblastoma lines D54P, D54TR, D54OTR, H80P, H80TR, H80OTR, F3, F37, F5 and F19 (gifts from Henry Friedman, Duke University) were maintained in ZO-MEM with 40 mM HEPES, 0.9% sodium bicarbonate, and 20% FBS. Remaining glioblastoma and medulloblastoma lines were obtained from the Duke University Preston Robert Tisch Brain Tumor Center and maintained in RPMI medium 1640 supplemented with 10% FBS. HeLa cells were obtained from the Duke University Cell Culture Facility and cultured in DMEM supplemented with 10% FBS. Cells were transiently transfected using FuGENE 6 (Roche) according to the manufacturer's protocol. Sensory neurons from the DRG were microinjected by using 10 g/L cytochrome *c* as described (Wright *et*

*al.,* 2004). The microinjection solution contained 100 mM KCl, 10 mM KPi (pH 7.4), and 4 mg/mL rhodamine dextran to mark injected cells. Cell viability was determined by counting rhodamine positive cells with intact, phase-bright cell bodies.

## 2.2 Cell-free lysate preparation and caspase assays

### 2.2.1 Preparation of cytosolic lysates (extracts)

Cytosolic extracts from cultured neurons were prepared as described (Wright *et al.,* 2004). Brain tumor cell lines, xenograft tumors, and human cortical tissues were harvested, washed with cold PBS, and pelleted. Pellets were resuspended in hypotonic lysis buffer [20 mM Hepes (pH 7.5), 10 mM KCl, 1.5 mM MgCl2, 1 mM EDTA, 1 mM EGTA, 1 mM DTT, 1 mM PMSF, 5 μg/mL leupeptin, and 5 μg/mL aprotinin] with 250 mM sucrose (to protect mitochondrial membrane integrity), and incubated for 15 minutes on ice. Tissues were homogenized by using a 0.5-mL Bellco glass homogenizer and centrifuged for 30 minutes at 14,000 rpm (Eppendorf 5415C) at 4°C, and the supernatant was preserved as extract. Extracts were quantitated by using the Bradford method. Xenograft tumors, human cortical tissue, and human high-grade glioma tissue were provided by the Tisch Brain Tumor Center. Tissues were diced on ice into 1-$mm^3$ pieces, and extracts were prepared as above. Cytosolic lysate was prepared from *Xenopus laevis* eggs according to standard protocols (Kornbluth and Evans, 2001).

### 2.2.2 Cell-free caspase assays

#### 2.2.2.1 Mammalian caspase assays

Assays were performed as described (Wright *et al.,* 2004; Schafer *et al.,* 2006). In brief, extracts were incubated with 10 μM either mammalian or yeast cytochrome *c* and 1 mM dATP at 37°C for 30 minutes before addition of the fluorogenic substrate, Ac-DEVD-afc (Biomol). Alternatively, extracts alone or with 8 μM cytochrome *c* were incubated as above before addition of the colorimetric substrate Ac-DEVD-pNA (Biomol) to 200 μM, and absorbance was measured at 405 nm.

#### 2.2.2.2 *Xenopus* caspase assays

20 μl cytosolic extract was supplemented with horse cytochrome *c,* yeast cytochrome *c,* or cytochrome *c* peptide fragments and allowed to incubate for 30 minutes at room temperature. 5 μl aliquots of those reactions were then incubated with 85 μl DEVDase buffer (50 mM HEPES [pH 7.5], 100 mM NaCl, 0.1% CHAPS, 10 mM DTT, 1 mM EDTA, 10% glycerol) and 10 μl of the substrate Ac-DEVD-pNA (200 μM) at 37°C for 30–60 min. Absorbance was measured at 405 nm.

## 2.3 Antibodies and immunoblotting

Antibodies used include: anti-cytochrome *c* (556433, BD Pharmingen), anti-caspase-9 (M0543, MBL International; 9504, Cell Signaling), anti-procaspase 3 (9665; Cell Signaling), anti-active(cleaved) caspase 3 (9661, Cell Signaling), anti-Apaf-1(13F11

and 2E12; Alexis; AAP-300, Assay Designs), anti-p53 (DO1; Santa Cruz), anti-E2F1 (C-20; Santa Cruz), anti-flag (F3165, Sigma), anti-α-tubulin (T9026; Sigma), and anti-β-actin (A5316 and A1978, Sigma). The anti-XLX serum was a gift from Jean Gautier (Columbia University), and the purified anti-xXIAP was a gift from Shigeru Yamashita (Toho University). Either Alexa Fluor secondary antibodies (Invitrogen) or streptavidin-AF680 (S32358, Invitrogen) were used with the LI-COR Odyssey IR Imaging System or HRP-conjugated secondary antibodies (Pierce Chemical) along with an ECL-Plus detection system (Amersham Biosciences). Protein array of human astrocytomas was from the BioChain Institute (A1235713-1).

## 2.4 Real-time RT-PCR

Medulloblastoma tumor cells were isolated for reverse transcriptase polymerase chain reaction (RT-PCR) as described (Oliver *et al.,* 2005). RNA was isolated by using the small-scale RNAqueous Kit and treated with DNase I (Ambion). Isolated mRNA from pre-sorted CD133+ and CD133- populations of glioma cells were a kind gift from Jeremy Rich's laboratory (Cleveland Clinic). For RT-PCR, first-strand cDNA was synthesized with an oligo(dT) primer by adding ≈300 μg of RNA with SuperScript III Reverse Transciptase (Invitrogen). Real-time PCR was performed by using iQ SYBR Green Supermix (BioRad), 5 ng of cDNA, and 10 μM of the following forward and reverse Apaf-1 primers: Human, 5'- ATA TGG AAT GTC TCA AAC GGT GAG C -3' and 5'- GGT CTG TGA GGA TTC CCC A -3', and mouse, 5'- ATA TGG AAT GTC TCA GAT GGC CAG C -3' and 5'- GGT CTG TGA GGA GTC CCC A -3'. Real-time

quantitation was performed by using a BioRad iCycler iQ System. Data were normalized to $\beta_2$-microglobulin (mouse samples) or GAPDH (human samples), and fold change was determined by using the $2^{-\Delta\Delta CT}$ method (Livak and Schmittgen, 2001). For RT-PCR agarose gel analysis, reactions were performed as above except with iQ Supermix (BioRad).

## 2.5 Microarray data analysis

Three independent gene profiling studies (Sun *et al.,* 2006; Freije *et al.,* 2004; Phillips *et al.,* 2006) publicly available on the Oncomine Cancer Profiling Database (www.oncomine.org) were used to investigate Apaf-1 mRNA levels in human brain cancers. The resulting data were analyzed as described by Turley *et al.* (2007). Briefly, the mean Apaf-1 expression and the standard deviation were calculated for each study. Differences in Apaf-1 expression between epileptic patient brain and glioblastoma were displayed by using a standard box-and-whisker plot. For data from the other two studies (Freije *et al.,* 2004; Phillips *et al.,* 2006), we calculated the standard difference in means of Apaf-1 mRNA expression between grade III and grade IV astrocytomas by using the statistical program Comprehensive Metaanalysis (Biostat). Microarray data from CD15+/- mouse medulloblastoma cell mRNA was provided by Rob Wechsler-Reya (Duke University), and is available through the NCBI Gene Expression Omnibus site (http://www.ncbi.nLm.nih.gov/geo/) under the accession number GSE12430.

## 2.6 Chromatin immunoprecipitation

ChIP was performed by using the EpiQuik Tissue Chromatin Immunoprecipitation Kit (Epigentek P-2003). DNA was purified by using a QIAquick PCR purification kit (Qiagen), and PCR was performed by using iQ Supermix (BioRad) and the Apaf-1 primers utilized for RT-PCR. Approximately 2% of the input chromatin and 7% of the ChIP samples were used as template in each case. Amplicons were visualized with ethidium bromide in 2.5% agrarose gels.

## 2.7 Cloning, protein expression and mRNA synthesis

Cytochrome *c*-eGFP (pCyt *c*-EGFP-N1)and eGFP-cytochrome *c* (pEGFP-C1-cyt *c*) were gifts from Doug Greene (St. Jude Children's Research Hospital, Memphis TN). Yeast heme lyase in pcDNA3.1 was a generous gift from Mohanish Deshmukh (University of North Carolina Chapel Hill, NC), and was cloned into the pmCherry-C1 vector (Clontech).

Cloning, expression and purification of Mos and Emi2 (aa 489-651) T545,551A were as described (Wu, Q *et al.,* 2007). *Xenopus* Bok was cloned from an EST clone of the NIBB *Xenopus laevis* project. Initially xBok cDNA was amplified utilizing an EcoRI forward primer (GGA ATT CTA ATG GAG ATG CTA AGA CGA TC), and an XhoI reverse primer (GCT CGA GTT ACC GCT CAC GGA GGA C). For mRNA production, xBok was cloned into the pSP64T vector to contain an N-terminal FLAG tag. For mRNA

synthesis, constructs were digested with SmaI or HindIII, and mRNAs produced using the mMessage mMachine RNA kit (Ambion).

Human Apaf-1 in pFastBac was a generous gift from Xiaodong Wang (University of Texas Southwestern), and was utilized to produce human Apaf-1 protein from a baculovirus expression system. The Apaf-1 expression plasmid was transformed into DH10Bac *Escherichia coli* cells (Invitrogen, Carlsbad, CA), according to the manufacture's manual. The recombinant baculovirus was then produced in accordance with the Invitrogen Bac-To-Bac protocol. In brief, Sf9 cells were infected with the baculovirus for 24 hours and then recombinant protein was purified as previously described (Zhou et al., 1999).

## 2.8 Intermolecular crosslinking and mass spectrometry

### 2.8.1 Covalent crosslinking and gel analysis of crosslinked proteins

Crosslinking of horse cytochrome *c* (Sigma) and recombinant human Apaf-1 with $BS^3$ $d_0/d_4$ (21590 and 21595, Pierce) was performed according to the manufacturer's suggested protocol (Pierce). Briefly, proteins were mixed in equal molar amounts (5 μg Apaf-1 and 0.6 μg cytochrome *c)* in 20 mM HEPES buffer, pH 7.5. The $BS^3$ $d_0/d_4$ was prepared in a 1:1 ratio and added to the protein solution at either 50 μM or 250 μM. Control solutions were prepared with adding dimethylsulfoxide (DMSO) (Thermo Scientific) in lieu of the crosslinking reagent solution. For initial crosslinking optimization, aliquots of the solution were analyzed at various time points. For immunoblot and mass spectrometry analysis, the reactions were allowed to proceed for

30 minutes. Reactions were terminated by adding $NH_4HCO_3$ to a final concentration of 20 mM. SDS-PAGE sample buffer was added to all samples and they were resolved by SDS-PAGE for either immunoblot analysis or silver staining. Silver stained bands of interest were excised from the gel and transferred to a clean eppendorf. Gel bands were de-stained for 10 minutes in a 1:1 mixture of 100 mM sodium thiosulfate and 30 mM potassium ferricyanide. De-stained bands were washed 3 times with water for 15 minutes per wash and submitted to the Duke Proteomics Facility for mass spectrometry analysis.

### 2.8.2 Sample preparation (performed by the Duke Proteomics Facility)

#### 2.8.2.1 In-gel digestion

Excised gel bands were reduced for 30 minutes at room temperature using 10 mM dithiolthreitol in 50 mM ammonium bicarbonate, pH 8.0. Samples were then alkylated for 30 minutes at room temperature with 20 mM iodoacetamine in 50 mM ammonium bicarbonate, pH 8.0 prior to in-gel proteolytic digestion with 50 ng of sequencing grade modified trypsin (Promega) at 37°C for 18 hours. Peptides were extracted into 200uL 50% acetonitrile, 1% formic acid with 10 minutes of bath sonication, brought to dryness using a vacuum centrifuge and resuspended in 20 uL 2% acetonitrile, 0.1% TFA.

#### 2.8.2.2 In-solution digestion

Rapigest acid labile surfactant (Waters Corp) was added to samples to a final concentration of 0.1%. Samples were reduced in 10 mM dithiolthreitol for 15 minutes at 70°C followed by alkylation with 20 mM iodoacetamide for 30 minutes at room

temperature followed by proteolytic digestion with trypsin at a ratio of 50:1 (protein:enzyme, w/w) for 18 hours at 37°C . Digested samples were brought up to 1% TFA and incubated at 60C for 2 hours to hydrolyze Rapigest surfactant.

### 2.8.3 LC-MS/MS (performed by the Duke Proteomics Facility)

Approximately 50% of the total peptide extracted from the gel slices were loaded onto a Waters NanoAcquity HPLC equiped with a 180 um x 2 cm Symmetry guard column (Waters Corp.) coupled in-line with a 75 um x 15 cm BEH130 UPLC analytical column (Waters Corp.) packed with 1.7 um C18 reversed-phase particles. Peptides were eluted using a linear gradient from 5% acetonitrile/0.1% formic acid to 40% acetonitrile/0.1% formic acid over 60 minutes at a flow rate of 300 nL/min. Analytical column temperature was maintained at 55°C throughout analysis. The NanoAcquity system was coupled to a Waters Synapt HDMS mass spectrometer or a Thermo LTQ-Orbitrap XL mass spectrometer through an electrospray ionization interface. Ionization was accomplished by applying 4.5 kV (Waters Synapt HDMS) or 1.9 kV (Thermo LTQ-Orbitrap XL) to a PicoTip Emitter (New Objective) with a 10 um spray tip.

The Waters Synapt HDMS mass spectrometer was operated in V-mode with 0.95 s precursor MS scans from m/z 50-1990. Up to 8 sequential product ion MS/MS scans from m/z 50-1990 were acquired in a data-dependent mode for all precursor ions which were at least 2+ charged and had a threshold of 20 counts/s. MS/MS fragmentation was accomplished using collision-induced dissociation CID with He gas in the quadrupole region of the instrument. Each product ion selected for MS/MS fragmentation was

subsequently placed on an exclusion list for 200 seconds to increase dynamic range. To improve mass accuracy, a precursor MS scan from m/z 50-1990 of 200fmol/ul Glu-Fib in 50% acetonitrile, 0.1% formic acid was acquired every 30 seconds using a lockspray modified interface.

The Thermo LTQ-Orbitrap XL mass spectrometer was operated in full FT-FT mode with precursor scans from m/z 400-2000 in the orbitrap at a resolution of 30,000 and 3 MS/MS scans in the orbitrap at a resolution of 7500 for precursor ions which were 2+ charged and above ions above a threshold of 10000 counts. MS/MS fragmentation was accomplished using collision-induced dissociation (CID) with Argon gas with a CID setting of 35%. Each product ion selected for MS/MS fragmentation was subsequently placed on an exclusion list for 60 seconds to increase dynamic range.

### 2.8.4 MS data analysis (performed in collaboration with the Duke Proteomics Facility)

Data generated from both Waters Synapt HDMS and Thermo LTQ-Orbitrap were processed using Mascot Distiller and were then searched using the Mascot database searching algorithim against a SwissProt FASTA database containing all mammalian entries. A static mass modification of +57.0 Da was applied to all cysteines, corresponding to carbamidomethylation during alkylation. Dynamic mass modifications of +16.0 Da on methionine corresponding to oxidation, +266.0 Da on lysine corresponding to $BS^3$ $d_0$ modification with a water loss, +270.0 Da on lysine corresponding to $BS^3$ $d_4$ modification with a water loss, +284.0 Da on lysine corresponding to $BS^3$ $d_0$ modification with a free carboxylic acid end, and +288.0 Da on

lysine corresponding to $BS^3$ $d_4$ modification with a free carboxylic acid end. Precursor scan tolerance were 20 ppm for data acquired on the Waters Synapt HDMS and 10 ppm for data acquired on the Thermo LTQ-Orbitrap XL. Product ion scans tolerances were 0.1 Da for data acquired on the Waters Synapt HDMS and 0.02 Da for data acquired on the Thermo LTQ-Orbitrap XL. Searches were set to onLy include fully tryptic peptides (N- and C-terminal) with up to 2 missed cleavages per peptide.

For samples subjected to both heavy ($BS^3$ $d_4$) and light ($BS^3$ $d_0$) crosslinking reagents, data was imported to Rosetta Elucidator (Rosetta Biosoftware) and subjected to a labeled-pair workflow. Briefly, the data was converted to a three-dimensional image (m/z, retention time, and intensity) and pairs of "features" (i.e. signals corresponding to peptides) whose M+H were within 4.025 Da (+/- 15 ppm) and whose retention time was within 12 seconds, were placed in "preliminary" identification table. Preliminary identifications were manually verified for the presence of both heavy and light isotopes, with significant signal-to-noise, and in ratios under 1:2.

#### 2.8.4.1 Dead-end crosslinked products

To identify dead-end crosslinked products in which one end of the crosslinking reagent reacted with a lysine while the other end was hydrolyzed by water, Mascot results were searched for peptides containing a mass modification of +284.0 Da ($BS^3$ $d_0$) or +288 Da ($BS^3$ $d_4$). These spectra were manually verified to ensure adequate sequence coverage and the presence of an unmodified C-terminal Lysine residue, if applicable (i.e. trypsin cannot cleave C-terminal to a $BS^3$ modified Lysine).

#### 2.8.4.2 Intrapeptide crosslinked products

To initially identify intrapeptide crosslinked products, Mascot results were searched for a peptide containing two non-C-terminal lysine residues, in which one of the lysines contained a mass modification of +266.0 Da ($BS^3$ $d_0$) or +270.0 Da ($BS^3$ $d_4$). To further validate the identification, the labeled-pair was verified for the presence of both light and heavy versions, which co-eluted within 12 seconds, and were present in a ratio under 1:2 from the Rosetta Elucidator labeled-pair results. To identify intrapeptide crosslinks not initially identified in Mascot, a theoretical list of all possible crosslinked products was generated using ProteinXXX. These results (output as M+H values) were blasted against a table of all identified M+H values recorded by Rosetta Elucidator within an error of 30 ppm (Waters Synapt HDMS) or 20 ppm (Thermo LTQ-Orbitrap XL). Potential hits were verified for the presence of both light and heavy versions, which co-eluted within 12 seconds, and were present in a ratio under 1:2.

#### 2.8.4.3 Interpeptide crosslinked products

Since no database searching algorithims are able to interpret interpeptide crosslinked products, identifications were made using accurate mass, ratio data of light and heavy $BS^3$ labeled peptides (if available), and retention-time co-elution. Briefly, a list of m/z's corresponding crosslinked peptides were generated using the program ProteinXXX (a standalone crosslinking application within the GPMAW suite of programs from Lighthouse Data, Denmark). The following constraints were applied to

peak list generation: crosslinking reagent targeting Lysine residues, up to four missed cleavages, and an upper mass limit of 12000 Da. Only interpeptide crosslinks were considered. M/z's of all precursor ions selected for MS/MS analysis were searched against the theoretical list generated by ProteinXXX using a match tolerance of 20ppm for data acquired on the Waters Synapt HDMS and 10ppm for data acquired on the LTQ Orbitrap XL. Potential matches were validated by visually inspecting the raw data for adequate signal-to-noise, appropriate heavy to light isotope ratios (if applicable), and the presence of at least 2 product ions for each of the peptides involved in the crosslink.

## 2.9 Cell imaging

Imaging of transfected mammalian cells was performed at the Duke Light Microscopy Core Facility using either an Olympus IX-70 inverted microscope with fluorescence capability or a Zeiss Axio Observer Z1 motorized microscope with fluorescence capability and images were captured using a Hamamatsu Orca-ER monochrome cooled-CCD camera or a Coolsnap EM high resolution CCD camera, respectively. Images were analyzed using Metamorph 7.5 software.

Infrared fluorescence in oocytes was imaged using the Odyssey Infrared Imaging system (LI-COR). Three to five oocytes per well in a black-walled 96-well plate (Corning Costar) were scanned at a focus offset of 3.0 mm, resolution of 84 um, and intensity settings of 5 in the 700 channel and 0.5 in the 800 channel. Embryos were imaged as above except at a resolution of 21 μm and intensity settings of either 5 or 2.5 in both channels. Analysis of fluorescence (including quantitation) was performed with the

Odyssey software, v2.1 (LI-COR). Reflected light images of oocytes and embryos were captured using a Stemi SV6 Stereomicroscope (Zeiss) with an attached PowerShot A620 digital camera (Canon). Alternatively, a WolfVision Professional Visualizer was used to capture reflected light images of some of the embryos.

## 2.10 *Xenopus* oocyte isolation, maturation and lysate preparation

Stage VI oocytes were prepared from ovaries manually excised from frogs primed with PMSG (Calbiochem), digested with 2.8 U of Liberase (Roche) in OR-2 buffer (82.5 mM NaCl, 2 mM KCl, 1 mM $MgCl_2$, 5 mM HEPES [pH 7.5]) for 1.5 hr at room temperature, washed with OR-2 and stored in OR-2 + 10% fetal bovine serum (Gibco) + 0.2% gentamicin (Invitrogen) at 18°C. To induce maturation, oocytes were treated with 200 μM progesterone (Sigma) in OR-2. Oocyte lysate was made by crushing oocytes in oocyte lysis buffer (20 mM HEPES pH 7.5, 20 mM β-glycerophosphate, 15 mM $MgCl_2$, 20 mM EGTA, and 1 mM PMSF) followed by centrifugation to remove insoluble material. For Western blot analysis, three oocyte equivalents were loaded per lane. For analysis of caspase activity, the lysate was diluted 10-fold with PBS, and incubated at 37°C in the presence of the colorimetric substrate Ac-DEVD-pNA (Biomol). Absorbance was then measured using a Bio-Rad 680 microplate reader at 405 nm.

## 2.11 *Xenopus in vitro* fertilization

Testes were manually excised and used to fertilize fresh eggs laid from PMSG-primed frogs injected human chorionic gonadotropin (Sigma). Fertilized eggs were

washed with 0.1x MMR buffer (10x MMR: 1 M NaCl, 20 mM KCl, 10 mM MgSO4, 25 mM $CaCl_2$, 5 mM HEPES pH 7.8, 0.8 mM EDTA), and then de-jellied following cortical rotation using 2% cysteine (Sigma).

## 2.12 Microinjection of *Xenopus* oocytes and embryos

Oocytes were typically injected with 40 nL solution contained in a capillary needle using a PV830 pneumatic picopump (WPI). If multiple rounds of injection were performed in a single cell, the injection volume was modified such that 40 nL was injected in total. Cytosolic volume of an oocyte was taken to be 1 mL, and used to calculate the final intracellular concentration of injected reagents. Microinjected reagents include: IRDye® 800CW/QC-1 CSP-3 substrate (LI-COR) at 200-400 nM/oocyte, cytochrome *c* from equine heart or from *Saccharomyces cerevisiae* (Sigma), caspase-8-cleaved Bid (tBid) (Calbiochem)), z-VAD-fmk (Biomol), Smac (gift from Mohanish Deshmukh, University of North Carolina) used at 280 nM/oocyte, dextran AlexaFluor680 3000 MW and dextran AlexaFluor 10,000 MW (Invitrogen/Molecular Probes). For mRNAs, 20 ng encoding β-globin or FLAG-xBok were injected per oocyte. Embryos were kept in a solution of 0.3x MMR buffer containing 4% Ficoll 400 (w/v) for microinjection; one blastomere was assumed to have a volume of 0.5 mL, and they were injected with 8 nL solution.

## 2.13 Protein binding assays

Cytochrome *c* peptides were synthesized by Bruce Kaplan at the Beckman Research Institute of the City of Hope (Duarte, CA). Each peptide was synthesized with an amino-terminal biotin and a carboxy-terminal amide and HPLC-purified. 1-2 μg of recombinant human Apaf-1 was incubated with either soluble cytochrome *c* peptides or cytochrome *c* peptides pre-bound to streptavidin-sepharose (GE Healthcare) for 30 minutes at room temperature and then retrieved on the streptavidin-sepharose. Alternatively, soluble cytochrome *c* peptides were incubated with his-tagged Apaf-1 for 30 minutes at room temperature and then retrieved on Ni-NTA agarose (Qiagen). Samples were washed, eluted with SDS-PAGE sample buffer and resolved by SDS-PAGE for immunoblot analysis.

# 3. Differential Apaf-1 levels allow cytochrome *c* to induce apoptosis in brain tumors but not in normal neural tissues

(This chapter is reproduced from: Proc Natl Acad Sci USA. 2007 Dec 26; 104(52): 20820-20825.)

## 3.1 Introduction

Primary brain tumors arise from cells intrinsic to the brain and intracranial cavity. Although these tumors account for only a small percentage of cancers, they cause a disproportionate share of cancer-related morbidity and mortality (Newton, 1994). Despite resection in conjunction with chemoradiation, the 5-year survival rate for glioblastoma, the most common histologic subtype, remains only 3% (CBTR, 2002). Although survival rates for childhood medulloblastoma are better, long-term neurological deficits secondary to radiation therapy remains a significant problem (Rutkowski and Kaufman, 2004). Therefore, therapeutic strategies that selectively induce apoptosis in brain tumors while sparing surrounding neural tissue could offer significant clinical promise.

Apoptosis is a form of programmed cell death required for proper embryonic development and tissue homeostasis. Aberrant signaling allows malignant cells to evade apoptosis, thus fostering tumor progression (Hanahan and Weinberg, 2000). In the intrinsic pathway of apoptosis, death-inducing signals converge upon the mitochondria, causing release of cytochrome *c*. Cytosolic cytochrome *c* binds to Apaf-1, leading to recruitment of procaspase-9 and formation of the apoptosome. Apoptosome-mediated

activation of caspase-9 activates executioner caspase-3 and caspase-7, which promote cell death (Danial and Korsmeyer, 2004).

Cytosolic cytochrome *c* is sufficient to induce apoptosis in many dividing cells, including fibroblasts, HEK293, and HeLa (Liu *et al.,* 1996; Li *et al.,* 1997). In contrast, differentiated sympathetic neurons are highly resistant to apoptosis induced by cytochrome *c* (Wright *et al.,* 2004). This differential susceptibility to cytochrome *c*-induced death in cycling cells and neurons led us to hypothesize that activating apoptosis with cytochrome *c* might selectively induce death in dividing brain tumor cells while sparing neurons in the brain parenchyma. However, this idea was tempered by the fact that various tumors have been shown to differ markedly in their sensitivity to cytochrome *c*. Although ovarian cancers and melanomas appear resistant to cytochrome *c*-induced apoptosis (Wolf *et al.,* 2001; Soengas *et al.,* 2001), breast cancers are hypersensitive to cytochrome *c* (Schafer *et al.,* 2006).

We show here that, despite the remarkable resistance of mature neurons and brain tissues to cytochrome *c*, both high-grade astrocytoma and medulloblastoma are susceptible to cytochrome *c*-mediated apoptosis. Importantly, although normal brain exhibits nearly undetectable levels of Apaf-1, we demonstrate that brain tumors express high levels of Apaf-1 through transcriptional induction of Apaf-1 mRNA. These results identify direct activation of the apoptosome as a potential therapeutic strategy for brain tumors that would eliminate cancer cells while sparing surrounding neural tissue.

## 3.2 Results

### 3.2.1 Multiple types of neurons become resistant to cytochrome *c* upon maturation

We recently reported that decreased Apaf-1-dependent apoptosome activity, which accompanies neuronal differentiation, renders sympathetic neurons resistant to cytochrome *c*-mediated apoptosis (Wright *et al.,* 2004). To determine whether the development of cytochrome *c* resistance is seen in other neurons, including those in the CNS, we examined neurons from the dorsal root ganglion (DRG), cerebellum, and cortex. Because these neurons mature at different times, we chose two time points for each neuronal type, corresponding to early and late stages of differentiation. Sensory neurons from the DRG were isolated from embryonic day 15 (E15) and postnatal day 2 (P2) mice. Microinjection of cytochrome *c* into E15 DRG neurons after 1 day in culture (E16 equivalent) induced extensive death within 3 hours. In contrast, P2 DRG neurons injected after 1 day in culture (P3 equivalent) were remarkably resistant to cytochrome *c* (Figure 3.1A).

To examine the sensitivity of cerebellar granule neurons (CGN) and cortical neurons to cytochrome *c*, we used a cell-free assay, as the small size of these neurons is unsuitable for microinjection. In this assay, addition of cytochrome *c* to cytosolic lysates (extracts) prepared from either primary tissue or cultured cells can recapitulate caspase-dependent apoptosis (Liu *et al.,* 1996). Although cytochrome *c* induced robust caspase activation in extracts of P5 CGN maintained 1 day in culture (P6 equivalent), no significant caspase activation was detected in extracts of P5 CGN maintained 14 days in

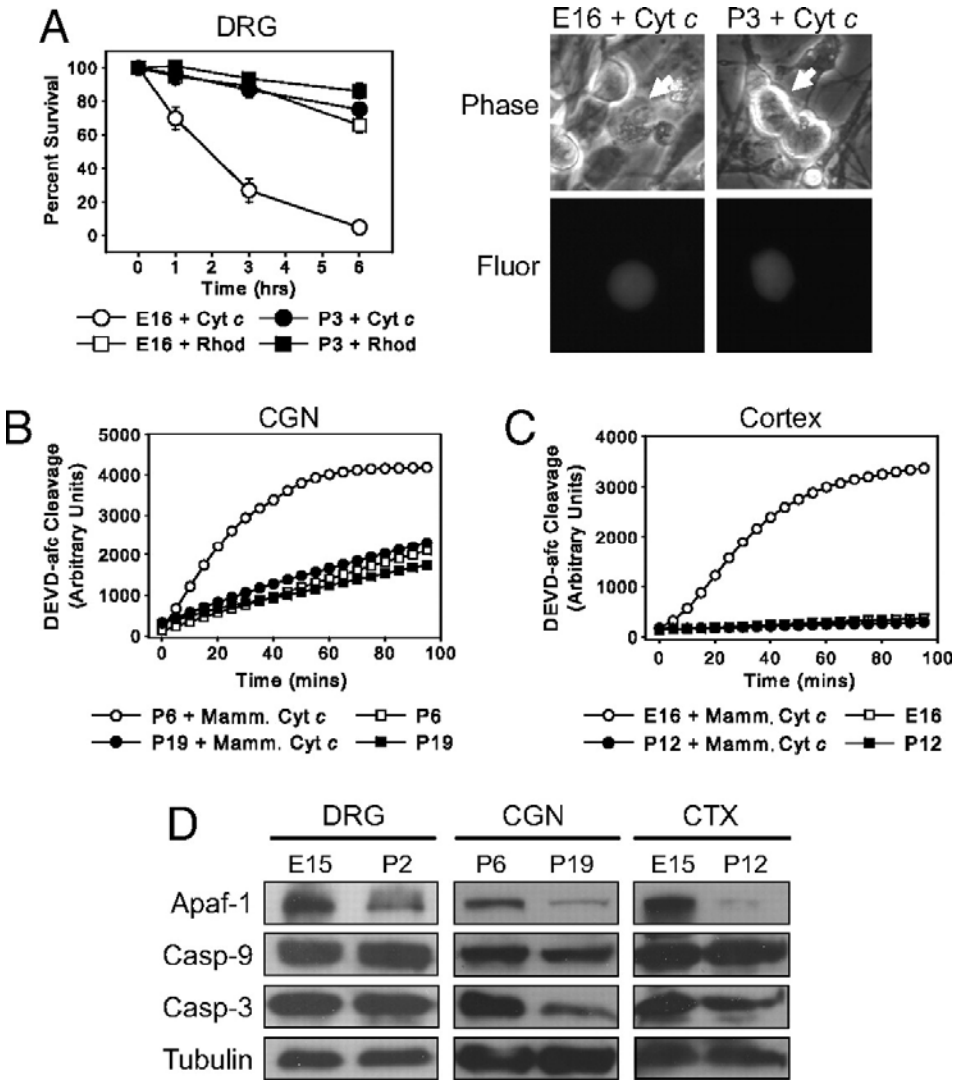


**Figure 3.1: Cytochrome *c* is incapable of activating caspases and inducing apoptosis in mature neurons**

**Figure 3.1**: **A**, E16 and P3 neurons from DRG were microinjected with 10 µg/µl cytochrome *c* and rhodamine dextran (for visualization). Data shown are neuronal survival at times after injection and are mean ± SEM of three independent experiments. In corresponding images, arrows indicate microinjected cells (Magnification: ×400). **B** and **C**, Cytosolic lysates from CGN, **B**, and whole cortex (CTX), **C,** at early and late stages of neuronal maturation were assessed for caspase activation after the addition of 10 µM cytochrome *c*. Caspase activation was monitored via cleavage of DEVD-afc. Yeast cytochrome *c*, which cannot bind Apaf-1 (Wright *et al.,* 2004), was added to extracts as a negative control. **D**, Immunoblotting shows protein levels of Apaf-1, caspase-9, and caspase-3 in DRG, CGN, and whole cortex at early and late stages of neuronal differentiation.

culture (P19 equivalent) (Figure 3.1B). Next, we examined whether cortical extracts exhibited a similar resistance to cytochrome *c* with maturation. Addition of cytochrome *c* was sufficient to activate caspases in cortical extracts from E16 but not P12 mice (Figure 3.1C). Together, these results show that our previous observations in sympathetic neurons, in which cytochrome *c* sensitivity is dramatically decreased upon maturation, can be generalized to multiple neuronal cell types, including those of the CNS.

To determine whether the resistance to cytochrome *c* upon neuronal maturation correlated with Apaf-1 down-regulation, we examined components of the apoptotic machinery in early and late stages of neuronal differentiation. Immunoblot analysis confirmed that, in all neuronal cell types examined, Apaf-1 levels were high in early-stage neurons but markedly decreased with maturation (Figure 3.1D).

### 3.2.2 Cytochrome *c* induces robust caspase activation in brain tumor cells

Unlike in neurons, in many dividing cells the introduction of cytosolic cytochrome *c* induces apoptosis. This difference prompted us to investigate whether brain tumors would be sensitive to cytochrome *c* while surrounding neural tissue would be resistant. We first confirmed that components of the apoptotic machinery were present in extracts from neuroblastoma (SH-SY5Y), medulloblastoma (UW228, D341MED, MCD1), and glioblastoma (MGR3, MGR1, D54MG, D247MG, H392) cell lines (Figure 3.2A). Next, we found that cytochrome *c* elicited robust caspase activation in all of the brain tumor cell line-derived extracts, but not in extracts of mouse cortex or cerebellum (Figure 3.2B).

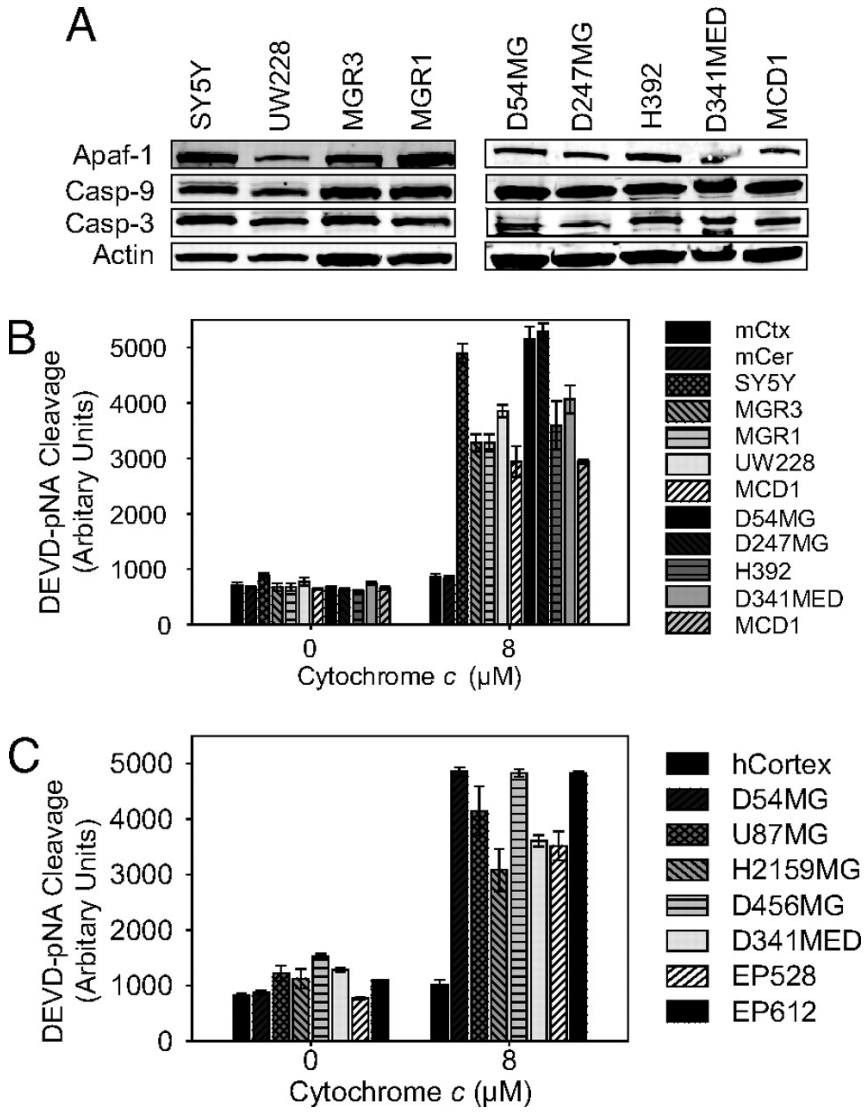


**Figure 3.2: Brain cancer cells are hypersensitive to cytochrome *c*-induced apoptosis.**

**Figure 3.2:** **A**, Protein levels of Apaf-1, caspase-9, and caspase-3 were examined in human brain tumor cell lines by immunoblotting. SY5Y, neuroblastoma; UW228, D341MED, and MCD1, medulloblastoma; MGR3, MGR1, D54MG, D247MG, and H392, glioblastoma. **B**, Extracts from human brain tumor cell lines or mouse neural tissue were supplemented with 8 μM cytochrome *c*. Caspase activation was monitored via cleavage of Ac-DEVD-pNA. Data shown are mean ± SEM of three independent experiments. mCtx, mouse cortex; mCer, mouse cerebellum. **C**, Extracts from human non-neoplastic temporal cortex and xenograft tumors were assessed for their ability to activate caspases as in **B**. U87MG and D54MG, adult glioma; H2159MG and D456MG, pediatric glioma; D341MED, medulloblastoma; EP528 and EP612, ependymoma.

As an alternative to working with cultured cells, we examined whether human brain tumor cells grown subcutaneously in immunocompromised mice also exhibited cytochrome *c* sensitivity. Xenograft extracts were prepared from human medulloblastoma (D341MED), human glioma from adults (D54MG, U87MG) and children (H2159MG, D456MG) and ependymoma (EP528, EP612). Consistent with the cultured cell data, addition of cytochrome *c* to the xenograft extracts elicited marked caspase activation. In contrast, extract from adult human cortex did not induce caspase activation upon cytochrome *c* addition (Figure 3.2C).

### 3.2.3 Endogenous mouse models of high-grade astrocytoma and medulloblastoma demonstrate selective cytochrome *c*-induced caspase activation in tumor tissue

To extend relevance of these results to brain tumor models where spontaneously forming lesions within the brain more accurately mimic human disease, we examined whether cytochrome *c* could induce caspase activation in tumors from both high-grade astrocytoma and medulloblastoma mouse models. These models enabled us to compare tumor tissue with surrounding neural tissue from the same animal. In the high-grade astrocytoma model, mice have been engineered to achieve somatic pRb inactivation and constitutive K-ras$^{G12D}$ activation with or without PTEN deletion, specifically in adult astrocytes. Tumors from these mice have been histopathologically characterized as predominantly anaplastic astrocytoma (WHO grade III) or glioblastoma (WHO grade IV) (Q.Z., C. R. Miller, C. Yin, C. Y. Yang, E. Bullitt, K. D. McCarthy, T. Jacks, D. N. Louis, and T.V.D., unpublished data). Extracts from these tumors exhibited strong

caspase activation upon addition of cytochrome *c*, whereas extracts prepared from adjacent neural tissue did not (Figure 3.3A). Next, we examined the ability of cytochrome *c* to activate caspases in tumors from *Patched* heterozygous mice that develop medulloblastoma (Oliver *et al.,* 2005; Goodrich *et al.,* 1997). Caspases were activated in medulloblastoma extracts after cytochrome *c* addition, whereas no caspase activation was detected in extracts of adjacent cerebellar tissue (Figure 3.3B). Consistent with apoptosome-mediated apoptosis, caspase-9 processing was observed in both high-grade astrocytoma and medulloblastoma extracts supplemented with cytochrome *c*, but not in extracts prepared from adjacent neural tissue (Figure 3.3C). These data illustrate the potential of cytochrome *c* to activate caspases selectively in brain tumors *in vivo*.

### 3.2.4 Apaf-1 expression levels determine the differential sensitivity to cytochrome *c* in normal and malignant brain tissue

In considering the molecular basis for the differential cytochrome *c* sensitivity of brain tumor and normal brain tissue, we reflected on our earlier observations that cytochrome *c* resistance in differentiated sympathetic neurons was caused by low Apaf-1 levels (Wright *et al.,* 2004). Low Apaf-1 expression was also observed in mature cerebellar and cortical neurons (Figure 3.1D) (Yakovlev *et al.,* 2001). In contrast, Apaf-1 expression was clearly evident in the brain cancer cell lines (Figure 3.2A). Importantly, Apaf-1 immunoblotting revealed markedly higher Apaf-1 protein levels in both high-grade astrocytoma and medulloblastoma tumors compared with adjacent neural tissues (Figure 3.4A). A similar difference was observed in human high-grade gliomas compared with normal human cortex (Figure 3.4D).

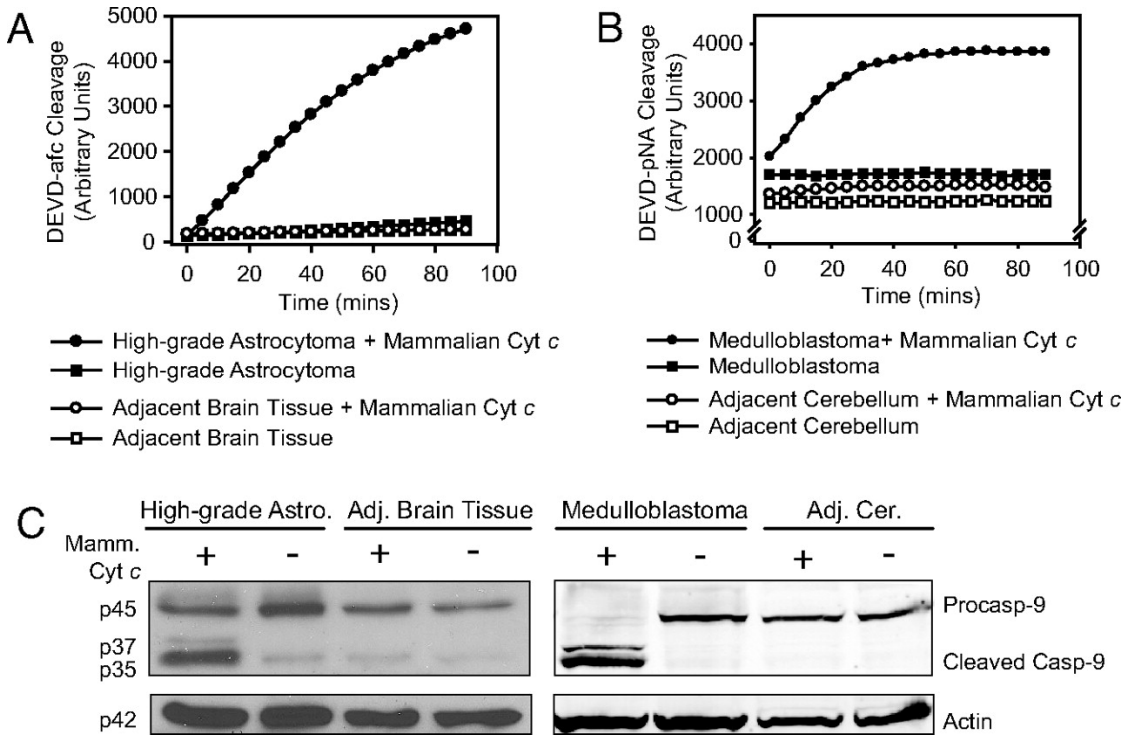


**Figure 3.3: Brain tumors from mouse models of high-grade astrocytoma and medulloblastoma display sensitivity to cytochrome *c*-mediated apoptosis.**

**Figure 3.3:** **A** and **B**, Extracts prepared from tumor tissues and adjacent neural tissues of two brain tumor mouse models, high-grade astrocytoma, **A**, and medulloblastoma, **B**, were supplemented with cytochrome *c* and caspase activation was monitored. **C,** Immunoblotting shows caspase-9 cleavage in extracts treated in *A* and *B*. Astro., astrocytoma; Adj. Cer., adjacent cerebellum.

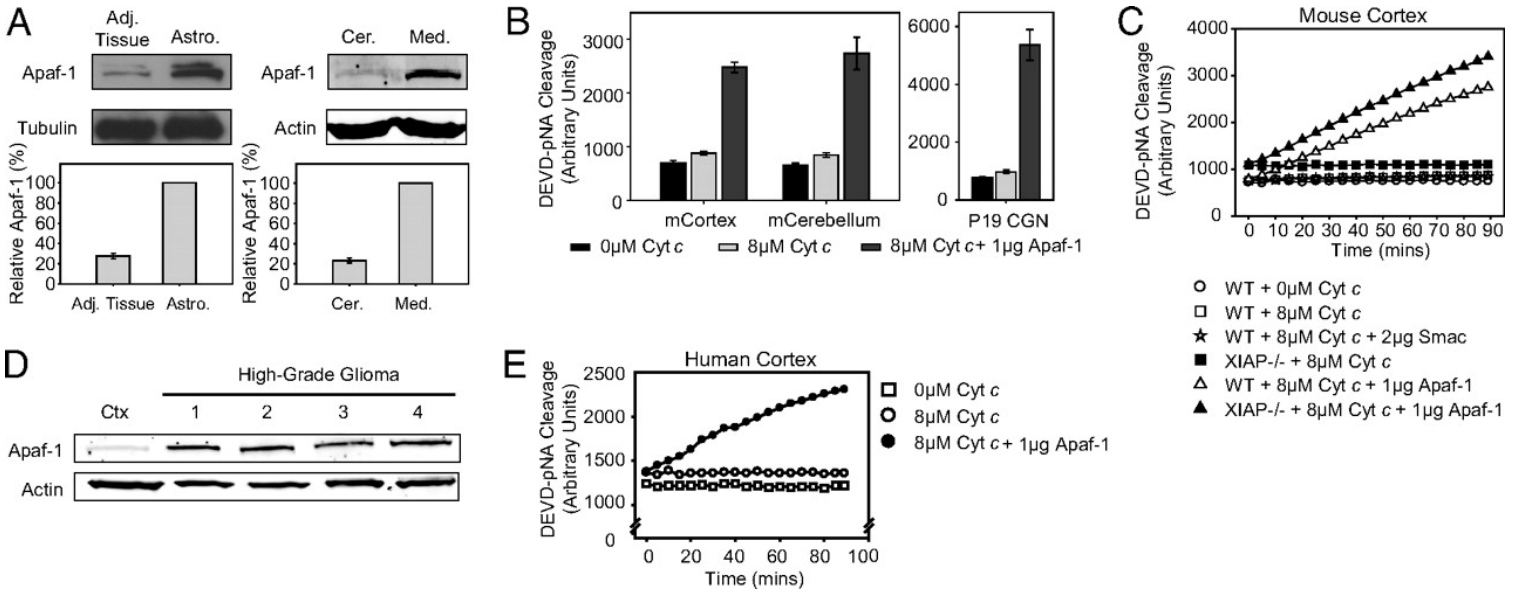




**Figure 3.4: A marked increase in Apaf-1 causes the increased sensitivity of brain tumor tissues to cytochrome *c***

**Figure 3.4: A**, Immunoblots demonstrating Apaf-1 protein levels in high-grade astrocytoma (Astro.) and medulloblastoma (Med.) relative to their respective adjacent neural tissue (Cer.: cerebellum). Quantitation of Apaf-1 (mean ± SEM of three independent experiments) is shown. **B**, Caspase activation in extracts from mouse cortex, cerebellum, and P19 CGNs was assessed in the presence of no cytochrome *c*, 8 μM cytochrome *c*, or 8 μM cytochrome *c* along with 1 μg of recombinant Apaf-1. **C**, *In vitro* assay assessing caspase activation in mouse cortical extracts when IAPs were inactivated (by Smac addition) or when XIAP was genetically removed ($XIAP^{-/-}$). **D**, Immunoblots showing relative Apaf-1 levels in human cortex (Ctx) versus four samples of high-grade gliomas. **E**, Caspase activation assay on human cortical extracts in the presence of no cytochrome *c*, 8 μM cytochrome *c*, or 8 μM cytochrome *c* along with 1 μg of recombinant Apaf-1.

To investigate whether differences in Apaf-1 expression were responsible for the differential sensitivity to cytochrome *c*, we added recombinant Apaf-1 protein to extracts prepared from late-stage CGNs, adult mouse cortex and cerebellum. Although no caspase activation was observed with cytochrome *c* alone, the addition of Apaf-1 and cytochrome *c* was sufficient to induce caspase activation (Figure 3.4B). Likewise, human cortical extracts showed caspase activation with cytochrome *c* and Apaf-1 but not with cytochrome *c* alone (Figure 3.4E).

We wanted to determine whether the low levels of Apaf-1 were sufficient to activate caspases in the mature brain if caspase inhibition by IAPs was relieved. Addition of Smac, an IAP inhibitor, to extract from wild-type adult mouse cortex did not promote increased caspase activation (Figure 3.4C). Additionally, extracts of $XIAP^{-/-}$ and wild-type adult mouse cortex displayed similar resistance to cytochrome *c* (and similar sensitivity upon Apaf-1 addition) (Figure 3.4C). These data illustrate that the low levels of Apaf-1 in adult mouse cortex (Figure 3.4C) and cerebellum (data not shown) could not induce caspase activation even upon inactivation or removal of IAPs.

### 3.2.5 Levels of Apaf-1 in normal and malignant brain tissue are transcriptionally regulated

Having found that levels of Apaf-1 protein underlie the observed sensitivity to cytochrome *c*, we examined whether this difference could be traced back to transcriptional regulation. Quantitative RT-PCR revealed that Apaf-1 mRNA was significantly more abundant in medulloblastoma than in adjacent cerebellum (Figure 3.5A). Importantly, Apaf-1 mRNA levels in isolated medulloblastoma cells were

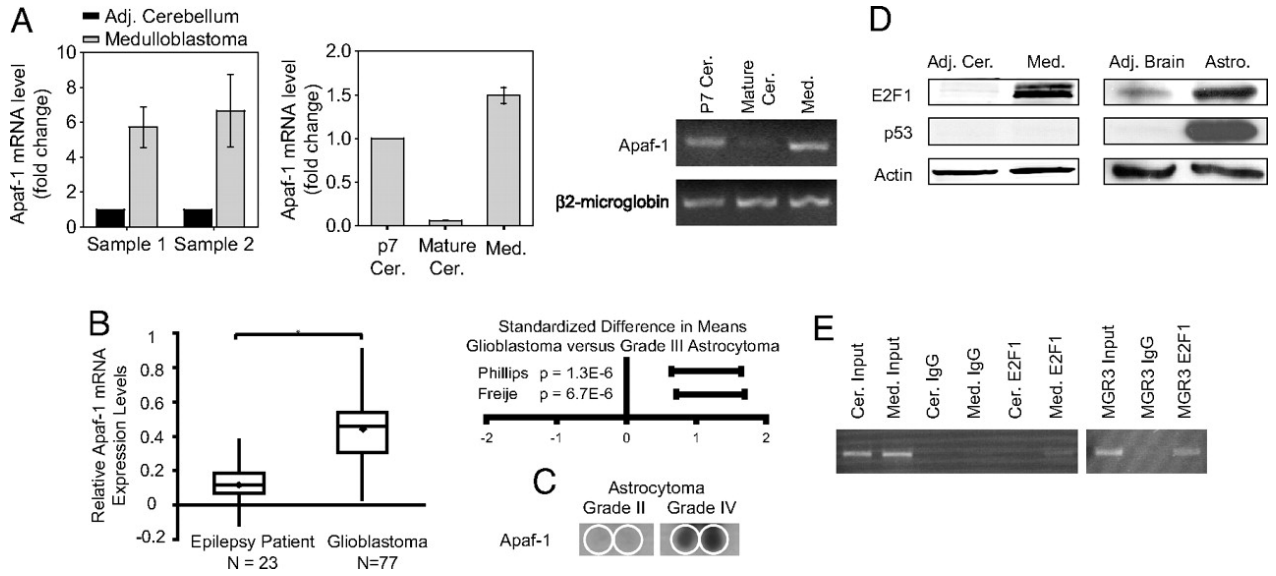


**Figure3.5: Transcriptional regulation of Apaf-1 mRNA levels contributed by E2F1.**



**Figure 3.5:** **A**, Quantitative analysis from RT-PCR shows the fold changes of Apaf-1 mRNA from dissected medulloblastoma and adjacent cerebellar tissues. Cells isolated from medulloblastoma tumor (Med.) were compared with normal P7 and adult cerebellar tissue. Data display the fold changes of Apaf-1 mRNA relative to normal P7 cerebellum, which is arbitrarily set as 1, and a corresponding agarose gel is shown for the PCR. **B**, Oncomine analysis of three independent gene profiling studies, with data from Sun *et al.* (Sun *et al.,* 2006) used to compare Apaf-1 mRNA expression levels in brain from epilepsy patients and in glioblastoma (*, $P < 0.0001$, independent two-tailed *t* test) and with data from Phillips *et al.* (2006) and Freije *et al.* (2004) analyzed by using the Comprehensive Metaanalysis software to plot the standard difference in means along with the 95% confidence intervals for Apaf-1 mRNA in grade III astrocytoma (corresponds to 0 on the *x* axis) compared with glioblastoma (positive values indicate an increase in Apaf-1 expression in glioblastoma versus grade III astrocytoma). **C**, A human tissue dot blot with duplicated samples demonstrates Apaf-1 levels in grade II astrocytoma and glioblastoma. Areas within the white circles represent sample location. **D**, Immunoblotting shows levels of E2F1 and p53 in brain tumor tissues versus adjacent brain tissue from mouse models of medulloblastoma and high-grade astrocytoma. **E**, ChIP assay demonstrates E2F1 asssociation with Apaf-1 promoter in mouse medulloblastoma tissue and in the human glioblastoma cell line MGR3.

comparable with developing P7 cerebellum, which is comprised of granule cell precursors; levels in both were significantly higher than in mature cerebellum (Figure 3.5A).

We then investigated Apaf-1 mRNA abundance in human astrocytomas by analyzing data from published gene profiling studies available in the Oncomine Gene Profiling Database. Analysis of data from Sun *et al.* (Sun *et al.,* 2006) demonstrated a statistically significant increase in Apaf-1 mRNA levels in glioblastoma compared with brain from epilepsy patients (Figure 3.5B). In two additional studies (Frieje *et al.,* 2004; Phillips *et al.,* 2006), relative Apaf-1 mRNA expression was increased in glioblastoma (grade IV astrocytoma) compared with grade III astrocytoma (Figure 3.5B). Similarly, a human tissue dot blot revealed a marked increase in Apaf-1 protein expression from a low-grade astrocytoma to a glioblastoma (Figure 3.5C). These data suggest not only that Apaf-1 expression is differentially regulated in normal versus tumor cells, but also that Apaf-1 expression increases with increasing tumor grade.

To elucidate the mechanism of Apaf-1 mRNA up-regulation in brain tumors, we examined the levels of E2F1 and p53, two previously identified transcriptional activators of Apaf-1 (Fortin *et al.,* 2001; Moroni *et al.,* 2002; Furukawa *et al.,* 2002). Levels of E2F1, but not p53, were consistently up-regulated in tumor tissues and low in adjacent brain tissues (Figure 3.5D). Additionally, many tumors, including two of the brain tumor lines we analyzed (MGR1 and MCD1), have mutations in p53 (Moore *et al.,* 1996; Francis Ali-Osman, personal communication). We therefore focused on determining

whether E2F1 was associated with the Apaf-1 promoter in brain tumors. Indeed, chromatin immunoprecipitation assays demonstrated that E2F1 specifically associates with the Apaf-1 promoter in mouse medulloblastoma tissue and the human glioblastoma cell line MGR3 (Figure 3.5E). In aggregate, the coordinated up-regulation of E2F1 and Apaf-1 in brain tumor cells, the previously reported ability of E2F1 to drive Apaf-1 transcription, and the ability of E2F1 to bind Apaf-1 promoter in brain tumors all suggest that E2F1 contributes to Apaf-1 expression in brain tumors.

## 3.3 Discussion

### 3.3.1 Low Apaf-1 levels offer protection from cytochrome *c*-dependent apoptosis in differentiated neurons and neural tissue

Resistance to cytochrome *c*-induced apoptosis in neuronally differentiated rat pheochromocytoma PC12 cells and differentiated sympathetic neurons has been reported (Wright *et al.,* 2004). In this study, we show that this striking development of resistance to cytochrome *c* during maturation is seen in multiple types of neurons, including those of the CNS. Specifically, we demonstrate this resistance in isolated late-stage neurons (Figure 3.1) and extracts from adult mouse cortex and cerebellum (Figure 3.2B) and human cortex (Figure 3.2C).

We have examined the mechanistic basis for this neuronal resistance to cytochrome *c*-mediated apoptosis and identified a link between Apaf-1 expression levels and the developmental state of a neuron. As neurons mature they dramatically decrease their levels of Apaf-1. Reconstitution with recombinant Apaf-1 protein in late-stage

neurons and mature neural tissue (Figure 3.4B and 3.4E) restores sensitivity to cytochrome *c*-induced apoptosis, thus providing strong evidence that down-regulation of Apaf-1 is the critical factor underlying the observed apoptotic resistance.

Similarly, other studies in rodent brain (Yakovlev *et al.,* 2001, Madden *et al.,* 2007) and mouse retina (Donovan and Cotter, 2002) have reported that neuronal maturation leads to inhibition of apoptosis, which parallels a decrease in Apaf-1 expression. We theorize that the reduction in Apaf-1 levels accompanying neuronal maturation may be a way of restricting unwanted apoptosis in differentiated neurons, in which long-term survival is necessary. Thus, up-regulation of Apaf-1 is predicted to be necessary and sufficient for these neurons to undergo cytochrome *c*-mediated apoptosis under pathological conditions. Indeed, during DNA damage-induced neuronal death (Fortin *et al.,* 2001, Vaughn and Deshmukh, 2007) and after fluid percussion-induced traumatic brain injury (Yakovlev *et al.,* 2001), Apaf-1 levels were markedly increased.

### 3.3.2 Brain tumor susceptibility to cytochrome *c*-induced apoptosis

Although inhibition of apoptosis is a hallmark of cancer, different cancers use distinct mechanisms to serve this purpose. In some instances, cancer cells evade apoptosis by preventing mitochondrial cytochrome *c* release in response to apoptotic stimuli. Other tumors display resistance to cytoplasmic cytochrome *c* because of defective apoptosome formation (Schafer and Kornbluth, 2006; Johnstone *et al.,* 2002). In contrast, we have previously shown that breast cancers are actually hypersensitive to

cytochrome *c*-induced apoptosis relative to normal mammary epithelial cells (Schafer *et al.,* 2006).

Given this unexpected phenomenon in breast cancer cells, we decided to investigate the sensitivity of primary brain tumors to cytochrome *c*-induced apoptosis. Using cultured human brain tumor cells (Figure 3.2B), human brain cancer-derived xenograft tumors (Figure 3.2C), and *in vivo* mouse models of high-grade astrocytoma and medulloblastoma (Figure 3.3), we found that, unlike their normal counterparts, brain tumors are susceptible to cytochrome *c*-induced apoptosis. Our mouse model data confirm this differential sensitivity between tumor tissue and adjacent neural tissue despite common genetic alterations in both tissues in the engineered mice. Although the sensitivity of breast and brain cancers to cytochrome *c* is superficially similar, the underlying mechanisms governing this sensitivity appear to be entirely distinct. Specifically, breast cancer cytochrome *c* hypersensitivity reflects overexpression of the apoptosome activator PHAPI, without alterations in levels of core apoptosome components (Schafer *et al.,* 2006). However, we report here that brain tumor sensitivity to cytochrome *c* is controlled through elevation of Apaf-1 expression relative to the extremely low levels present in mature neurons and neural tissue (Figure 3.4).

Moreover, this difference in Apaf-1 is transcriptionally regulated (Figure 3.5A). Of note, Oncomine analysis of publicly available microarray data suggests that Apaf-1 mRNA levels are not only higher in glioblastoma relative to normal brain, but also that Apaf-1 mRNA levels increase with increasing tumor grade (Figure 3.5B). It may be that,

because Apaf-1 transcription can be regulated by E2F1, increased Apaf-1 levels are an inexorable consequence of the increased E2F1 levels associated with (and in part responsible for) increased proliferation in tumor cells. According to this model, we would expect elevated Apaf-1 levels in poorly differentiated, highly proliferative brain tumors, which we did indeed observe in comparing glioblastoma (grade IV astrocytoma) with well differentiated grade II astrocytoma (Figure 3.5C). Furthermore, expression of E2F1 has recently been shown to be sufficient to cause brain tumors in mice (Olson *et al.,* 2007). Here, we show that brain tumors harbor high levels of E2F1, whereas levels in normal brain are quite low (Figure 3.5D). Furthermore, our ChIP studies suggest a physiological role for E2F1 in promoting Apaf-1 transcription in brain tumors (Figure 3.5E).

Although Apaf-1 can be regulated at the transcriptional level, it has been reported previously that Apaf-1 translation initiates via an internal ribosomal entry segment (IRES) (Coldwell *et al.,* 2000). One known factor in IRES-mediated Apaf-1 translation, nPTB, is expressed in neuronal cell lines (Mitchell *et al.,* 2003; Boutz *et al.,* 2007). Therefore, keeping Apaf-1 protein levels low in mature neurons may critically depend on keeping Apaf-1 mRNA levels low. It is attractive to speculate that neurons are poised to translate Apaf-1 should the message be produced, for example, under conditions of neuronal damage where reinstatement of Apaf-1-dependent apoptosis might be desirable.

### 3.3.3 Apoptosome activation as a therapeutic strategy

In aggregate, our data show that activating apoptosis with cytochrome *c* induces caspase activation in brain tumors but not in mature neural tissue. We have demonstrated that this differential sensitivity to cytochrome *c* is caused by a transcriptionally regulated difference in Apaf-1 levels. Although apoptotic resistance upstream of mitochondrial cytochrome *c* release likely renders brain tumors refractory to standard chemotherapeutics, our results show that they remain sensitive to apoptosis induced by cytochrome *c*.

Exploiting this vulnerability by directly activating the apoptosome with peptides or small molecules that mimic cytochrome *c* is therefore an attractive therapeutic approach for cancer cells that maintain functionally active apoptosome components. Importantly, our results from extracts of neural tissue, which are comprised of both neurons and glia, suggest that, like mature neurons, glia are also likely to be resistant to cytochrome *c*. Therefore, we believe that the development of a cytochrome *c* mimetic would be particularly beneficial in the context of brain tumors where it would selectively induce apoptosis in tumor cells while sparing adjacent brain tissue.

Because local delivery of a cytochrome *c* mimetic would be necessary to avoid potential systemic side effects, wafer implant technology would be one feasible approach. During brain tumor excision, gel wafers embedded with chemotherapeutics are inserted into the space previously occupied by tumor, resulting in slow release of drug precisely in the region of persisting malignant cells (Fleming and Saltzman, 2002). Ongoing studies

are focused on the development of a cytochrome *c* mimetic that could be delivered in such a manner to eliminate brain tumor cells without harming surrounding neural tissue.

# 4. The cytochrome *c*—Apaf-1 interaction and development of a cytochrome *c* mimetic

## 4.1 Introduction

Apoptotic signaling occurs along an intrinsic pathway when triggered by cellular insults such as chemotherapeutic-induced DNA damage (Norbury and Zhivotovsky, 2004). When the cell deems the damage irreparable, it engages pro-apoptotic Bcl-2 family members, which initiate apoptosis by triggering permeabilization of the mitochondrial outer membrane (Costanzo *et al.,* 2002). Mitochondrial permeabilization allows release of the electron transfer protein cytochrome *c* into the cytosol (Galluzzi *et al.,* 2007). Once cytosolic, cytochrome *c* interacts with an adaptor protein Apaf-1, thereby altering the conformation of Apaf-1, exposing a caspase recruitment domain (CARD) and triggering Apaf-1 dATP hydrolysis/exchange and oligomerization. The assembled heptameric structure containing cytochrome *c* and Apaf-1 is referred to as the apoptosome (Bao and Shi, 2007). The Apaf-1 CARD recruits an initiator caspase, procaspase-9, to the oligomerized complex in such a manner that results in dimerization-induced activation of caspase-9 (Li *et al.,* 1997; Shi, 2005). Apoptosome-bound caspase-9 activates downstream effector caspases, which are responsible for cleaving a host of target proteins, resulting in cell death (Earnshaw *et al.,* 1999).

Apaf-1 is a critical component within this pathway, serving to link the upstream signaling product (cytosolic cytochrome *c*) to the downstream executioners (active caspases). Interestingly, neuronal cells down-regulate Apaf-1 as they differentiate and

exit the cell cycle, rendering them resistant to cytochrome *c*-induced apoptosis (Wright *et al.,* 2004). Although the loss of Apaf-1 expression or activity has been reported in melanomas and ovarian cancers (Soengas *et al.,* 2001; Wolf *et al.,* 2001; Liu *et al.,* 2002), we previously demonstrated that brain cancer cells express Apaf-1 and are sensitive to cytochrome *c*-mediated caspase activation (Johnson *et al.,* 2007). Based on these findings, we hypothesize that a cytochrome *c* mimetic could be clinically beneficial in the treatment of brain cancers, specifically targeting malignant cells for apoptosis while sparing the surrounding brain parenchyma.

Treatment of brain tumors has been hampered by the difficulty of targeting chemotherapeutics across the protective blood-brain-barrier (BBB) (Lesniak and Brim, 2004). This challenge has not only led researchers to hone in on lipid soluble chemotherapeutics capable crossing the BBB, such as temozolomide (Agarwala and Kirkwood, 2000), but also to develop approaches for local drug delivery. For example, in the treatment of advanced gliomas, the most common and deadly primary brain tumor in adults, Gliadel wafers are now approved for clinical use (Westphal *et al.,* 2003). These carmustine(BCNU)-embedded biodegradable wafers are surgically placed immediately following tumor excision. The wafers slowly degrade, releasing drug into the region to kill any remaining cancerous cells. Additionally, treatment of CNS lymphomas and leukemias and primary brain tumors has utilized intrathecal drug delivery, in which chemotherapeutics are delivered to the cerebrospinal fluid, literally bathing the brain with drug (Ruggiero *et al.,* 2001; Patchell *et al.,* 2002). For example, the Ommaya reservoir is

an intraventricular catheter system that can be inserted through brain parenchyma into a ventricle (or specific region of the brain) and used to infuse drug locally to a region of interest.

These approaches for local drug delivery significantly decrease the risk of systemic toxicity (Rainov *et al.,* 2006), offering potential for testing newly-developed therapeutics that might be intolerable if delivered systemically. A cytochrome *c*-based therapeutic fits that profile because such an agent would be expected to induce apoptosis of many normal cells in the body, but in the brain it would be expected to induce apoptosis selectively in brain tumor cells. The notion of targeting the apoptosome as a cancer therapy has been described (Ledgerwood and Morison, 2009), and we believe the potential of this approach could be realized in the treatment of brain cancers. So although pursuing development of such an agent is certainly risky, we judged it appropriate given the dire need for new brain cancer treatments and the available technology that would enable local delivery of any developed compounds.

Here we show that drug-resistant brain tumors and brain tumor stem cells express Apaf-1 and are capable of activating caspases in response to cytochrome *c,* further confirming the apoptosome as a valid therapeutic target. We proceed to employ a multi-tiered strategy aimed at developing a cytochrome *c*-based therapeutic. We probe the fundamental binding interaction between cytochrome *c* and Apaf-1, reasoning that knowledge of the binding sites could aid in rational drug design. We also design a construct encoding a cytosolic version of cytochrome *c,* attempting to express active,

cytosolic cytochrome *c* within brain tumor cells. Finally, we engineer and optimize a screening modality to search for a small-molecule cytochrome *c* mimetic. Although we have not yet identified any candidate therapeutics, the small-molecule screen is ongoing and the data presented herein provide direction for continued research in this area.

## 4.2 Results

### 4.2.1 Temozolomide-resistant glioblastoma cells remain sensitive to cytochrome *c*-mediated caspase activaiton

Our findings in chapter 3 demonstrate that brain tumor cells activate caspases in response to cytosolic cytochrome *c*. However, those studies did not evaluate brain tumors harboring drug resistance, which is a significant clinical problem in the treatment of advanced gliomas, such as glioblastoma. The first-line chemotherapeutic for these tumors is the DNA-alkylating agent temozolomide. Although the drug increases overall survival, the benefit is short-lived, as all tumors develop temozolomide resistance (Chakravarti and Palanichamy, 2008). The primary mechanism underlying resistance is thought to be the upregulation of a DNA repair protein, $O^6$-alkylguanine-DNA alkyltansferase (AGT), which allows the cancerous cells to tolerate temozolomide-induced DNA damage (Stupp *et al.,* 2007). Cellular AGT can be inactivated with $O^6$-benzylguanine ($O^6$-BG), and although combinatorial therapy including $O^6$-BG kills temozolomide resistant cells *in vitro* and in xenograft tumors, the cocktail does not improve patient outcomes over treatment with temozolomide alone (Quinn *et al.,* 2009). Although unclear why the cocktail lacks improved efficacy, it is thought that some tumors are either innately resistant or develop resistance to $O^6$-BG, implying the presence of an additional

mechanism of apoptotic resistance that is not understood on a biochemical level. Thus, we were curious to evaluate whether these $O^6$-BG- and temozolomide- (OT) resistant brain cancers were able to activate caspases in response to cytochrome *c.* This information would be a first step toward identifying the mechanism of OT-resistance, and would also provide an indication of whether drug-resistant glioblastomas would be good candidates for a cytochrome *c*-based therapeutic.

To address this question, we utilized two pairs of glioblastoma cell lines that had been cultured as parental lines (P), and also cultured in the presence of temozolomide and $O^6$-BG until becoming resistant to both drugs. Immunoblot analysis confirmed the continued expression of Apaf-1 in these OT-resistant lines (Figure 4.1A), and cytosolic lysates from both OT-resistant lines activated caspases similarly to their respective parental cell line in response to cytochrome *c* (Figure 4.1B). Notably, cells cultured with temozolomide alone until becoming temozolomide-resistant (TR) were also tested in these assays, demonstrating Apaf-1 expression and sensitivity to cytochrome *c*-induced caspase activation (data not shown). Because OT-resistance was developed *in vitro,* the mechanism for resistance might be a distinct process from what occurs in the clinic. Therefore, we also analyzed a panel of glioblastoma cell lines derived from patients who had failed temozolomide therapy. These glioblastomas, including one demonstrating marked OT-resistance (F3), were all capable of activating caspases in response to cytochrome *c* (Figure 4.1C). Immunoblot analysis of these glioblastoma cell lines demonstrated invariable expression of Apaf-1, and caspase-9 processing in response to

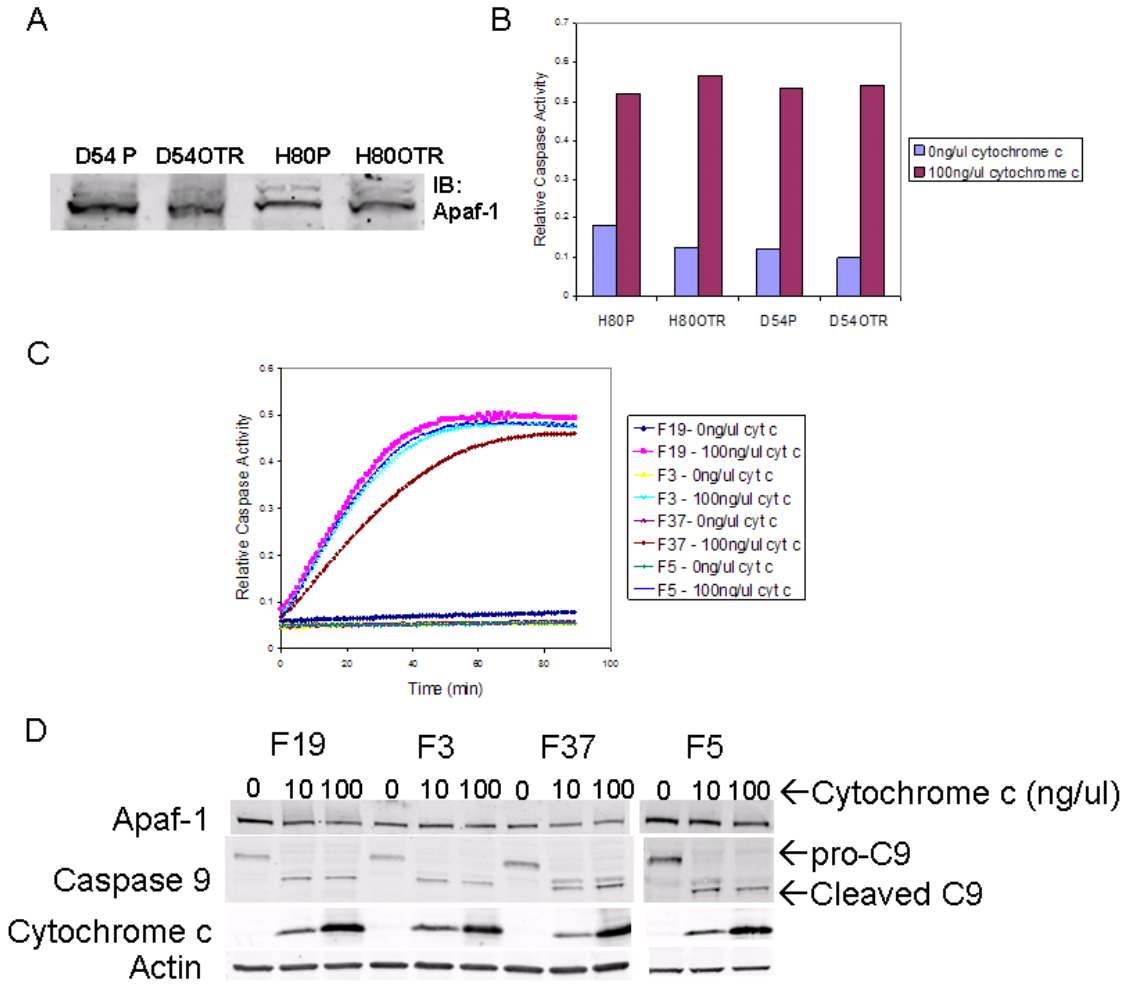


**Figure 4.1: Drug-resistant glioblastoma cells remain sensitive to cytochrome *c***

**Figure 4.1: A**, Immunoblot analysis demonstrating Apaf-1 expression in parental glioblastoma lines, D54P and H80P, and in lines resistant to both temozolomide and $O^6$-BG, D54OTR and H80OTR. **B**, Cytosolic extracts from parental (P) and resistant (OTR) lines were supplemented with cytochrome *c,* and caspase activity was monitored via cleavage of Ac-DEVD-pNA. **C**, Cytosolic extracts derived from advanced gliomas (F19, F3, F37 and F5) were supplemented with cytochrome *c* and monitored for caspase activation over time. **D**, Immunoblot analysis demonstrating expression of Apaf-1 and caspase-9 processing in response to cytochrome *c*.

cytochrome *c,* confirming apoptosome-mediated caspase activation (Figure 4.1D). Together, these data indicate that drug-resistant glioblastomas would be sensitive to apoptosis induced by cytosolic cytochrome *c,* and also reveal that the apoptosome components are functional in OT-resistant glioblastomas.

### 4.2.2 Brain tumor stem cells express Apaf-1 mRNA

Research over the past several years has demonstrated that a small subset of cells within a tumor, known as cancer stem cells, is highly proliferative and possesses the ability to reconstitute a tumor (Huntly and Gilliland, 2005). These tumor-propagating cells tend to be present in vast minority within a tumor but are highly resistant to most therapeutics (Bao *et al.,* 2006). Unfortunately this means that even aggressive treatments demonstrating promising tumor shrinkage are incomplete because resistant cancer stem cells survive and are capable of continued proliferation. We became interested in this subpopulation of brain tumor cells, wondering whether they would be sensitive to cytochrome *c*-induced apoptosis. We hypothesized that proliferating cancer stem cells would express Apaf-1 and be sensitive to cytochrome *c*, based on our previous finding that E2F1, a transcription factor critical for promoting cell cycle progression, drives the expression of Apaf-1 in brain cancers (Johnson *et al.,* 2007).

The isolation and culture of brain tumor stem cells is limited by the small number of stem cells present in tumors and by their retaining stemness for a very limited time in culture (Galli *et al.,* 2004). We were fortunate to receive mRNA prepared from glioma cell populations that had been sorted according to their status for a well-characterized

brain tumor stem cell marker, CD133 (Singh *et al.,* 2003). Performing RT-PCR to examine Apaf-1 mRNA levels in the past, we had observed significantly more abundant transcript in brain tumors than in normal brain (Figure 4.2A). Comparatively, our RT-PCR analysis in CD133+/- cells from both an adult and a pediatric glioma demonstrates roughly equivalent levels of Apaf-1 mRNA in the two tumor sub-populations (Figure 4.2B). Interestingly, both CD133+ samples had slightly higher levels of Apaf-1 mRNA than the CD133- samples. However we were not able to obtain additional samples to determine whether this small difference is reproducible or biologically significant. Finally, recent work published by our close collaborator, Dr. Robert Wechsler-Reya, has identified CD15 as a marker for tumor-propagating cells in medulloblastoma (Read *et al.,* 2009). Gene expression profiling was performed to compare CD15+/- medulloblastoma cell populations, and we were fortunate to be able to probe the resulting database for Apaf-1 expression levels. As was observed with the CD133+/- glioma cells, CD15+/- medulloblastoma cells express equivalent amounts of Apaf-1 mRNA (Figure 4.2C). Although interpretation of these results is limited because we were not able to obtain enough material to perform immunoblotting or caspase assays in these cell populations, they certainly suggest that brain tumor stem cells express Apaf-1 and thus are expected to be sensitive to cytochrome *c*-induced apoptosis.

### 4.2.3 Cytochrome *c* fragments are incapable of binding Apaf-1 or mediating caspase activation

In order to develop a cytochrome *c*-based therapeutic, a fundamental understanding of how cytochrome *c* binds Apaf-1 would be extremely beneficial. Apaf-1

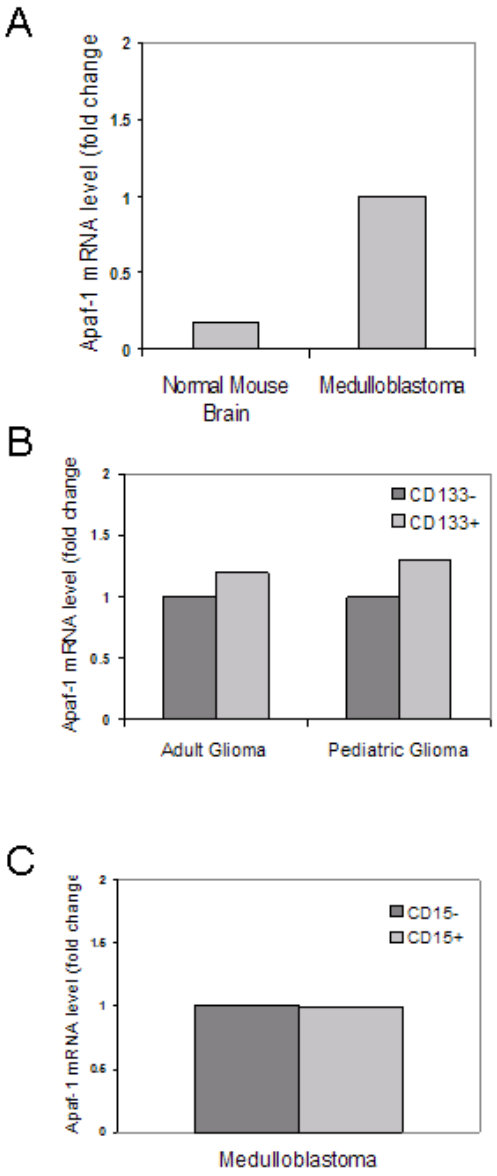


**Figure 4.2: Brain tumor stem cells express Apaf-1 mRNA.**

**Figure 4.2:** **A**, Quantitative analysis from RT-PCR shows the fold changes of Apaf-1 mRNA from dissected mouse medulloblastoma and adjacent cerebellar tissue. Data display the fold changes of Apaf-1 mRNA relative to the medulloblastoma, which is arbitrarily set at 1. **B**, Quantitative analysis from RT-PCR shows the fold changes of Apaf-1 mRNA from CD133- and CD133+ sub-populations from cell lines derived from adult and pediatric gliomas. Data display the fold changes of Apaf-1 mRNA relative to the CD133- sub-population, which is arbitrarily set at 1. **C**, Data from microarray gene expression profiling in mouse medulloblastoma CD15- and CD15+ sub-populations. Data display the fold changes of Apaf-1 mRNA relative to the CD15- sub-population, which is arbitrarily set at 1.

is a large protein (120 kDa) containing an N-terminal caspase recruitment domain (CARD), a central nucleotide-binding and oligomerization domain (NOD), and 13 WD40 repeats (Riedl *et al.,* 2005). The Apaf-1 WD40 repeats, with which cytochrome *c* is theorized to interact (Acehan *et al.,* 2002), render the gene prone to recombination and consequently make it difficult to clone. On the other hand, cytochrome *c* is quite small (12 kDa) and has been well-characterized due to its role in the mitochondrial electron transport chain. It is translated in the cytoplasm in an "apo" form, and is rapidly transported into the mitochondria where it heme modified by cytochrome *c* heme lyase, becoming holocytochrome *c* (Mayer *et al.,* 1995). The heme modification of cytochrome *c* has been shown to be required for its ability to trigger apoptosome formation (Kluck *et al.,* 2000). Moreover, several surface-exposed lysine residues on opposite faces of cytochrome *c* have been shown to be important for Apaf-1 binding (Yu *et al.,* 2001) (Figure 4.3A), suggesting that the three-dimensional structure of heme-modified cytochrome *c* is important for dictating its interaction with Apaf-1. Perhaps surprisingly then, one study demonstrated in cells that apocytochrome *c,* while incapable of triggering apoptosis, does retain its ability to bind Apaf-1 (Martin and Fearnhead, 2002). The same group later reported that apocytochrome *c* binding to Apaf-1 actually prevents apoptosome formation and subsequent caspase activation (Martin *et al.,* 2004).

Intrigued by these findings and eager to determine whether we could identify a minimal region of cytochrome *c* required for Apaf-1 binding, we designed and synthesized four overlapping cytochrome *c* peptide fragments (Figure 4.3B). The

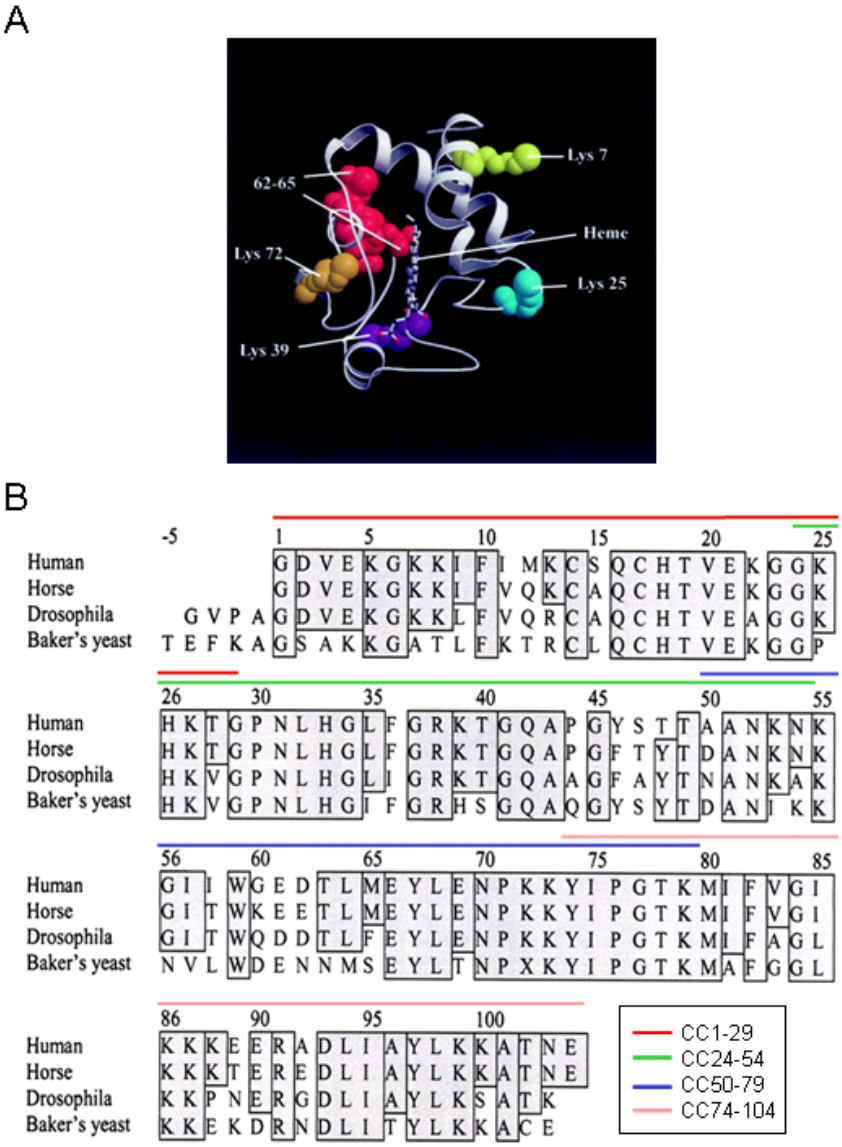


**Figure 4.3: Critical lysine residues in cytochrome *c* and diagram of synthesized cytochrome *c* fragments.**

**Figure 4.3:** **A**, Horse cytochrome *c* protein is shown as helix and strand with important residues indicated as space-filled balls. This figure was generated by Raster 3D and MOLSCRIPT based on PDB file 1HRC and is from Yu *et al.* (2001), with permission from Elsevier. **B**, Sequence alignment for horse, human, *Drosophila,* and yeast cytochromes *c* with the horst numbering system utilized, from Yu *et al.* (2001), with permission from Elsevier. This figure has been modified to illustrate the four overlapping cytochrome *c* peptides that were synthesized for use in the described experiments.

peptides were synthesized to include N-termimal biotinylation, allowing us to perform binding assays in which we pulled down soluble Apaf-1 on peptide-linked avidin beads. However, none of the cytochrome *c* peptide fragments were able to pull-down Apaf-1 while cytochrome *c* readily pulled down Apaf-1 (data not shown). We also performed the converse experiment, in which we utilized His-tagged Apaf-1 on nickel beads to query whether we could pull down any of the soluble peptides. Although cytochrome *c* readily bound Apaf-1, none of the cytochrome *c* peptide fragments displayed Apaf-1 binding (data not shown).

In addition to these binding assays, we also performed a series of functional studies to assess whether the cytochrome *c* peptide fragments were able to influence formation of the apoptosome. We first examined whether peptide addition to cytosolic lysate was capable of inducing caspase activation. Shown in figure 4.4A, although cytochrome *c* addition to cytosol is sufficient to trigger caspase activity, none of the peptides showed any such activity. Then, we proceeded to investigate if any of the peptides could dampen (or block) cytochrome *c*-induced caspase activation, but were disappointed to observe that the cytochrome *c* peptide fragments were unable to negate the effects of cytochrome *c* (Figure 4.4B).

### 4.2.4 Intermolecular crosslinking and mass spectrometry analysis of cytochrome *c*—Apaf-1 complexes: can we use this approach to map molecular interaction surfaces?

As a distinct approach for mapping the binding sites between Apaf-1 and cytochrome *c* we pursued the use of intermolecular crosslinking followed by mass

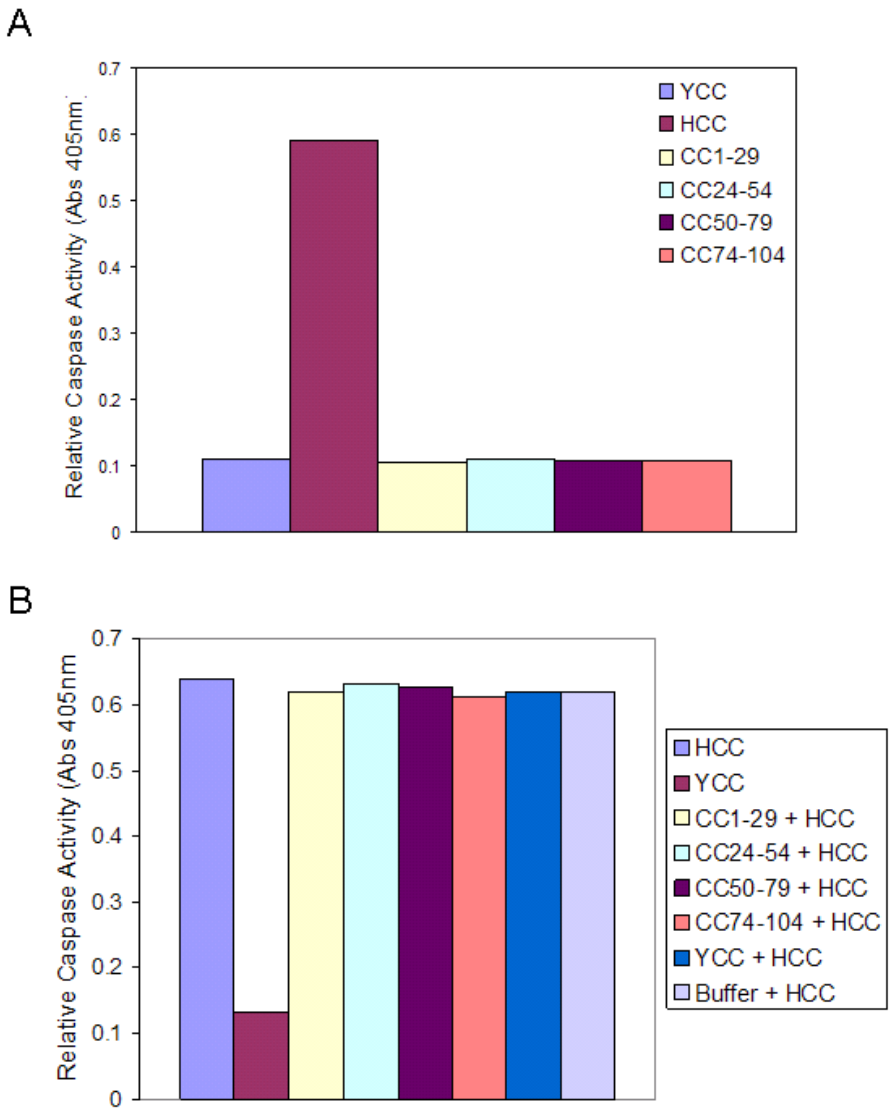


**Figure 4.4: Peptide fragments of cytochrome *c* neither activate nor inhibit caspase activation.**

**Figure 4.4: A,** *Xenopus* egg-derived cytosolic extract was supplemented with either yeast cytochrome *c* (YCC), horse cytochrome *c* (HCC) or a cytochrome *c* peptide fragment (as illustrated in figure 4.3B) and analyzed for caspase activity via cleavage of Ac-DEVD-pNA. **B,** *Xenopus* egg-derived cytosolic extract was supplemented with cytochromes *c* or horse cytochrome *c* and a cytochrome *c* peptide fragment as detailed by the legend, and these reactions were then analyzed for caspase activity via cleavage of Ac-DEVD-pNA.

spectrometry (MS) analysis as a collaborative effort with the Duke Proteomics Facility. Crosslinking reagents have been used as tools in a variety of biological applications, from identifying interacting proteins on cell-surfaces to evaluating whether a transcription factor is bound to a specific region of DNA. When combined with mass spectrometry analysis, crosslinking can be used to identify the molecular contact surfaces between two interacting proteins (Sinz, 2003). To this end, a pair of crosslinking reagents have been developed which differ only in the number of deuterium atoms in their composition, such that one reagent is exactly four mass units heavier than the other. By incorporating the two reagents in an equal ratio, crosslinked peptides in low abundance can be identified following MS analysis by searching the resulting grand list of peptide hits for any peptide products differing by exactly four mass units (Sinz, 2006). Further analysis of identified crosslinked peptides can ultimately yield three-dimensional structural insight into a given protein-protein interaction (Back *et al.,* 2003; Dihazi and Sinz, 2003; Muller *et al.,* 2001; Kalkhof *et al.,* 2005).

In our particular case we hoped to identify peptide sequences within Apaf-1 and cytochrome *c* involved in their interaction. Thus, our strategy was to crosslink the interacting proteins in solution, analyze the products by SDS-Page, submit excised bands of interest to the proteomics facility for MS analysis, and finally probe the resulting data sets to identify crosslinked products (Figure 4.5). We were successfully able to obtain crosslinked product based on immunoblot analysis of cytochrome *c* and Apaf-1 in the presence of crosslinker (Figure 4.6). These data actually provided a significant amount of

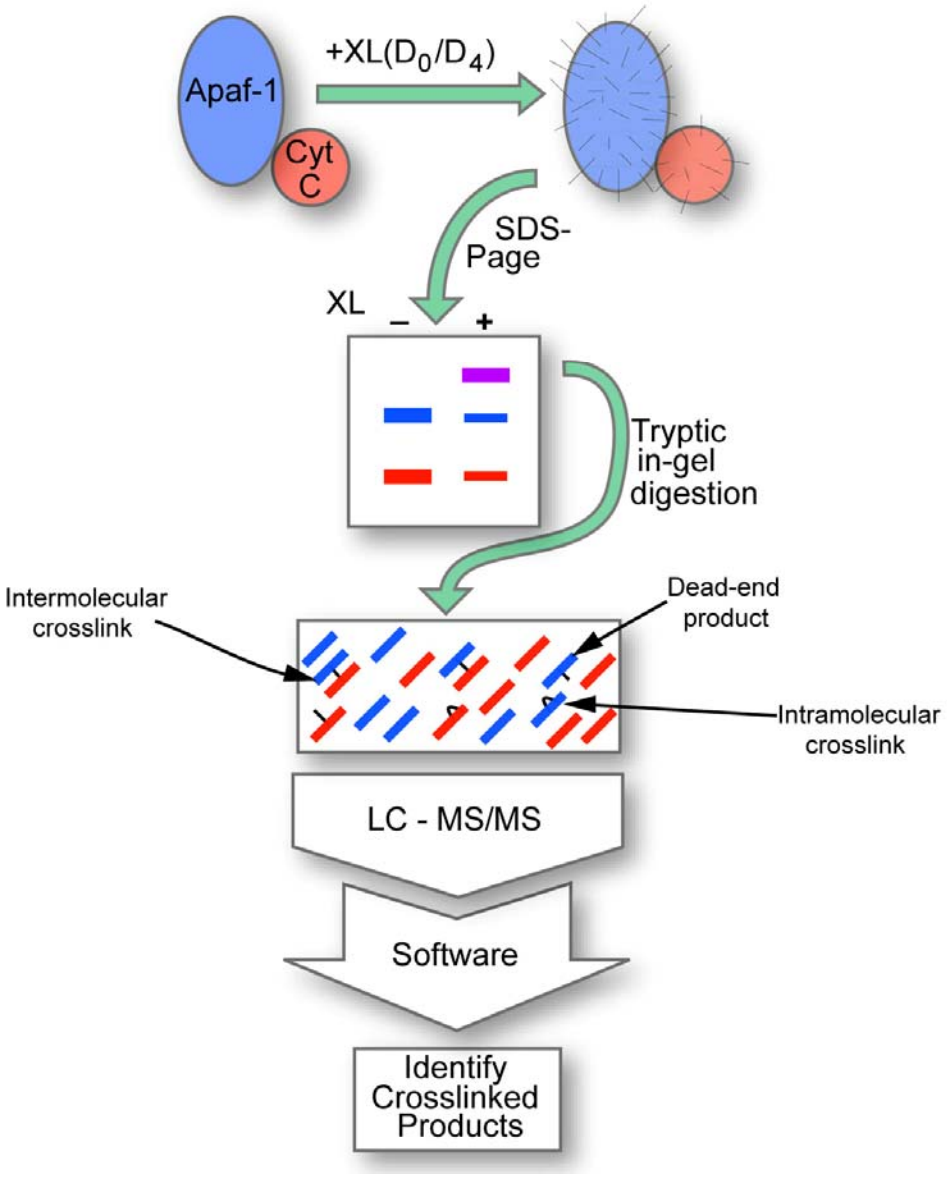


**Figure 4.5: Crosslinking strategy to map the cytochrome *c*—Apaf-1 binding sites.**

**Figure 4.5:** A schematic overview of the strategy employed to detect crosslinked products resulting from the cytochrome *c*—Apaf-1 interaction. Briefly, Apaf-1 and cytochrome *c* are incubated in the presence of a 1:1 ratio of heavy and light crosslinkers ($XL(D_0/D_4)$), analyzed by SDS-Page and the resulting crosslinked product (purple band) is proteolytically digested. The resulting tryptic peptides, containing predominantly un-crosslinked products but also some peptides that have reacted with the crosslinker forming either dead-end products, intramolecular or intermolecular crosslinks, are submitted for mass spectrometry analysis (LC-MS/MS).

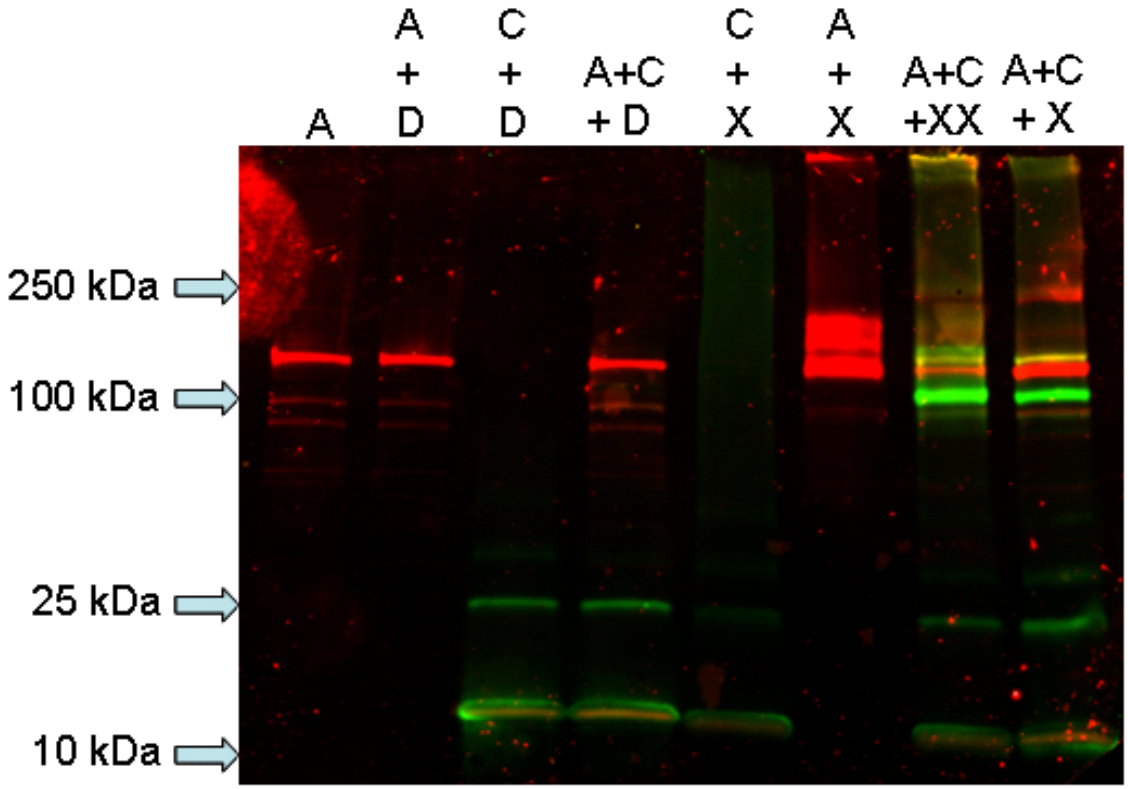


**Figure 4.6: Immunblot analysis of cytochrome *c*—Apaf-1 covalent crosslinking.**

**Figure 4.6:** Apaf-1 (A; red signal) and cytochrome *c* (C; green signal) are incubated in the presence of either a DMSO control (D) or crosslinking reagent (X = $BS^3$ $d_0/d_4$ low dose; XX = $BS^3$ $d_0/d_4$-treated high dose). Crosslinked products are visualized as yellow bands, reacting with both Apaf-1 and cytochrome *c* antibodies.

information, some of it pertinent to the cytochrome *c*—Apaf-1 interaction, and so our interpretation of the immunoblot will be described here. First, in the absence of crosslinker, recombinant human Apaf-1 purified from Sf9 insect cells is detected primarily as a single band at roughly 120 kDa, but at least two potential breakdown products are also recognized by the employed Apaf-1 antibody (lanes 'A' and 'A+D'). Note that purified horse cytochrome *c* runs at approximately 12 kDa, but there is also a larger (approximately 25kDa) band that we routinely observe, which may represent cytochrome *c* dimerization that is stable in the presence of SDS- and reducing agent (lanes 'C+D' and 'A+C+D'). When incubated with the crosslinker, monomeric Apaf-1 is still detectable, but some of the protein has shifted upwards into larger molecular weight products, including a product larger than 250 kDa (lane 'A+X'). This implies transient aggregation or oligomerization of Apaf-1 occurring in solution even in the absence of cytochrome *c.* When a mixture of cytochrome *c* and Apaf-1 is incubated with crosslinker, we observe a yellow band (indicating crosslinked cytochrome *c*—Apaf-1) slightly higher than monomeric Apaf-1 (lanes 'A+C+XX' and 'A+C+X'), and a second yellow band greater than 250 kDa (lane 'A+C+XX'). We interpret these bands to represent one molecule of Apaf-1 crosslinked with one molecule of cytochrome *c* and multiple oligomerized Apaf-1 molecules all crosslinked to multiple cytochromes *c*, respectively. In order to provide the Duke Proteomics Facility with the simplest possible protein complex, we submitted the smaller of the two yellow bands for MS analysis. Finally, there is a prominent green band observed around 100 kDa in the cytochrome *c*—Apaf-1

crosslinked samples, which indicates the presence of cytochrome *c* at this molecular weight. We believe this is due to cytochrome *c* binding to a breakdown product of Apaf-1 that is not recognizable by the Apaf-1 antibody. Importantly, because the Apaf-1 antibody was developed against the N-terminal CARD domain, this result demonstrates that cytochrome *c* does not require the CARD for interacting with Apaf-1.

After optimizing our crosslinking conditions, we submitted the excised cytochrome *c*—Apaf-1 band to the Duke Proteomics Facility for in-gel tryptic digestion followed by LC-MS analysis. Simultaneously, we submitted control samples, including Apaf-1 and cytochrome *c* incubated individually in the presence of crosslinker. MS analysis identified the proteins in the samples as Apaf-1 and cytochrome *c*. Furthermore, intrapeptide crosslinked products could be identified from the control crosslinked cytochrome *c* sample, demonstrating that the technique and analytic strategies employed were capable of detecting crosslinked peptides (Figure 4.7). However, although "dead-end" crosslinked products were identified in Apaf-1 alone or cytochrome *c*—Apaf-1 samples (indicating that the crosslinking reagent had found Apaf-1 and reacted with a few accessible lysines), no thru-space crosslinked peptides were detected. In addition to traditional database searching of the MS/MS spectra for mass modifications corresponding to the crosslinking reagents, the Duke Proteomics Facility also employed an alternative approach of converting the LC-MS run into a three-dimensional image (m/z, retention time, intensity). These images were searched for the presence of co-eluting peaks differing in mass by 4.025 Da, corresponding to the mass difference

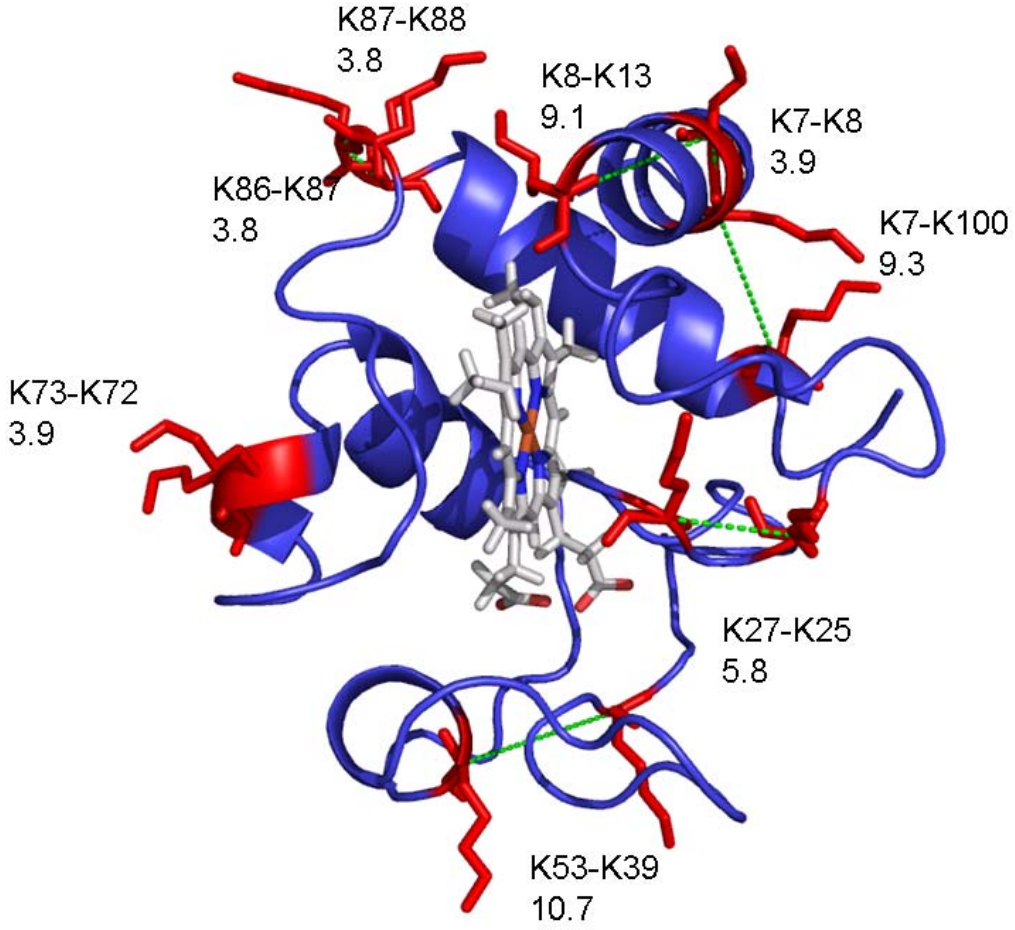


**Figure 4.7: Intramolecular crosslinking of cytochrome *c*.**

**Figure 4.7:** Horse cytochrome *c* protein is shown as helix and strand with identified crosslinked lysine (K) residues in red with connecting dashed lines in green (generated in PyMol).

between $d_0$ and $d_4$ labeled crosslinking reagents. However, this approach did not yield additional identifications, likely due to the large dynamic range of peak intensities within a single LC-MS run. Finally, because our method relied upon in-gel retrieval of tryptically-digested peptides, it is possible that poor yield in the gel extraction step resulted in our negative results. Therefore we crosslinked Apaf-1 alone and submitted the sample in-solution for MS analysis. Unfortunately, even in this situation no crosslinked peptides were identified.

### 4.2.5 Expressing active, cytosolic cytochrome *c* in brain cancer cells

As one approach for developing a cytochrome *c*-based therapeutic without knowing the binding sites between Apaf-1 and cytochrome *c,* we designed a gene therapy strategy that would ultimately enable viral delivery of a construct encoding an active, cytosolic form of cytochrome *c.* In order for this to be possible, we would have to prevent mitochondrial localization of cytochrome *c* and heme lyase, the enzyme that catalyzes its heme modification. However, we would have to do that in such a way as to retain the ability for heme lyase to heme-modify cytochrome *c* and retain the structure of cytochrome *c* so that it would still bind Apaf-1 and induce apoptosome formation. We began by fusing fluorescent proteins to our proteins of interest, hoping that these fluorescent protein tags would enable visual tracking of expression and prevent mitochondrial localization (Figure 4.8A). When compared to a mitochondrial staining pattern characteristic of cytochrome *c* expression (Figure 4.8B), fusion of cytochrome *c* with green fluorescent protein (GFP) at either the N- or C-terminus successfully disrupts

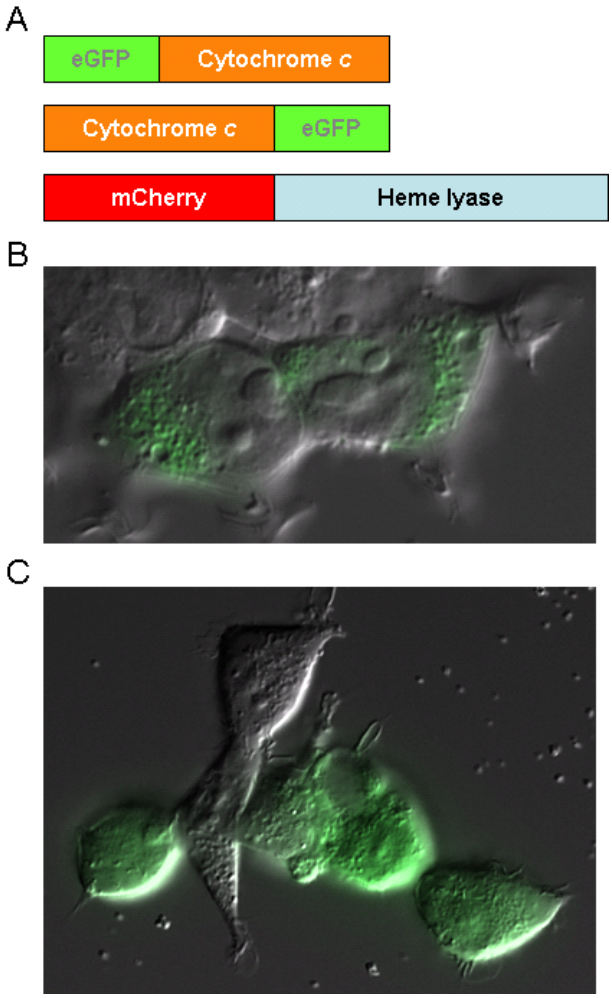


**Figure 4.8: Cytosolic expression of cytochrome *c* and heme lyase.**

**Figure 4.8:** **A**, Schematic of expression constructs utilized for expressing cytochrome *c* and heme lyase in the cytosol, including eGFP fused to both N- and C-terminals of cytochrome *c* and mCherry fused to the N-terminus of yeast heme lyase. **B**, Representative image of HeLa cells transfected with mito-eGFP, illustrating a mitochondrial staining pattern. **C**, HeLa cells transfected with cytochrome *c*-eGFP, demonstrating a cytosolic staining pattern.

this pattern and results in staining consistent with cytosolic expression (Figure 4.8C). Fusion of the red fluorescent protein derivative, mCherry, to the N-terminus of yeast heme lyase was similarly able to prevent mitochondrial localization of the lyase (data not shown).

We then performed a series of co-expression studies to determine whether cytosolic expression of the two fusion proteins would trigger caspase activity, as expected if the mCherry-heme lyase could modify the GFP-apocytochrome *c* and the resulting GFP-holocytochrome *c* was then able to bind Apaf-1. Our first experiments were performed in HeLa cells, and we were encouraged by our observations that cells expressing both GFP-cytochrome *c* and mCherry heme lyase appeared apoptotic (Figure 4.9A). Even in less clear-cut images, cells expressing both constructs tended to look unhealthy compared with cells expressing only one of the constructs (Figure 4.9B). We proceeded to test these constructs in additional cell types, including two brain tumor cell lines. In these cases, although some double-expressing cells appeared apoptotic, the majority appeared healthy, regardless of when they were examined (range from several hours post-transfection through four days post-transfection) (Figure 4.9C and D).

### 4.2.6 Development of a small-molecule screen to identify a cytochrome *c* mimetic

For our final approach we were hoping to identify compounds that act similarly to cytochrome *c* by binding Apaf-1 and inducing apoptosome formation. To that end, we developed and optimized a small-molecule screen that tests the ability of a given compound to substitute for cytochrome *c* in activating caspases. The assay utilizes the

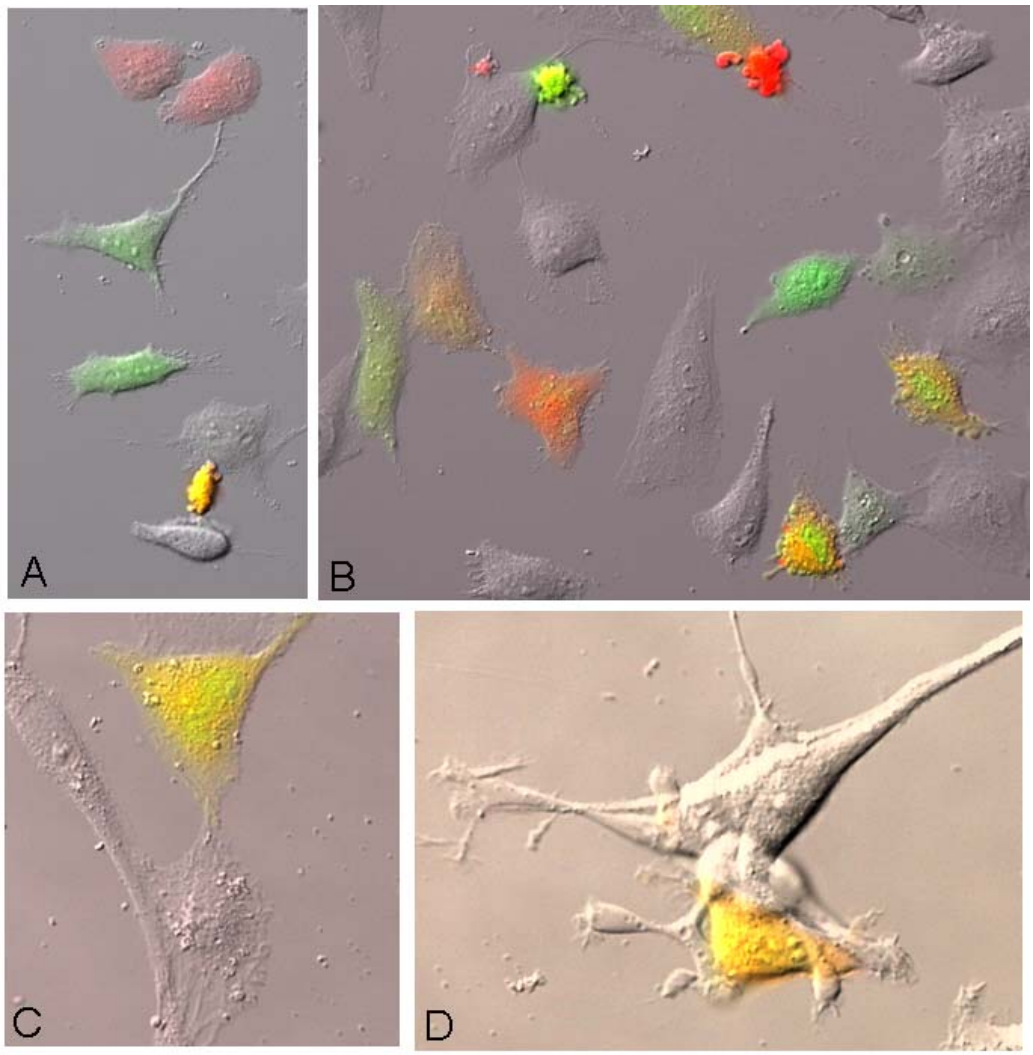


**Figure 4.9: Co-expression of cytosolic cytochrome *c* and heme lyase.**

**Figure 4.9:** **A**, HeLa cells transfected with both cytochrome *c*-eGFP (green) and mCherry-heme lyase (red), with the cell expressing both proteins (yellow) clearly apoptotic (rounded up with pronounced membrane blebbing). **B**, Additional image of cells treated as in **A**. **C**, MGR3 glioblastoma cells transfected with eGFP-cytochrome *c* and mCherry-heme lyase. **D**, D54 glioblastoma cells transfected with cytochrome *c*-eGFP and mCherry-heme lyase.

*Xenopus* cell-free system, in which large volumes of concentrated cytosolic lysate can be prepared from eggs. Because components of the apoptosome are highly conserved across species, this extract approximates a human cytosolic lysate for screening purposes while offering the advantage of being easily prepared in large volumes. For the assay, cytosol is aliquoted into either a 96-well or 384-well plate (volumes and concentrations of reagents have been optimized for both formats), to which a small-molecule and a fluorogenic (or colorimetric) caspase substrate are added. After one hour incubation at 37°C plates are read in a fluorometer (or spectrophotometer) to evaluate individual wells for the presence of caspase activity. Each plate includes positive (cytochrome *c*) and negative (water or yeast cytochrome *c*) controls in triplicate. Utilizing this screening technique in collaboration with the laboratory of Francis Ali-Osman, we have evaluated over 8,000 small-molecule compounds. Demonstrated in figure 4.10 are results from a small subset of compounds, in which a certain threshold value of relative caspase activity is deemed significant based on comparisons with negative control wells. The potential hits we have identified thus far in the screen have been further analyzed utilizing a caspase assay similar to the one described here except with cytosolic lysate prepared from Apaf-/- mouse embryonic fibroblasts. This secondary screen allows us to determine whether any of the compounds function in an Apaf-1-dependent manner. Additional screening modalities with compounds of interest include survival assays in brain tumor cell lines to examine if the compounds are able to kill brain cancer cells *in vitro.* Although we have

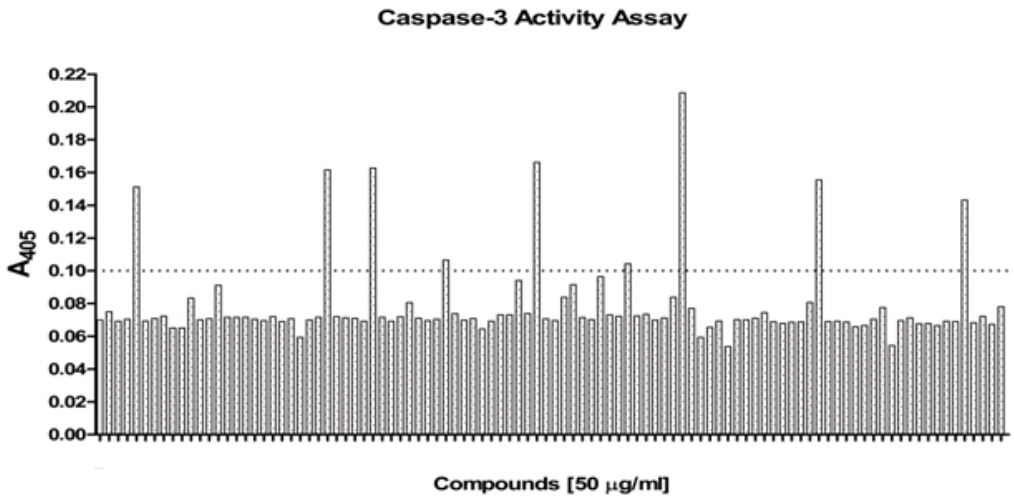


**Figure 4.10: A small-molecule screen to identify cytochrome *c* mimetics.**

**Figure 4.10:** Representative data obtained from screening small-molecules for their ability to activate caspases in cytosolic lysate, with relative caspase activity measured on the y-axis (here with absorbance at $A_{405}$ based on cleavage of Ac-DEVD-pNA).

identified several compounds that killed glioblastoma cells in culture, they failed to act in an Apaf-1-dependent manner.

## 4.3 Discussion

### 4.3.1 Drug-resistant brain cancer cells can be targeted for apoptosis with cytosolic cytochrome *c*

We had previously demonstrated the susceptibility of brain cancer cells to cytochrome *c*-induced apoptosis. Here we show that this sensitivity is seen in multiple types of drug-resistant brain cancer cells. Specifically, we demonstrated cytochrome *c*-induced caspase activity in glioblastomas resistant to both temozolomide and $O^6$-BG. We also detected Apaf-1 mRNA expression in notoriously difficult-to-treat brain cancer stem cells. These data support the notion that brain cancer cells could be triggered to undergo apoptosis in response to cytosolic cytochrome *c*. Furthermore, these data suggest that even drug-resistant cancer cells and tumor-propagating cells would be susceptible to apoptosis induced in this manner.

One important limitation of this work was our inability to directly examine levels of Apaf-1 protein or sensitivity to cytochrome *c*-induced caspase activity in the cancer stem cells. Because of the low abundance of tumor-propagating cells, it was simply impractical to obtain enough cellular material to perform such experiments. However, future experiments in continued collaboration with Robert Wechsler-Reya and Jeremy Rich could address these questions by collecting any available cancer stem cell lysate slowly over time until enough was accumulated to perform immunoblotting and caspase activity assays. Additionally, it would be interesting to extend these investigations to

examine whether normal neural stem cells are sensitive to cytochrome *c.* Collaborative experiments with Chay Kuo at Duke University could be pursued to characterize the sensitivity of neural stem cells to cytosolic cytochrome *c* during postnatal development and adulthood. We predict that adult neural stem cells, present in stem cell niches but less active than during development (Price, 2001; Kuo *et al.,* 2006), might demonstrate increased resistance to cytochrome *c* when compared to actively proliferating brain tumor stem cells.

Our results with OT-resistant glioblastomas demonstrate that the apoptotic pathway downstream of cytochrome *c* remains intact, and thus the mechanism of OT-resistance must lie upstream of this point. Future studies hoping to delineate the mechanism of resistance should first examine whether cytochrome *c* gets released from the mitochondria following OT treatment. Based on our observations with addition of exogenous cytochrome *c*, we would predict that cytochrome *c* is not being released, and that the apoptotic signal never gets delivered to the mitochondria. If indeed this is true, it would be interesting to further examine OT-resistant cells for activation of checkpoint kinases, p53/73, and Bcl-2 family members. Based on emerging clinical data, in which combination therapy with temozolomide and $O^6$-BG offered no improvement over temozolomide alone, priority should be placed on determining the mechanism of OT-resistance. Understanding this resistance could unveil a new target for therapeutic development. Ultimately, novel approaches for treating advanced gliomas are absolutely

essential. Based on our work, we believe one promising strategy is apoptosome activation with the use of a cytochrome *c*-based therapeutic.

### 4.3.2 Mapping the cytochrome *c*—Apaf-1 binding sites

The interaction of cytochrome *c* and Apaf-1 is critical for inducing apoptosome formation. Cytosolic cytochrome *c* binds to Apaf-1 in such a manner that leads to Apaf-1 oligomerization and recruitment of procaspase-9. The region of Apaf-1 with which cytochrome *c* interacts remains unknown, and although several residues on cytochrome *c* are thought to be important for mediating binding to Apaf-1, whether a minimal binding region of cytochrome *c* exists has been unclear. Here we show that peptide fragments of cytochrome *c* are unable to bind Apaf-1 or to regulate apoptosome formation in any measurable way. These results confirm that the three-dimensional structure of cytochrome *c* is essential for enabling binding to Apaf-1. Unfortunately, our cytochrome *c* fragment experiments have not provided us with any novel binding site information that could be applied in the design of an apoptosome-activating therapeutic.

We also utilized crosslinking followed by mass spectrometry in the hope of identifying molecular contact surfaces involved in the cytochrome c—Apaf-1 interaction. Importantly, immunoblot analysis of chemical crosslinking revealed that the Apaf-1 CARD is not required to mediate the cytochrome *c*—Apaf-1 interaction. This has been assumed in the field for some time, but empirical evidence of this has been lacking. Future studies with a variety of Apaf-1 antibodies could be utilized to further delineate regions of Apaf-1 required for the binding interaction. Our mass spectrometry results

with cytochrome *c* establish the approach as a valid strategy for identifying crosslinked peptides. We were, however, unable to detect crosslinked products from Apaf-1 or cytochrome c—Apaf-1 samples. The most likely explanation is that crosslinked products are at such low abundance relative to non-derivatized tryptic peptides in these samples that their signals were masked from being detected. This challenge is routinely encountered when using MS to analyze very large crosslinked proteins, like Apaf-1, which generate vast numbers of tryptic peptides and highly complex MS spectra (Sinz, 2006). A common strategy for overcoming this obstacle for other species in low abundance, such as phosphorylated peptides, is the use of enrichment techniques prior to MS analysis. For phosphorylated samples, all of the peptides are subjected to a $TiO_2$ column which selectively retains phosphate-containing peptides, thus significantly reducing the influence of protein size or complexity in the MS analysis (Pinkse *et al.*, 2004). Similarly, our experiments would be greatly aided by a tagged crosslinking reagent that would allow us to isolate only crosslinked products, thus enriching them in our sample prior to MS analysis. An alternative approach would utilize crosslinking reagents that incorporate a labile bond within the linker which dissociates under low-energy, enabling independent isolation and sequencing of crosslinked peptides during the mass spectrometry analysis (Soderblom *et al.,* 2007). Although such reagents are not commercially available, we believe that re-visiting these experiments would be a worthwhile endeavor once an appropriate crosslinker becomes obtainable.

### 4.3.3 Developing a therapeutic to activate the apoptosome

Collectively, our data indicate that brain cancer cells maintain functionally active apoptosome components and thus could be targeted to die with cytosolic cytochrome *c*. We believe that the cytochrome *c* resistance of normal neural tissue and the ability to deliver drugs locally to the brain make apoptosome activation a particularly attractive strategy for the treatment of primary brain tumors. Here we have described our work towards developing a cytochrome *c* therapeutic, pursuing both screen-based and gene therapeutic approaches. Our gene therapy strategy was based on expressing an active, cytosolic version of cytochrome *c* within brain cancer cells. Although we successfully expressed tagged cytochrome *c* (GFP-cytochrome *c* and cytochrome *c*-GFP) in the cytosol, co-expressing cytosolic cytochrome *c* with tagged heme lyase (mCherry-heme lyase) did not yield obvious apoptosis in glioblastoma cell lines. Interpretation of these results is limited since we did not perform a quantitative measurement of apoptosis in these cells compared with control-transfected cells. Moreoever, these cells were transiently transfected using lipid-based reagents, yielding relatively low transfection efficiencies. Future experiments should first clone the fluorescent fusion proteins into a viral vector, infect brain cancer cells with the viral construct, and then quantitatively analyze infected cells for induction of apoptosis utilizing flow cytometry with a fluorescent antibody against cleaved caspase 3. These experiments, although requiring a significant time commitment, are required to establish the potential utility of such an approach. One additional limitation is our lack of an assay to analyze whether the tagged

heme lyase is functional in modifying the cytochrome *c.* We attempted to design such an assay (data not shown), but were not successful. Development of this assay would help us determine if the fusion cytochrome *c* protein is getting modified when co-expressed with the tagged heme lyase.

In this work we have been able to successfully develop a screening modality to search for compounds that act like cytochrome *c* to induce caspase activity. This assay was purposefully designed in cytosolic lysates with caspase activation as the measured endpoint so that we can cast a wide net and identify any compound that triggers caspase activation in the absence of cytochrome *c.* For example, a small-molecule that induces caspase-9 activation and thus leads to activation of effector caspases, would register as a potential hit in our assay. Although secondary screening of this compound would reveal that it does not act in an Apaf-1-dependent manner, it would still be a useful tool and a compound warranting further characterization. The most important component of the assay design is the absence of cytochrome *c,* which allows us to identify compounds that mimic cytochrome *c.* This is in contrast to previously reported small-molecule screens, which have identified apoptosome modulators that enhance caspase activation in the presence of cytochrome *c* (Nguyen and Wells, 2003; Jiang *et al.,* 2003). Additionally, this assay can be performed in a high-throughput manner that will enable screening of incredibly vast small-molecule libraries. Our screening efforts to date have not identified any compounds of interest, but we have only screened roughly 8,000 compounds. Certainly continued screening is warranted, and we are optimistic that interesting

compounds exist to be found. That being said, we do appreciate the complex binding interaction between cytochrome *c* and Apaf-1. The conformation of Apaf-1 that is induced (or stabilized) in response to cytochrome *c* binding may be difficult to mimic with a small-molecule. Fortunately our screening approach does not necessitate the small-molecule work in exactly the same way as cytochrome *c,* but merely that it leads to apoptosome formation and subsequent activation of effector caspases.

# 5. Features of programmed cell death in intact Xenopus oocytes and early embryos revealed by near-infrared fluorescence and real-time monitoring

(This chapter has been submitted for publication and is currently under review.)

## 5.1 Introduction

Apoptosis is a form of programmed cell death executed by caspases. These cysteine proteases exist in the cytosol as zymogens until death stimuli trigger their activation (Earnshaw et al., 1999). Apoptotic signals can originate from extracellular ligands binding to cell-surface death receptors (extrinsic pathway) or from internal cues (e.g. DNA damage) inducing mitochondrial release of cytochrome *c* (intrinsic pathway) (Schultz et al., 2003). In both cases, the resulting adaptor protein complexes recruit initiator caspases, leading to their dimerization-induced activation (Shi, 2005). Effector caspases are then processed by initiator caspases, greatly enhancing their enzymatic activity, freeing them to cleave an array of cellular substrates resulting in tidy cell dismantling (Shi, 2002).

Further study of the biochemical intricacies governing apoptotic signaling pathways is warranted, given that dysregulation of apoptosis contributes to the development of several important human pathologies, such as cancer and neurodegeneration (Bellamy et al., 1995). Monitoring caspase activation is a critical component of studying apoptotic death, and numerous techniques that measure caspase activity have been developed (Köhler et al., 2002). Traditionally these have relied upon

biochemical analyses of lysates prepared from large numbers of cells. More recently, fluorescence resonance energy transfer (FRET)-based caspase substrates have been developed that enable monitoring of caspase activity in mammalian cells (Rehm *et al.,* 2002; Morgan and Thorburn, 2001; Liu *et al.,* 2002). These assays generally implement cellular expression of a construct encoding two fluorescent proteins linked by a short peptide containing a caspase cleavage site (e.g., DEVD); caspase activation in a cell results in separation of the two fluorescent proteins and a consequent change in fluorescence emission ratios. Although a powerful tool, the strategy relies on treatment of cell populations with apoptosis-inducing drugs and fluorescence imaging (microscopy or flow cytometry) over many hours. Moreover, use of such genetically-encoded FRET indicators to monitor developmental programmed cell deaths would require production of transgenic animals and robust expression during embryogenesis.

The *Xenopus* system has traditionally been used as a powerful tool for studying both early embryonic development and cell cycle control (Jones and Smith, 2008; Philpott and Yew, 2005). Given the critical role of apoptosis in developmental processes and the emerging interplay between cell cycle and cell death regulators, this system has great potential to aid in the delineation of these crucial connections. Although extracts prepared from *Xenopus* eggs develop caspase activity over time (that can be monitored using a variety of fluorescent and colorimetric indicators in vitro), these activities reflect the "death" of multiple pooled eggs in aggregate, rather than the real-time apoptosis of individual cells (Newmeyer et al., 1994; Kornbluth and Evans, 2001). Microinjection of

cytochrome *c* into *Xenopus* oocytes has been demonstrated to reliably induce apoptosis, but detection of death has depended on changes in oocyte morphology (which take hours to occur) or on indirect markers of caspase activation (e.g., plasma membrane depolarization) (Bhuyan et al., 2001). Unfortunately, changes in membrane potential are not specific for apoptotic death, lack the sensitivity of the cell-free system, and cannot be recorded for more than one oocyte at a time. Thus, to date, there has been no means for directly measuring caspase activity in an intact *Xenopus* oocyte or early embryo.

Here we report a novel method based on a near-infrared dye caspase substrate that allows measurement of caspase activation in real-time in living *Xenopus* oocytes. By applying this technique we have studied the kinetics of caspase activation, assessed the role of IAPs in determining sensitivity to cytochrome *c*, compared caspase activation during different phases of the cell cycle, and imaged caspase activity in the early *Xenopus* embryo. These studies have revealed important subtleties in apoptotic regulation and also suggest the utility of this system as a tool for identifying novel apoptotic regulators.

## 5.2 Results

### 5.2.1 A near-infrared caspase substrate enables the detection of caspase activity in *Xenopus* oocytes

Recently, a near-infrared (NIR) caspase substrate became commercially available from LI-COR, Inc. (X. Peng *et al*., 2009). This IRDye® 800CW/QC-1 CSP-3 substrate (IRDye) emits fluorescence only after being cleaved by effector caspases at a canonical DEVD cleavage motif, which separates non-fluorescent quencher and NIR donor dyes, thereby restoring donor signal (Figure 5.1A). To determine if the IRDye would be

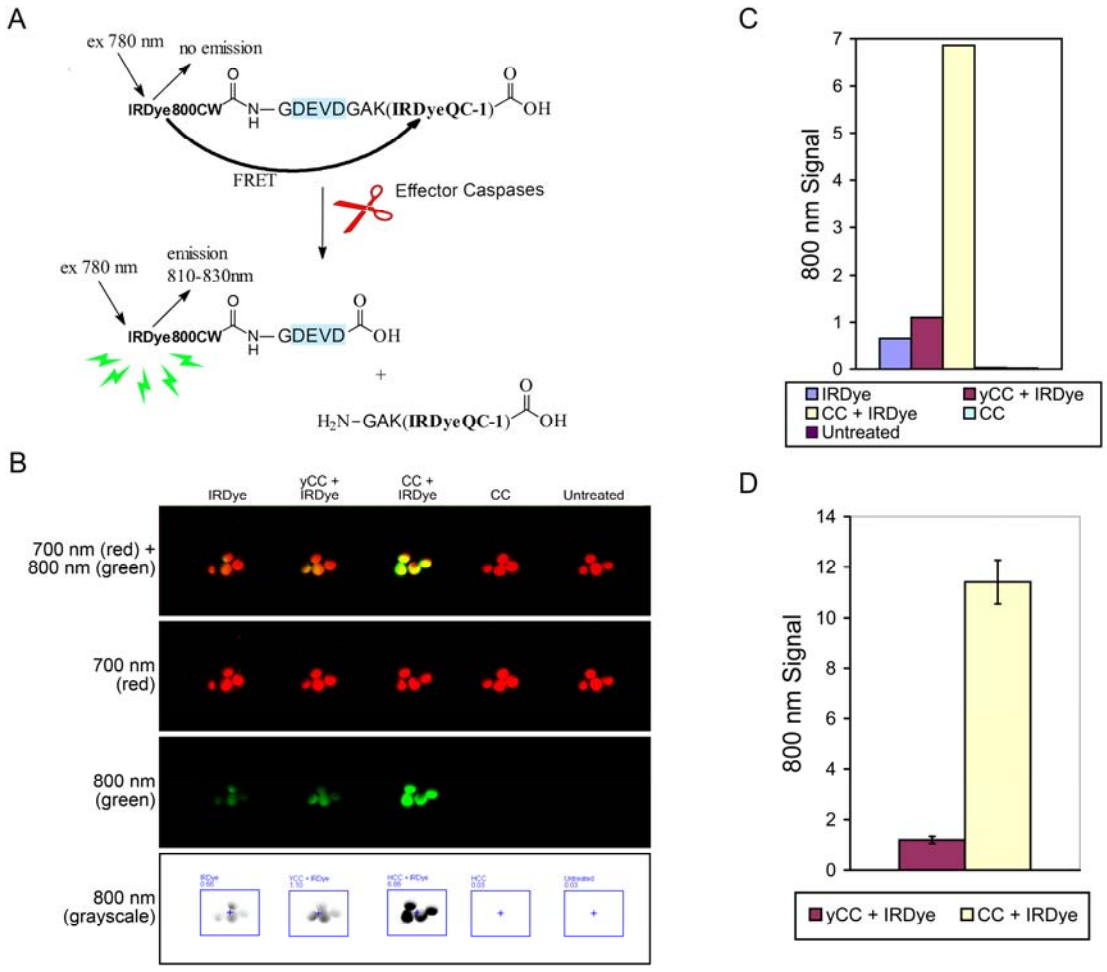


**Figure 5.1: Fluorescence can be detected in oocytes microinjected with the IRDye and cytochrome *c*.**

**Figure 5.1:** **A**, Schematic of the LI-COR IRDye® 800CW/QC-1 CSP-3, which contains a non-fluorescent quencher (IRDyeQC-1) conjugated to a donor (IRDye800CW) by a DEVD-containing peptide. Proteolytic cleavage by active effector caspases separates the dyes, abolishing fluorescence resonance energy transfer (FRET) thereby restoring the donor dye fluorescence. **B**, Oocytes were injected as indicated and imaged 30 minutes later. yCC, yeast cytochrome *c,* and CC, cytochrome *c,* both injected at 67 nM/oocyte. **C**, Graphical representation of quantitated signal in the 800 nm channel from **B**. **D**, Mean fluorescence in the 800 channel from 21 independent microinjection experiments of IRDye with either yCC or CC is displayed +/- S.E.M.

suitable for detecting caspase activation in intact *Xenopus* oocytes, we microinjected oocytes with cytochrome *c* and the IRDye. As controls, we microinjected either IRDye, cytochrome *c*, or IRDye and *Saccharomyces cerevisiae* cytochrome *c* (yeast cytochrome *c*), which is structurally similar to mammalian cytochrome *c* but lacks the ability to trigger caspase activation (Yu et al., 2001). The NIR fluorescence of microinjected (or untreated control) oocytes was imaged and results are shown in figure 5.1B. Signal detected in the 700 nm channel was caused by oocyte autofluorescence (each red spot represents a single oocyte) while the 800 nm signal resulted from fluorescence of cleaved IRDye, with intense signal emanating from oocytes co-injected with cytochrome *c* and the IRDye (Figure 5.1C). These data strongly suggest that this method is well-suited for detecting caspase activity in intact oocytes. Designating the signal obtained from oocytes co-injected with yeast cytochrome *c* and IRDye as background, oocytes co-injected with cytochrome *c* and IRDye reliably yielded a 9-fold signal increase above background when imaged 30 minutes to 1 hour after microinjection (Figure 5.1D).

To demonstrate that the observed oocyte fluorescence truly reflected caspase activation, we first asked whether the signal could be negated by a caspase inhibitor or induced by factors that trigger the release of endogenous cytochrome *c*. Microinjection of the broad-spectrum caspase inhibitor z-VAD-fmk inhibited the signal while microinjection of tBid, a truncated form of Bid that induces cytochrome *c* release from mitochondria (Li et al., 1998), produced a signal comparable to that of the microinjected cytochrome *c* (Figure 5.2A). Furthermore, expression of Bok, a multi-domain pro-

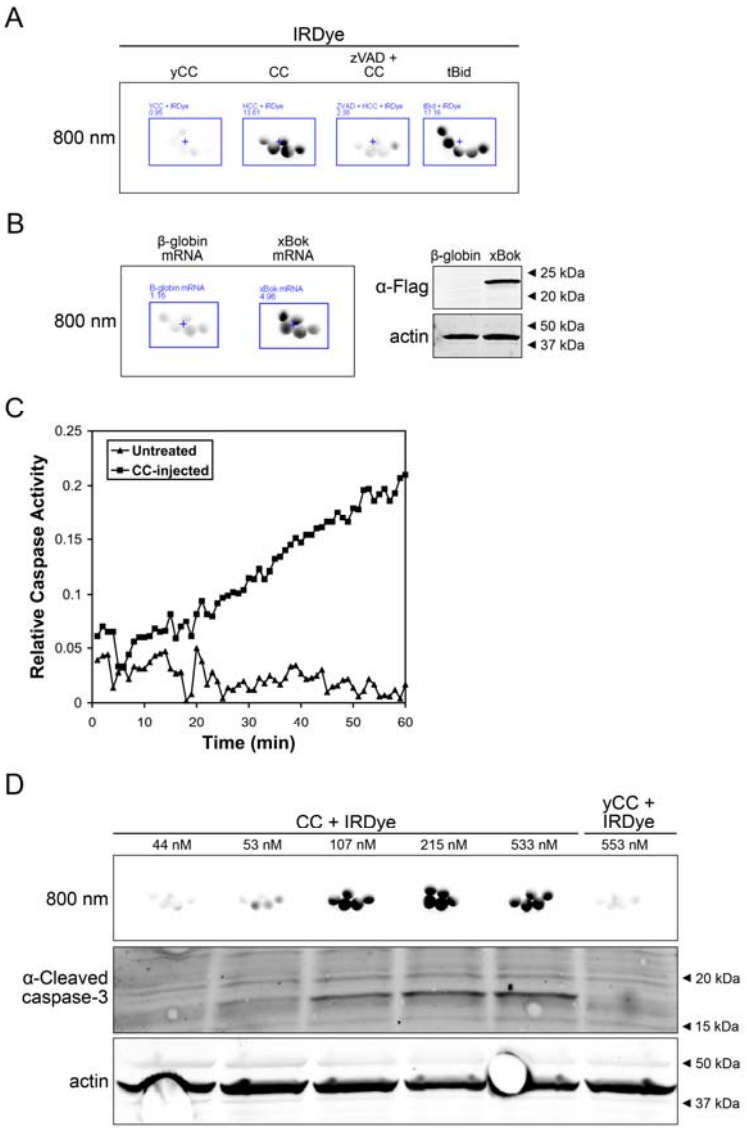


**Figure 5.2: Oocyte fluorescence is due to activation of effector caspases.**

**Figure 5.2:** **A**, Oocytes were injected with the IRDye and either yCC (267 nM), CC (267 nM), CC (267 nM) + z-VAD-fmk, or tBid and imaged after 1 hour. **B**, (Left) IRDye and 20 ng of either B-globin or flag-tagged Xenopus Bok (xBok) mRNA was injected into oocytes, allowed to express for 5 hours at room temperature and them imaged. (Right) Oocyte lysates immunoblotted with anti-flag antibody demonstrated xBok expression. **C**, Cell-free lysates were prepared from untreated or CC-injected oocytes, and analyzed for caspase activity over time after the addition of the colorimetric caspase substrate Ac-DEVD-pNA. **D**, (Top) Oocytes were injected with the IRDye and increasing doses of CC or yCC and imaged after 1 hour. (Bottom) Lysates prepared from these oocytes immunoblotted for active caspase 3.

apoptotic member of the Bcl-2 family implicated in cell death in the ovary (Hsu et al., 1997), triggered apoptosis in oocytes that could be detected by the IRDye signal (Figure 5.2B). Additionally, we prepared cell-free lysates from cytochrome *c*-microinjected oocytes to confirm the presence of active caspases, which we analyzed using both an *in vitro* colorimetric caspase assay (Figure 5.2C) and immunoblotting of active caspase-3 (Figure 5.2D). In aggregate, these data validate microinjection of the IRDye as a robust technique for imaging effector caspase activity within intact oocytes.

### 5.2.2 Caspases are rapidly activated and long-acting, but are required for a limited period of time to ensure cell death

The morphological changes that occur during apoptosis in *Xenopus* oocytes have been described previously (Bhuyan et al., 2001). In response to microinjected cytochrome *c,* oocytes initially appear unchanged, but approximately two hours post-injection they develop mottling of the animal pole pigment (Figure 5.3A). Once an oocyte exhibits this characteristic morphological feature it will invariably die, but it is thought that caspase activation commits the cell to an apoptotic death prior to any detectable change in morphology (Shi, 2002). Caspase activation in response to cytosolic cytochrome *c* is thought to be a rapid event (Berger et al., 2006), and indeed, the IRDye-based in vivo oocyte caspase assay characterized above yielded detectable fluorescence within five minutes of cytochrome *c* microinjection (Figure 5.3B). This IRDye-based signal was detected for more than twenty-four hours after microinjection, suggesting that the cleaved IRDye remained stable within the dying cell (Figure 5.3C). Microinjection of cytochrome *c* alone followed by microinjection of the IRDye at various time points resulted in a

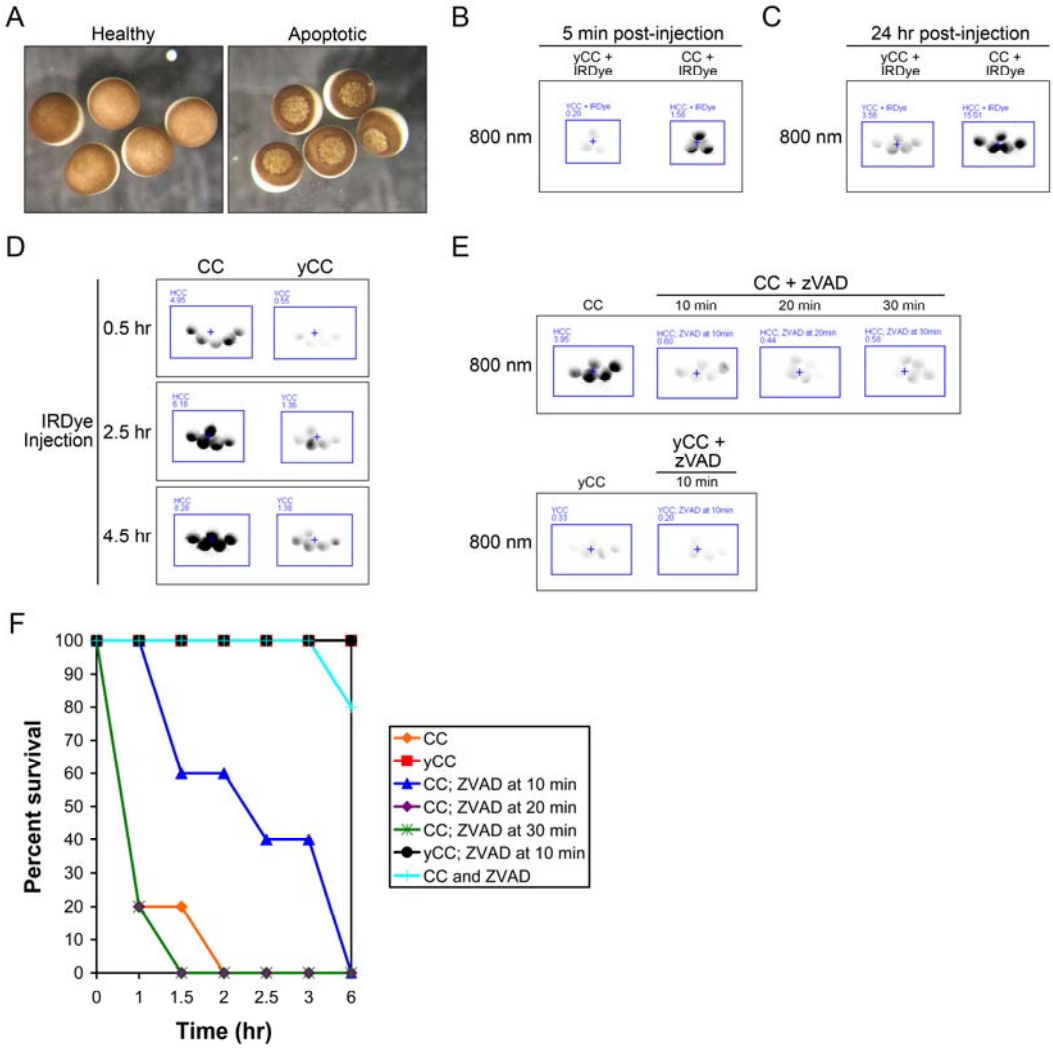


**Figure 5.3: Caspases are rapidly activated in response to cytochrome *c;* caspases remain active for hours although their activity is only required for 10 minutes to ensure apoptosis.**

**Figure 5.3:** **A**, Oocytes were injected with yCC (healthy) or CC (apoptotic) at 106 nM, and photographed 3 hours later. **B**, Oocytes microinjected with IRDye and either yCC or CC at 67 nM were imaged for fluorescence after 5 minutes. **C**, Oocytes microinjected with IRDye and either yCC or CC at 533 nM were imaged after 24 hours. **D**, Oocytes microinjected with either CC or yCC at 80 nM at t=0 were then injected with IRDye at various times indicated, and imaged 30 minutes later. **E**, CC or yCC was microinjected at 533 nM at t=0, then IRDye and z-VAD-fmk were injected at times indicated and then imaged 30 minutes later. **F**, Survival curve based on observation of apoptotic morphology of oocytes that had been treated as described in **E**.

fluorescent signal for at least 4.5 hours after exposure to cytochrome *c,* suggesting that caspases remain active and capable of cleaving substrates throughout the apoptotic process (Figure 5.3D).

In order to evaluate how long caspase activity must be maintained to cause apoptotic death (i.e., the "point of no return") we microinjected cytochrome *c* followed by co-injection of IRDye and z-VAD-fmk at 10 minute intervals. As shown in Fig 3E, z-VAD-fmk effectively inhibited caspase activity as detected by quenching of detectable IRDye fluorescence. Remarkably, cytochrome *c*-injected oocytes whose caspase activity was inhibited after 10, 20 or 30 minutes all exhibited apoptotic death, with the time to development of apoptotic morphology unchanged in the 20 and 30 minute groups and only slightly delayed in the 10 minute group (Figure 5.3F). These data suggest that as little as 10 minutes of caspase activity is sufficient to promote cleavage of critical substrates and ensure death of the oocyte.

### 5.2.3 Inhibitor of apoptosis proteins serve as a brake to apoptosis in the oocyte

During the course of these studies, we observed the presence of a threshold value for intracellular cytochrome *c* concentration, below which caspases did not become active and oocytes remained healthy; this cytochrome *c* threshold seems to fall between 50 and 100 nM, (Figure 5.2D). These data suggested either that there must be a "buffer" preventing caspase activity in these cells and/or that the oocyte can tolerate a certain degree of caspase activity. In some systems (e.g., *Drosophila*), IAPs appear to play a critical role in determining cell survival/death. In vertebrates, it appears that IAPs play

variable cell-type-specific roles, with a particular importance in setting the apoptotic threshold in differentiating cells such as maturing neuronal cells, which harbor low levels of Apaf-1 (Wright et al., 2004). We hypothesized that IAP proteins might play a heretofore unsuspected role in setting the apoptotic threshold in the oocyte. To test this, we first confirmed expression of the two IAPs that have been described in *Xenopus,* XLX and xXIAP (data not shown) (Holley et al., 2002, Tsuchiya et al., 2005). We then microinjected oocytes with a sub-threshold dose of cytochrome *c* and Smac, an inhibitor of IAP function (Deshmukh et al., 2002). Based on IRDye fluorescence, Smac addition substantially lowered the dose of cytochrome *c* required to induce caspase activation while heat-inactivated Smac had no effect (Figure 5.4A). In the presence of Smac, titration of the cytochrome *c* concentration to below 25 nM resulted in a failure of caspases to activate, suggesting the presence of a residual threshold that is IAP-independent (Figure 5.4B).

Careful analysis of the cytochrome *c* titration studies revealed that individual oocytes varied in their response to a peri-threshold dose. For example, in one particular batch of oocytes, 90 nM cytochrome *c* induced caspase activation in 30% of oocytes, with IRDye fluorescence of 3 apoptotic and 3 living oocytes displayed in figure 5.4C. Unfortunately, we were unable to evaluate IAP levels directly in these two sub-populations because IAPs are rapidly degraded by active caspases and it is impossible to predict prior to cytochrome *c* microinjection which oocytes will survive and which will die (Figure 5.4D). As we have previously reported, an endogenous apoptotic program in

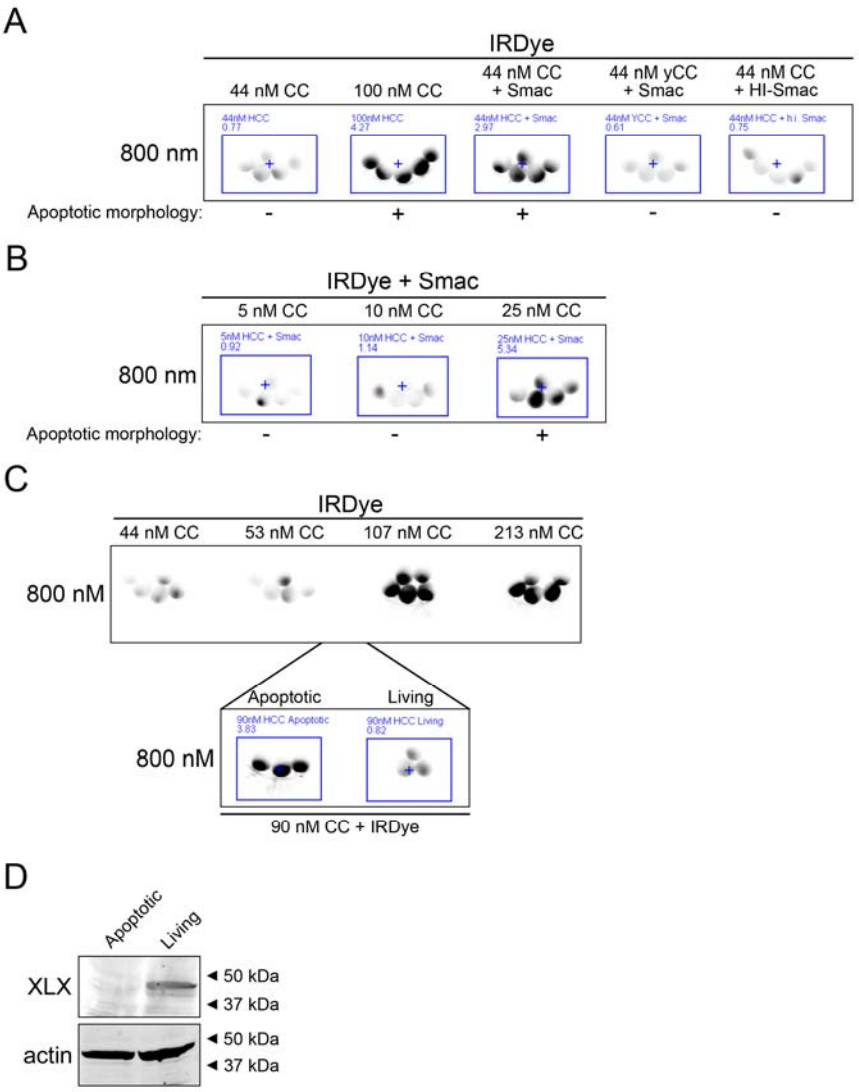


**Figure 5.4: Inhibitor of apoptosis proteins contribute to setting the cytochrome *c* threshold in oocytes.**

**Fgure 5.4:** **A**, Oocytes were microinjected with IRDye and either sub-threshold CC (44 nM), supra-threshold level of CC (107 nM), 44nM CC plus Smac protein, 44nM yCC plus Smac, or 44nM CC plus Smac that had been heat-inactivated by heating at 95°C for 5 minutes (HI-Smac) and then imaged after 40 minutes. **B**, Low doses of CC were injected with the IRDye and Smac and imaged after 30 minutes. **C**, Oocytes were injected with IRDye and increasing doses of CC and imaged after 45 minutes. The same batch of oocytes was re-injected with IRDye and 90nM CC, observed for apoptotic morphology and then 3 apoptotic and 3 living oocytes were imaged for fluorescence. **D**, Lysates were prepared from the apoptotic and living oocyte groups described in **C** and then immunoblotted for XLX.

oocytes, including mitochondrial cytochrome *c* release and caspase activation, is manifested when they are incubated on the bench, at least in part because they exhaust nutrient stockpiles required for viability (Nutt *et al.,* 2005). We have observed that the presence of Smac hastens the induction of apoptosis in oocytes aged on the bench (data not shown), further supporting the hypothesis that IAP levels function as a brake to apoptosis in the oocyte.

### 5.2.4 Meiotic oocytes develop resistance to cytochrome *c,* and death of oocytes arrested in meiosis is caspase-independent

Stage VI *Xenopus* oocytes are arrested in G2 of the cell cycle. Treatment with progesterone (PG) induces oocyte maturation, which is marked by germinal vesicle breakdown (GVBD) and high cdc2 activity indicative of re-entry into the cell cycle (Humphrey et al., 2005). GVBD results in a sharply demarcated loss of pigment in the animal pole (Maller, 2001), which, although distinct from apoptotic morphology, renders visual determination of whether a meiotic oocyte (post-GVBD) is undergoing apoptotic death challenging (Figure 5.5A). Using cell-free systems, we and others have reported that a meiotic state (M-phase) engenders resistance to cytochrome *c*-induced caspase activation (Allan and Clarke, 2007; Greenwood and Gautier, 2007; Kornbluth, 2002). A comparison of IRDye fluorescence in immature and mature (post-GVBD) oocytes microinjected with cytochrome *c* confirmed that sensitivity to cytochrome *c* decreases with maturation (Figure 5.5B). Approximately 30 minutes after stimulation with PG but well before GVBD, PG-treated and control oocytes displayed comparable sensitivity to cytochrome *c,* demonstrating that PG is not simply disrupting the IRDye-based assay, and

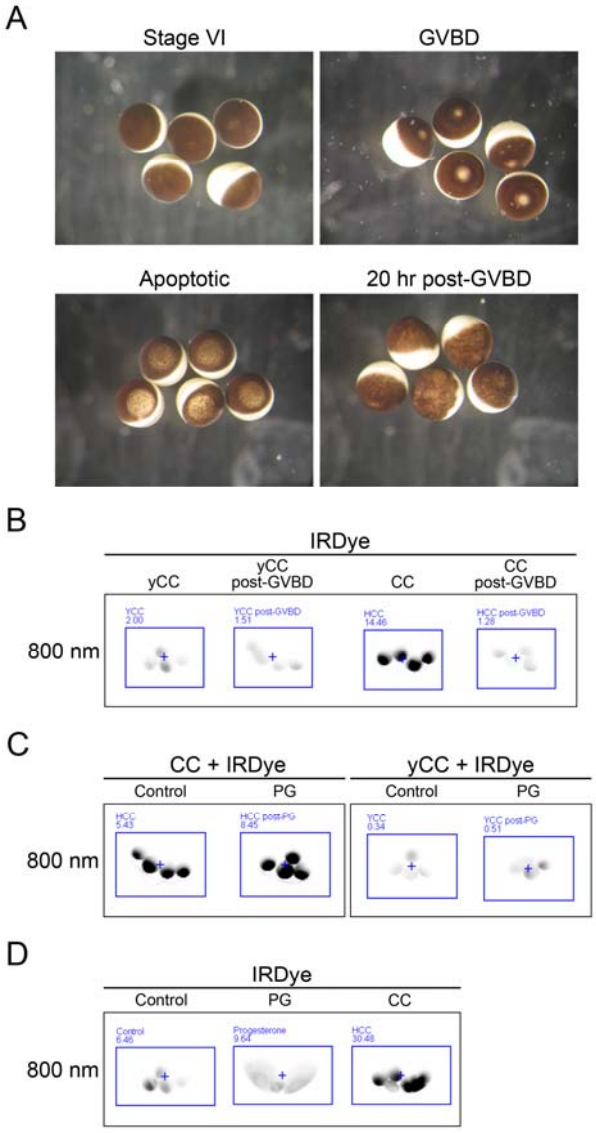


**Figure 5.5: Progesterone-induced oocyte maturation decreases sensitivity to cytochrome *c*.**

**Figure 5.5:** **A**, Reflected light images of oocytes as indicated. **B**, Oocytes were treated with progesterone and allowed to mature until GVBD, approximately 5 hours. Post-GVBD or control-treated oocytes were then injected with the IRDye and yCC or CC (at 67 nM), and then imaged after 1 hour. **C**, Oocytes were treated with progesterone for 30 minutes before injecting them or control-treated oocytes with the IRDye and yCC or CC (at 533 nM), and imaged after 1 hour. **D**, Oocytes were treated with progesterone or control, microinjected with IRDye after GVBD and then imaged for fluorescence 24 hours after progesterone treatment. Oocytes injected at the same time with IRDye and CC at 67 nM were included as a positive control.

strengthening the notion that resistance develops with entry into M-phase (Figure 5.5C). Notably, mature oocytes, arrested in meiosis II, that are not fertilized within several hours will die (Figure 5.5A). To determine if such death is caspase-mediated, we evaluated IRDye-based fluorescence over time in PG-treated oocytes. We observed that even 24 hours after PG treatment, when oocytes appeared, by morphological criteria, to be dying there was no indication of caspase activity based on the absence of IRDye fluorescence (Figure 5.5D), suggesting that death in these oocytes proceeds by a process other than classical apoptosis.

### 5.2.5 Apoptosis is not cell-autonomous in the early *Xenopus* embryo

We sought to extend our studies beyond the oocyte to determine if we could image caspase activation in the early embryo and to investigate if there were novel features of the apoptotic program at early times post-fertilization. Indeed, caspase activity was detected in fertilized eggs microinjected with IRDye and cytochrome *c* (Figure 5.6A). Further, individual blastomeres within the embryo were visualized, as in figure 5.6A, where it was evident that IRDye fluorescence was present in both blastomeres, as would be expected since microinjection occurred prior to cell division. In embryos with two blastomeres, we microinjected a single blastomere with IRDye and cytochrome *c,* and fluorescence was detected within half of the embryo, suggesting that the signal and therefore caspase activation was localized to the microinjected half of the embryo (Figure 5.6B). Surprisingly, under these circumstances morphological death occurred not only in the microinjected half of the embryo but also in the un-injected half, albeit with a slightly

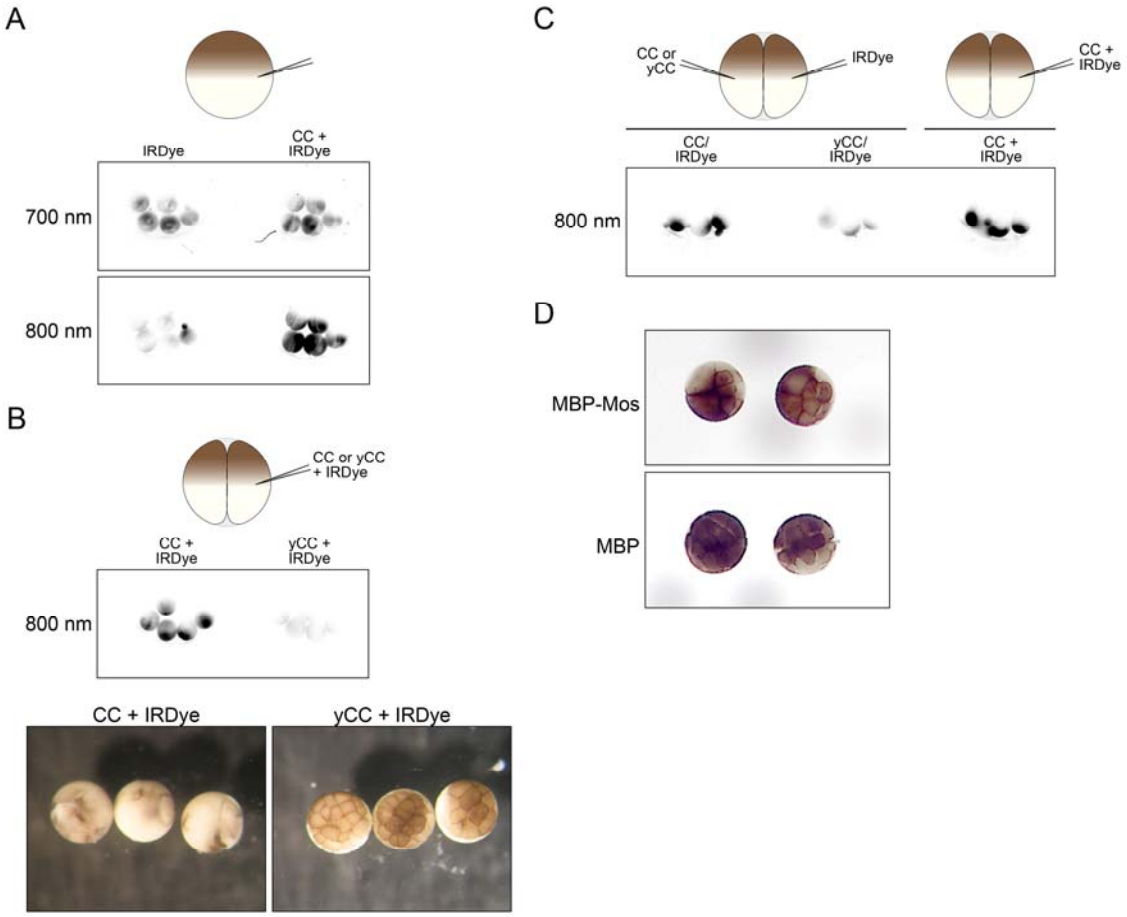


**Figure 5.6: Cytochrome *c*-induced apoptosis in the early embryo is not cell-autonomous.**

**Figure 5.6: A,** Fertilized eggs were injected prior to the first cell cleavage with the IRDye or IRDye and CC and then imaged during the 2-cell stage. Autofluorescence is shown in the 700 nm channel and caspase activity in the 800 nm channel. **B,** One blastomere of a two-cell embryo was microinjected with IRDye and either CC or yCC (at 270 nM). **Top,** injected embryos were imaged after 30 minutes (approximately 3 hours after fertilization). **Bottom,** photographs were taken of the embryos 4 hours after fertilization. **C,** Embryos were injected as indicated and then imaged 30 minutes later. **D,** Photograph of Mos-arrested embryos, with left half arrested while right half of embryos continue to divide.

delayed time course (Figure 5.6B). In order to determine whether the observed death of the un-injected blastomere involved caspase activity, we microinjected one blastomere with cytochrome *c* and the other with IRDye. Caspase-mediated fluorescence was detected in the IRDye-injected side, suggesting that cytochrome *c* introduction into one half of the embryo caused caspase activation on the opposite side (Figure 5.6C).

One explanation for this phenomenon would be movement of cytochrome *c* from one blastomere to the other via cytoplasmic bridges, which have been reported in the early *Xenopus* embryo (Byers and Armstrong, 1986; Cardellini et al., 1988; Landesman Y et al., 2000). To evaluate whether we could detect the presence of cytoplasmic bridges, we performed a series of experiments utilizing microinjection of cell cycle-arresting proteins and fluorescent dyes. Initially we used Mos protein, which has been previously shown to arrest the development of one half of an embryo when microinjected (Sagata et al., 1989), and confirmed that in our hands we observe arrest of only one side of the embryo (Figure 5.6D).

Next, we took advantage of two fluorescent dextrans, one approximating the molecular weight of the IRDye (dextran, AF680 3000 MW) and one roughly the size of cytochrome *c* (dextran, AF680 10000 MW). Patterns of fluorescence in microinjected fertilized eggs versus single blastomeres of 2-cell embryos were readily distinguishable, yielding a diffuse or partitioned signal, respectively (Figure 5.7A). We then microinjected embryos at the two-cell stage, one blastomere receiving cytochrome *c* and the 3000MW fluorescent dextran, and the opposite blastomere receiving the IRDye. As shown in

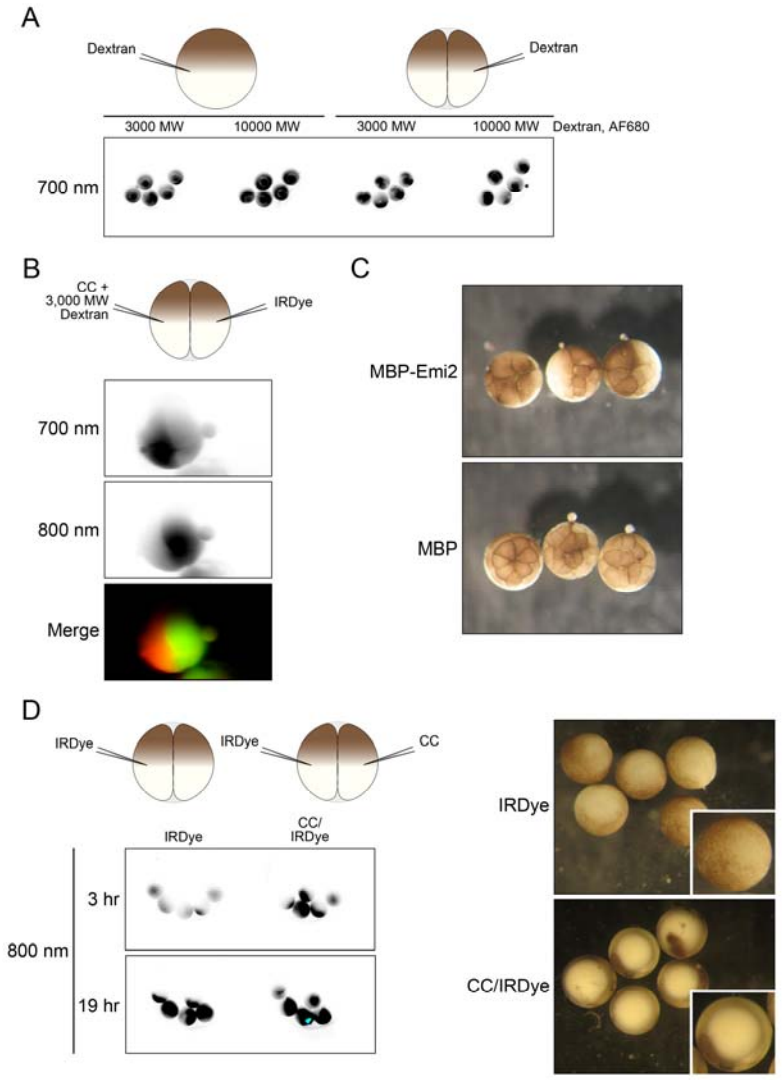


**Figure 5.7: Cytoplasmic transfer between blastomeres prevents cell-autonomous apoptosis.**

**Figure 5.7: A**, Fluorescent dextrans were injected as indicated and then embryos were imaged 30 minutes later. **B**, One embryo injected as indicated and imaged 30 minutes later. Signal in the 700 nm channel represent fluorescent dextran and signal in the 800 nm channel represents IRDye cleavage. **C**, Emi2 mutant protein was injected into one blastomere at the two-cell stage and photographs were taken approximately 4 hours post-fertilization. The embryo on the left demonstrates full arrest. **D,** Embryos were injected as indicated (approximately 2 hours post-fertilization) and imaged for fluorescence at the indicated times after fertilization. (Right) Photographs of the embryos 19 hours post-fertilization, confirming IRDye-injected embryos are dividing normally and show no signs of apoptosis.

Figure 5.7B, images of a single embryo illustrate 700 nm channel signal on one side (fluorescent dextran) and 800 nm channel signal on the other side (fluorescent IRDye), demonstrating that transfer of dyes either does not occur or is not detectable with this methodology. Finally, we microinjected a concentrated preparation of an active, non-degradable fragment of Emi2 protein (aa 489-651 T545,551A), known to inhibit the anaphase promoting complex, inducing a cell-cycle arrest similar to that of Mos protein (Tung et al., 2005). In the large majority microinjected embryos we observed the expected arrest of one half of the embryo, though in roughly one-third of cases we observed arrest of the entire embryo, which most likely reflects transfer of Emi2 across cytoplasmic bridges (Figure 5.7C). Collectively, these data strongly suggest that apoptosis in the early embryo is not cell-autonomous as it is in later embryogenesis and adulthood, but whether this reflects a signaling pathway that links blastomeres of the early embryo or a true cytoplasmic linkage that is below detection by fluorescent dye imaging is not clear. However, these data are consistent with the notion that it is preferable to eliminate the entire embryo when apoptosis initiates in a single cell at a point in development when the dying cell represents a significant portion of the embryo.

## 5.3 Discussion

We employed microinjection of an NIR dye caspase substrate to measure caspase activity in individual, living *Xenopus* oocytes and early embryos in real-time. This assay provides quantitation of caspase activity that can be obtained rapidly (and repeatedly over time), and is easily distinguishable from oocyte maturation-induced GVBD. Relative to

the traditional *Xenopus* cell-free system, this approach enables evaluation of individual cells, and has the unique strength of being able to monitor caspase activity and morphological apoptotic death in oocytes and developing embryos as separable entities (Figure 5.3E and F; Figures 6 and 7).

The *Xenopus* oocyte is easily microinjected and NIR imaging can be performed immediately following exposure to cytosolic cytochrome *c*. This enables us to address questions that have been technically impractical, a strength that is illustrated by our studies probing caspase activation kinetics. These experiments confirm that caspases become activated extremely rapidly in response to cytochrome *c* (in under five minutes). Additionally, we investigated whether continued caspase activity is required to cause apoptosis. Our data indicate that even short-term activation of caspases (as brief as 10 minutes of exposure to cytosolic cytochrome *c*) causes an oocyte to die via apoptosis, suggesting that only caspase substrates cleaved within this timeframe are essential for cell dismantling. In light of the vast number of identified caspase substrates (Lüthi and Martin, 2007; Dix et al., 2008; Mahrus et al., 2008) and the uncertainty of precisely how caspase-mediated proteolysis translates into organized cellular breakdown (Taylor et al., 2008), this result yields insight into how caspase substrates might be prioritized for further functional characterization.

In addition to the cytochrome *c*-induced caspase activity described, we also observed significant fluorescence of embryos microinjected with IRDye alone by nineteen hours after fertilization (Figure 5.7D). Sublethal caspase activity has been

reported in *Xenopus* oocytes as well as in human preimplantation embryos (Arnault et al., 2008; Martinez et al., 2002), and we hypothesize that our observations reflect the accumulation of minimal amounts of active caspases present at any given time that become significant only in summation. It is unclear whether these minimal amounts of caspase activity are important for development or are simply an inexorable consequence of rapid cell division that is tolerated by the embryo. Regardless, this observation prompted us reflect upon our IAP studies, where we saw that IAP inhibition could decrease the amount of cytochrome *c* required to activate caspases. Perhaps the levels of IAPs endowed to an oocyte determine whether an embryo will be able to limit the amount of caspase activation to within a tolerable range. One intriguing possibility warranting further investigation is that IAP levels decrease with age, making older oocytes more prone to apoptotic death following fertilization.

A series of studies performed in *Xenopus* embryos refer to the presence of cytoplasmic bridges between daughter cells (Byers and Armstrong, 1986; Cardellini et al., 1988; Landesman Y et al., 2000). Our studies in which we microinject cytochrome *c* into individual blastomeres and cause entire embryo apoptosis support this idea. It is well known that checkpoint activation does not occur in embryos until after the mid-blastula transition (Wroble and Sible, 2005); one important reason for such a delay might be to prevent the triggering of apoptosis by minor cellular damage during a time when death of an individual blastomere would lead to death of the entire embryo. Conversely, in the presence of a cell-damaging stimulus sufficiently strong to warrant induction of cell death

in a single cell, it would likely be advantageous to rapidly induce death of the entire embryo to avoid significant developmental anomalies.

Although our experiments with microinjected cytochrome *c* and Emi2 strongly support the notion of communicating cytoplasms, we were unable to image this phenomenon using fluorescent dyes. So although this assay offers a powerful means for detecting caspase activity within a single cell, it may be that this imaging modality lacks the sensitivity required to detect a very weak signal when in direct proximity to a very strong one.

Although clearly advantageous for monitoring apoptosis as part of an inquiry into basic cellular and developmental processes, the technique presented here might also be employed as a screening modality to identify apoptotic regulators. The 96-well format combined with the ease of oocyte microinjection make this system poised for either medium-throughput or secondary screens. Given our previous reports suggesting that an apoptosome-stimulating therapeutic might be useful in the treatment of breast and brain tumors (Schafer et al*.,* 2006; Johnson et al., 2007), it may prove worthwhile to employ this assay to screen small-molecule libraries for a cytochrome *c* mimetic. Moreover, *Xenopus* oocytes have been used to good effect in screening small pool cDNA libraries for novel cell cycle regulators (Ferby et al., 1999). A similar approach, using the NIR dye as an apoptotic indicator, may allow identification of novel cell death-regulating proteins.

.

# 6. Conclusions and perspectives

In 1996, the laboratory of Xiaodong Wang reported the requirement of cytosolic cytochrome *c* for activation of apoptotic proteases in vertebrates (Liu *et al.,* 1996). Since that discovery the field of apoptosis has exploded, and we now have a well-established model for how cytochrome *c* functions to induce apoptosis in the cell. Release of mitochondrial cytochrome *c* is induced by pro-apoptotic Bcl-2 family members, which permeabilize the outer mitochondrial membrane. Cytosolic cytochrome *c* binds an adaptor protein Apaf-1, triggering dATP hydrolysis/exchange on Apaf-1 and spontaneous oligomerization of Apaf-1 to form the apoptosome. This heptameric protein complex recruits procaspase-9 and induces its activation. Caspase-9-bound apoptosome functions to activate effector caspases, which serve to dismantle the dying cell. Each of these steps can be regulated, ultimately determining whether or not a cell will undergo apoptosis.

Work from this dissertation contributes to a better understanding of how different cell-types, including cancerous cells, respond to cytosolic cytochrome *c.* We demonstrate that brain cancer cells maintain functional apoptotic machinery downstream of the mitochondria and are thus sensitive to cytochrome *c*-induced caspase activation. Conversely, differentiated cells of the central nervous system, including neurons and glia, display marked resistance to cytochrome *c* due to down-regulation of Apaf-1. This differential sensitivity provides a new target for selectively killing brain cancer cells: activation of the apoptosome. Although we have not yet developed an apoptosome-activating agent, we did develop a novel assay that measures caspase activity in intact

cells which we believe will be useful in screening compounds for cytochrome *c*-like apoptotic activity. Moreover, utilization of this assay to study apoptosis in the oocyte has furthered our understanding of the oocyte's response to cytosolic cytochrome *c* and the post-mitochondrial regulation of apoptosis in this system.

## 6.1 Sensitivity of brain cancer cells to cytochrome *c*-induced apoptosis

Data from chapter 3 of this dissertation demonstrate an unexpected sensitivity of brain tumors to postmitochondrial induction of apoptosis. We were particularly interested in studying brain cancer cells because sympathetic neurons had been shown to develop resistance to cytochrome *c*-mediated apoptosis during differentiation (Wright *et al.,* 2004). Our findings in isolated neurons from mature cerebellum and cortex confirmed this resistance, and we were able to further demonstrate that normal brain tissue, comprised of both neuronal and glial cell types, does not activate caspases in response to cytosolic cytochrome *c.* These data suggest that mature glial cells resemble differentiated neurons in their resistance to cytochrome *c.*

Conversely, cytosolic lysates from a variety of malignant brain cancers readily activate caspases in response to cytochrome *c.* Sensitivity to cytochrome *c* was not only observed in brain cancer cell lines but also in xenograft brain tumors and cancers from mouse models of both high-grade astrocytoma and medulloblastoma. We found that differences in Apaf-1 expression underlie this differential sensitivity to cytochrome *c,* with protein levels of Apaf-1 being high in brain cancer cells and nearly undetectable in normal brain. In these cell types, Apaf-1 protein abundance correlates with Apaf-1

mRNA levels and with levels of E2F1, a known transcriptional activator of Apaf-1. In brain cancer cells, E2F1 is found bound to the Apaf-1 promoter, suggesting that E2F1 contributes to the expression of Apaf-1.

In light of these data, we believe that the expression of Apaf-1 in brain tumors reflects the requirement for E2F1 to drive malignancy-associated cell cycle progression and proliferation. This model is corroborated by our observations that Apaf-1 abundance increases with increasing tumor grade, as a cancer becomes increasingly proliferative and de-differentiated. Although we did not examine the relationship between E2F1 levels and tumor grade, at least one clinical study of human glioblastoma has reported that lower E2F1 expression correlates with longer median survival (Alonso *et al.,* 2005). Similarly, since we believe that Apaf-1 levels mirror E2F1 levels in brain tumors, we might expect that Apaf-1 expression levels could provide prognostic information, particularly for patients with glioblastoma.

Perhaps it seems contradictory that a cancerous cell would upregulate a pro-apoptotic protein like Apaf-1 (or that high levels of Apaf-1 might actually be a negative prognostic indicator for survival). Indeed, how can a brain cancer cell afford to be vulnerable to cytochrome *c*-induced apoptosis? The simplest explanation is that brain cancer cells, which are known to be highly resistant to apoptotic stimuli, employ effective anti-apoptosis mechanisms that function upstream of the mitochondria. Thus, these cells are usually not exposed to cytosolic cytochrome *c* and so the presence of Apaf-1 does not hinder their survival. In fact, one study examining the effects of Apaf-1 in glioma cells

observed reduced cellular proliferation when Apaf-1 is knocked down with siRNA, suggesting that Apaf-1 expression might be beneficial for cell-cycle progression (Kugler *et al.,* 2005). However, more recent work by the laboratory of Guido Kroemer has identified loss of Apaf-1 as compromising the DNA damage checkpoint and causing chromosomal instability, leading to the proposal that Apaf-1 functions as a tumor suppressor (Zermati *et al.,* 2007; Mouhamad *et al.,* 2007). Based on these contradictory findings we believe that any nonapoptotic role of Apaf-1 remains ambiguous and may depend upon the cell-type in question. However, our work studying apoptosis in brain cancers suggests that brain tumor survival is not negatively influenced by the expression of Apaf-1.

## 6.2 Selectively killing brain tumor cells with cytochrome *c*

We were excited to observe that brain cancer cells are sensitive to cytochrome *c*-induced apoptosis, particularly in light of our data demonstrating marked resistance of mature brain tissue to cytochrome *c.* These results suggest that triggering apoptosis downstream of the mitochondria, by introducing cytochrome *c* to the cytosol, would selectively kill brain cancer cells while sparing the surrounding brain parenchyma. The work presented in chapter 4 of this dissertation was aimed at pursuing this possibility by attempting to develop an apoptosome-activating strategy that could ultimately be utilized clinically in the treatment of brain tumors.

Although our multi-tiered approach has been unsuccessful in developing a cytochrome *c*-based therapeutic, we did obtain several important findings that should

help direct future research in this area. First, we demonstrated that multi-drug-resistant glioblastoma and brain cancer stem cells express Apaf-1 and are sensitive to cytochrome *c*-induced apoptosis. These data indicate that an apoptosome-activating strategy should be effective in targeting brain cancer cell populations that are highly-resistant to conventional treatments. In terms of the drug-resistant glioblastoma cells, it has been assumed that temozolomide resistance occurs due to upregulation of the DNA repair enzyme AGT. However, patients treated with temozolomide plus $O^6$-BG to eliminate AGT activity fare just as poorly as those treated with temozolomide alone, suggesting the presence of an additional mechanism of drug resistance (Quinn *et al.,* 2009. Our results demonstrate that these cancers retain apoptotic potential downstream of the mitochondria and thus the block to apoptosis must lie somewhere upstream of this point. Although future research is necessary to elucidate additional mechanisms mediating drug-resistance in these cells, our findings are corroborated by a study reporting that drugs causing mitochondrial permeability (and thus cytochrome *c* release) induce apoptosis in temozolomide-resistant glioma cells (Lena *et al.,* 2009). With regard to our finding that Apaf-1 is expressed in brain tumor stem cells, we are encouraged by these data but were unable to obtain enough material to confirm the sensitivity of these cells to cytochrome *c*-mediated apoptosis. CD133+ glioma cells have recently been shown to preferentially activate the DNA damage checkpoint in response to radiotherapy, and inhibition of checkpoint kinases disrupted the radioresistant-mediated survival of these cells (Bao *et al.,* 2006). Although indirect, these results suggest that CD133+ glioma cells are capable

of undergoing cytochrome *c*-mediated apoptosis once upstream apoptotic inhibition has been released (e.g., checkpoint activation and DNA repair).

A second important finding was that cytochrome *c* peptide fragments are incapable of binding to Apaf-1 or inhibiting cytochrome *c*-induced caspase activation. These results highlight the importance of the three-dimensional structure of cytochrome *c* for its interaction with Apaf-1. Previous work from George McLendon's laboratory identifying residues on several faces of the cytochrome *c* structure as being critical for the interaction was suggestive of a three-dimensional binding interface, but more recent work reported that apocytochrome *c,* which lacks three-dimensional structure, maintains the ability to bind Apaf-1 (Yu *et al.,* 2001; Martin and Fearnhead, 2002; Martin *et al.,* 2004). Our results are consistent with the earlier work, and call into question the findings that apocytochrome *c* interacts with Apaf-1 and prevents cytochrome *c*-induced apoptosome formation. Further, our crosslinking studies identified an Apaf-1 breakdown product that is unrecognized by an Apaf-1 CARD antibody but remains capable of binding cytochrome *c.* Mass spectrometry analysis of this crosslinked product confirmed the presence of both Apaf-1 and cytochrome *c,* with no tryptic peptide sequence obtained from the first 150 amino acid residues of Apaf-1, consistent with a CARD-lacking Apaf-1 breakdown product in this sample (Zhou *et al.,* 1999). This result provides empirical evidence that the Apaf-1 CARD is not required for the cytochrome *c*—Apaf-1 interaction, which has long been the proposed model but without experimental demonstration (Shi, 2008). Of note, we believe our approach to use chemical crosslinking followed by mass

spectrometry as a means of mapping protein interaction sites is a valid one. Unfortunately, a tagged crosslinker that would enable sample encrichment for crosslinked peptides prior to mass spectrometry analysis is not yet commercially available. Once such an agent becomes obtainable we believe that this approach should be revisited in order to elucidate cytochrome *c*—Apaf-1 interaction surfaces.

Finally, we have developed a high-throughput screening modality that should enable the identification of compounds that act like cytochrome *c* to induce caspase activation in cytosolic lysates. This assay should register any agent capable of activating the apoptosome in the absence of cytochrome *c.* Secondary screens can determine if the compound acts in an Apaf-1-dependent manner, which would be our goal for selectively inducing apoptosis in brain cancer cells while sparing normal brain tissue. Only 8,000 small-molecules have been screened to date, and we are hopeful that continued screening will be successful in discovering promising compounds that could ultimately be developed as an anti-cancer therapeutic.

## 6.3 Cytochrome *c*-induced apoptosis in the oocyte and early embryo

Our desire to have multiple ways in which to screen compounds for apoptosome-activating function led us to develop an assay that measures caspase activity in the intact *Xenopus* oocyte. Our work validating this assay and applying it to the study of cytochrome *c*-induced apoptosis in the oocyte are presented as chapter 5 of this dissertation. The assay itself utilizes a near-infrared caspase substrate that fluoresces only after being cleaved by active effector caspases. We were able to demonstrate that

microinjection of cytochrome *c* into oocytes induces the rapid development of oocyte fluorescence, and this fluorescence is due to activation of caspases. We further show that we can monitor caspase activation induced by apoptotic stimuli that trigger the release of endogenous cytochrome *c*, such as tBid and Bok. We believe that these experiments illustrate the potential of this assay as a screening modality for discovering novel apoptotic regulators. This *in vivo* screening technique would be expected to identify any compound that induces mitochondrial cytochrome *c* release or mimics the action of cytochrome *c* to induce apoptosome formation. However, the assay could be easily modified to include microinjection of Bcl-$X_L$, which would serve to protect mitochondrial membrane integrity, thus enabling identification of only those compounds that induce apoptosis downstream of the mitochondria. In addition to screening small-molecule libraries, we have obtained a *Xenopus* oocyte cDNA library that has been successfully employed in the discovery of Ringo, a cdc2-binding protein with the ability to induce meiotic maturation in the oocyte (Ferby *et al.,* 1999). We believe that this assay could be utilized in a similar manner to identify novel apoptotic regulator proteins.

In addition to its potential as a screening modality, we believe that this assay enhances our ability to study the subtleties of apoptosis kinetics and regulation. For example, the technique enabled us to probe the kinetics of caspase activation in response to cytochrome *c.* We observed activation of caspases within five minutes of cytochrome *c* microinjection, and to our knowledge, these results are the first *in vivo* demonstration of the rapidity of cytochrome *c*-induced caspase activation. By microinjecting the caspase

inhibitor z-VAD-fmk at various time points following injection of cytochrome *c* we were able to demonstrate that ten minutes of caspase activity is sufficient for ensuring an apoptotic cell death. This result implies that ample substrates get cleaved by effector caspases within ten minutes to execute apoptotic cellular dismantling. Interestingly, this work supports the notion that caspase cleavage creates a novel proteome, possessing stable functionality within the dying cell (Dix *et al.,* 2008; Mahrus *et al.,* 2008). Future studies should focus on the earliest-cleaved caspase substrates and their mediation of cell breakdown.

We were also able to identify the presence of a minimal cytochrome *c* concentration required for inducing apoptosis in the oocyte and demonstrate that this threshold is established, at least in part, by IAPs. Outside of neuronal cells, the physiological significance of IAPs has remained controversial (Wright *et al.,* 2004). Here we show that IAPs in the oocyte help to establish a cytochrome *c* threshold, effectively determining how much mitochondria cytochrome *c* leakage must occur before triggering an apoptotic response. We believe a cytochrome *c* threshold is likely to be present in most cell types (and regulated by IAP levels), but has been difficult to test experimentally. Thus, we believe a major strength of the oocyte microinjection system is that it enables us to carefully control the precise amount of cytochrome *c* (or other proteins, such as the IAP inhibitor Smac) delivered to the cytosol.

Further, we compared cellular cytochrome *c* sensitivity in S-phase and M-phase oocytes, demonstrating for the first time *in vivo* that M-phase cells are significantly more

resistant to cytochrome *c* than cells in interphase. Although this phenomenon has been reported using the *Xenopus* cell-free extract system, our data offer confirmation in an intact cell. Phosphorylation of caspase-9 has been reported as the underlying mechanism for the observed mitotic protection from cytochrome *c*-induced apoptosis (Allan and Clarke, 2007). However, we believe that additional mechanisms are at work during M-phase that all contribute to apoptotic resistance. Ongoing work in the Kornbluth laboratory is establishing a role for multiple inhibitory protein phosphorylations, including caspase-2 and Apaf-1, in producing mitotic apoptotic resistance. The assay described in this work has aided those studies, and promises to be useful for additional studies examining the interplay between apoptosis and cell cycle regulation.

Finally, we show that cytochrome *c* is capable of inducing apoptosis of the early *Xenopus* embryo. Surprisingly, microinjection of a single blastomere with cytochrome *c* at the two-cell stage induces caspase activation of the opposite blastomere and resulting death of the entire embryo. These results suggest that apoptosis in the early embryo is not a cell-autonomous process, a phenomenon we attribute to the presence of cytoplasmic bridges connecting individual blastomeres. The notion that apoptosis, at certain developmental stages or in certain cell types, may not be a cell-autonomous process is an intriguing one. In addition to the implications for development, which we believe warrant further study, we also find that these results may aid in our understanding of apoptosis regulation in other cell-types. Interestingly, skeletal muscle in the adult exists as differentiated, syncytial cells (Sandri and Carraro, 1999); perhaps Apaf-1 down-

regulation observed in these tissues is physiologically important for preventing apoptosis of the entire syncytium in response to leaky cytochrome *c* within an individual muscle fiber (Madden *et al.,* 2007).

## 6.4 The cellular response to cytosolic cytochrome *c*

In healthy cells, cytochrome *c* exists in the mitochondrial intermembrane space, where it shuttles electrons between respiratory complexes III and IV. Apoptotic signaling induces permeabilization of the outer mitochondrial membrane, releasing cytochrome *c* into the cytosol. In many cells this single event functions like turning a switch: cytosolic cytochrome *c* binds Apaf-1, the apoptosome forms, caspase-9 is recruited and activated, leading to activation of effector caspases. This post-mitochondrial apoptosis signaling pathway is remarkably rapid and efficient. Using the cytosolic presence of a previously organelle-sequestered protein as a trigger for activating death proteases allows the cell to respond in an all-or-none fashion. As the "appropriateness" of an apoptotic stimulus is evaluated upstream of the mitochondria by Bcl-2 proteins, once cytochrome *c* is released the cell simply needs to execute the plan. Thus, the apoptotic machinery remains continuously poised, awaiting the cytochrome *c* trigger.

However, in certain types of cells a flip of the switch (cytosolic cytochrome *c*) fails to turn on the light (caspase activation). These cells are the postmitotic, long-lived cells of the CNS and muscle, in which accidental caspase activation and ensuing death of individual cells could impair function of the entire system. Down-regulation of Apaf-1 expression in these cells ensures resistance to any cytosolic cytochrome *c* because the

function of cytochrome *c* in the cytosol depends on the presence of Apaf-1. Not only does this strategy provide an effective means of apoptotic resistance but it also offers a sophisticated system for apoptotic regulation. In the face of severe DNA damage or other overwhelming stress, the cell can, over time, reactivate expression of Apaf-1 to allow a cytochrome *c*-mediated apoptotic death to occur.

Cancerous cells have all acquired the ability to evade apoptosis. In theory, this could result from an inhibition of apoptotic signaling either upstream or downstream of the mitochondria. In practice it seems that many forms of cancer prevent apoptosis signaling upstream of the mitochondria, such that cytochrome *c* is not released from the mitochondria in response to even intense apoptotic stimuli. Thus, the cancer cell has managed to dramatically change what deems an "appropriate" reason to undergo cell suicide. In such cases inhibition of post-mitochondrial apoptotic signaling is unnecessary, and the cells maintain expression of the apoptosome components (perhaps in part because the expression of these proteins is linked to cellular proliferation, which benefits the cancer). Primary cancers of the CNS appear to adhere to this model—although aggressive gliomas are resistant to chemotherapeutics that function to stimulate apoptosis upstream of the mitochondria, these cancers remain capable of activating caspases in response to cytosolic cytochrome *c.* Regardless of the variety of mechanisms at play in preventing cytochrome *c* release in these cells, the cellular response to cytochrome *c* remains intact. Maintained functionality of downstream apoptotic signaling in these types of cancers

could be exploited therapeutically with an agent that mimics the function of cytosolic cytochrome *c.*

The presence or absence of Apaf-1 in a cell determines the cellular response to cytochrome *c* in an absolute, yes/no manner. Additional post-mitochondrial modes of regulation serve more to influence the degree of apoptosome formation/caspase activation. Certainly the physiological relevance of these types of regulatory mechanisms is questionable unless prevention of apoptotic death can be readily demonstrated. Studying the cellular response to cytosolic cytochrome *c* in the *Xenopus* oocyte offers a valuable model system for evaluating post-mitochondrial apoptosis regulation. The oocyte is sensitive to cytochrome *c*-induced apoptosis, and the amount of cytochrome *c* delivered to the cytosol can be readily manipulated by microinjection. Using this approach, the amazing rapidity of cytochrome *c*-induced caspase activation can be measured (and manipulated). Importantly, IAPs prevent caspase activation in response to low doses of cytochrome *c,* demonstrating significance of this post-mitochondrial form of apoptosis regulation in the oocyte. Further, in addition to enhancing our ability to study the cellular response to cytochrome *c,* the *Xenopus* oocyte microinjection system enables us to identify compounds that mimic the function of cytosolic cytochrome *c.*

## 6.5 Concluding remarks

The data presented in this dissertation have furthered our knowledge of how different cell-types respond to cytosolic cytochrome *c.* We observed an unexpected sensitivity of brain tumor cells to induction of apoptosis with cytochrome *c* while normal

brain tissue is remarkably resistant. Mechanistically we have demonstrated this differential sensitivity is due to high Apaf-1 levels in the tumor tissue with almost no Apaf-1 in surrounding non-neoplastic brain tissue. The transcription factor E2F1 contributes to the high expression of Apaf-1 in brain tumors. These findings raise the exciting possibility of apoptosome activation as an anti-cancer therapeutic strategy, which we pursued in this dissertation. We were able to develop both a high-throughput cytosolic lysate screening modality and a microinjection-based intact cell assay to assess caspase activation in response to small-molecules or expressed proteins. Future work will aim to continue the screening process using these established techniques in order to identify compounds that could act like cytosolic cytochrome *c,* triggering apoptosis selectively in brain tumors while sparing the surrounding normal brain parenchyma.

# References

Acehan d, Jiang X, Morgan DG, Heuser JE, Wang X and Akey CW Three-dimensional structure of the apoptosome: implications for assembly, procaspase-9 binding, and activation. Mol Cell. 2002; 9: 423-432.

Adelson PD and Kochanek PM Head injury in children. J Child Neurol. 1998; 13: 2-15.

Agarwala SS and Kirkwood JM Temozolomide, a novel alkylating agent with activity in the central nervous system, may improve the treatment of advanced metastatic melanoma. Oncologist. 2000; 5: 144-151.

Allan LA and Clarke PR Phosphorylation of caspase-9 by CDK1/cyclin B1 protects mitotic cells against apoptosis. Mol Cell. 2007; 26: 301-310.

Allen JD, Zhang XD, Scott CL, Boyle GM, Hersey P, Strasser A Is Apaf-1 expression frequently abrogated in melanoma? Cell Death Differ. 2005; 12: 680-681.

Alonso MM, Fueyo J, Shay JW, Aldape KD, Jiang H, Lee OH, Johnson DG, Xu J, Kondo Y, Kanzawa T, Kyo S, Bekele BN, Zhou X, Nigro J, McDonald JM, Yung WK and Gomez-Manzano C Expression of transcription factor E2F1 and telomerase in glioblastomas: mechanistic linkage and prognostic significance. J Natl Cancer Inst. 2005; 97: 1589-1600.

Arnault E, Tosca L, Courtot AM, Doussau M, Pesty A, Finaz C, Allemand I and Lefèvre B Caspase-2(L), caspase-9, and caspase-3 during in vitro maturation and fragmentation of the mouse oocyte. Dev Dyn. 2008; 237: 3892-3903.

Back JW, de Jong L, Muijsers AO and de Koster CG Chemical cross-linking and mass spectrometry for protein structural modeling. J Mol Biol. 2003; 331: 303-313.

Bao Q and Shi Y Apoptosome: a platform for the activation of initiator caspases. Cell Death Differ. 2007; 14: 56-65.

Bao Q, Lu W, Rabinowitz JD and Shi Y Calcium blocks formation of the apoptosome by preventing nucleotide exchange in Apaf-1. Mol Cell. 2007; 25: 181-192.

Bao S, Wu Q, McLendon RE, Hao Y, Shi Q, Hjelmeland AB, Dewhirst MW, Bigner DD and Rich, JN Glioma stem cells promote radioresistance by preferential activation of the DNA damage response. Nature. 2006; 444: 756-760.

Bar EE, Chaudhry A, Farah MH and Eberhart CG Hedgehog signaling promotes medulloblastoma survival via BclII. Am J Pathol. 2007; 170: 347-355.

Bedikian AY, Millward M, Pehamberger H, Conry R, Gore M, Trefzer U, Pavlick AC, DeConti R, Hersh EM, Hersey P, Kirkwood JM and Haluska FG Bcl-2 antisense (oblimersen sodium) plus dacarbazine in patients with advanced melanoma: the Oblimersen Melanoma Study Group. J Clin Oncol. 2006; 24: 4738-4745.

Beere H, Wolf B, Cain K, Mosser D, Mahboubi A, Kuwana T, Tailor P, Morimoto R, Cohen G and Green D Heat-shock protein 70 inhibits apoptosis by preventing recruitment of procaspase-9 to the Apaf-1 apoptosome. Nat Cell Biol. 2000; 2: 469-475.

Bellamy, CO, Malcomson RD, Harrison DJ and Wyllie AH Cell death in health and disease: the biology and regulation of apoptosis. Semin Cancer Biol; 1995: 6: 3-16.

Berger AB, Witte MD, Denault JB, Sadaghiani AM, Sexton KM, Salvesen GS and Bogyo M Identification of early intermediates of caspase activation using selective inhibitors and activity-based probes. Molecular Cell. 2006; 23: 509-521.

Bhuyan AK, Varshnev A and Mathew MK Resting membrane potential as a marker of apoptosis: studies on Xenopus oocytes microinjected with cytochrome c. Cell Death Differ. 2001; 8: 63-69.

Bittigau P, Sifringer M, Pohl D, Stadthaus D, Ishimaru M, Shimizu H, Ikeda M, Lang D, Speer A, Olney JW and Ikonomidou C Apoptotic neurodegeneration following trauma is markedly enhanced in the immature brain. Ann Neurol. 1999; 45: 724-735.

Boatright KM, Renatus M, Scott FL, Sperandio S, Shin H, Pedersen IM, Ricci JE, Edris WA, Sutherlin DP, Green DR and Salvesen GS A unified model for apical caspase activation. Mol Cell. 2003; 11: 529-541.

Boehning D, Patterson RL, Sedaghat L, Glebova NO, Kurosaki T and Snyder SH Cytochrome c binds to inositol (1,4,5) triphosphate receptors, amplifying calcium-dependent apoptosis. Nat Cell Biol. 2003; 5: 1051-1061.

Boutz PL, Stoilov P, Li Q, Lin CH, Chawla G, Ostrow K, Shiue L, Ares M Jr and Black DL A post-transcriptional regulatory switch in polypyrimidine tract-binding proteins reprograms alternative splicing in developing neurons. 2007; 21: 1636-1652.

Broniscer A and Gajjar A Supratentorial high-grade astrocytoma and diffuse brainstem glioma: two challenges for the pediatric oncologist. Oncologist. 2004; 9: 197-206.

Brown GC and Borutaite V Regulation of apoptosis by the redox state of cytochrome c. Biochim Biophys Acta. 2008; 1777: 877-881.

Brunelle JK and Letai A Control of the mitochondrial apoptosis by the Bcl-2 family. J Cell Sci. 2009; 122: 437-441.

Burgess DH, Svensson M, Dandrea T, Gronlund K, Hammarquist F, Orrenius S and Cotgreave IA Human skeletal muscle cytosols are refractory to cytochrome c-dependent activation of type-II caspases and lack APAF-1. Cell Death Differ. 1999; 6: 256-261.

Byers TJ and Armstrong, PB Membrane protein redistribution during Xenopus first cleavage. The Journal of Cell Biology. 1986; 102: 2176-2184.

Cain K, Bratton SB and Cohen GM. The Apaf-1 apoptosome: A large caspase-activating complex. Biochimie. 2002; 84: 203-214.

Cain K, Brown DG, Langlais C and Cohen GM Caspase activation involves the formation of the apoptosome, a large (approximately 700 kDa) caspase-activating complex. J Biol Chem. 1999; 274: 22686-92.

Cain K, Langlais C, Sun XM, Brown DG and Cohen GM Physiological concentrations of K+ inhibit cytochrome c-dependent formation of the apoptosome. J Biol Chem. 2001; 276: 41985-41990.

Cantley LC and Neel BG New insights into tumor suppression: PTEN suppresses tumor formation by restraining the phosphoinositide 3-kinase/AKT pathway. Proc Natl Acad Sci USA. 1999; 96: 4240-4245.

Cardellini P, Rasotto MB, Tertoolen LGJ and Durston AJ Intercellular communication in the eight-cell stage of Xenopus laevis development: a study using dye coupling. Developmental Biology. 1988; 129: 265-269.

Cecconi F, Alvarez-Bolado G, Meyer BI, Roth KA and Gruss P Apaf1 (CED-4 homolog) regulates programmed cell death in mammalian development. Cell. 1998; 94: 727-737. Central Brain Tumor Registry of the United Sates Statistical report: Primary brain tumors in the United States 1998-2002. 2005; CBTR, Chicago.

Chai J, Shiozaki E, Srinivasula SM, Wu Q, Datta P, Alnemri ES and Shi Y Structural basis of caspase-7 inhibition by XIAP. Cell. 2001; 104: 769-780.

Chai J, Wu Q, Shiozaki E, Srinivasula SM, Alnemri ES and Shi Y Crystal structure of a procaspase-7 zymogen: mechanisms of activation and substrate binding. Cell. 2001; 107: 399-407.

Chakravarti A and Palanichamy K Overcoming therapeutic resistance in malignant gliomas: current practices and future directions. Cancer Treat Res. 2008; 139: 173-189.

Chandra D, Bratton SB, Person MD, Tian Y, Martin AG, Ayres M, Fearnhead HO, Gandhi V and Tang DG Intracellular nucleotides act as critical prosurvival factors by binding to cytochrome c and inhibiting apoptosome. Cell. 2006; 125: 1333-1346.

Chao Y, Shiozaki EN, Srinivasula SM, Rigotti DJ, Fairman R and Shi Y Engineering a dimeric caspase-9: a re-evaluation of the induced proximity model for caspase activation. PLoS Biol. 2005; 3:e183.

Chen YR, Meyer CF, Ahmed B, Yao Z and Tan TH Caspase-mediated cleavage and functional changes of hematopoietic progenitor kinase 1 (HPK1). Oncogene. 1999; 18: 7370-7377.

Cheng CK, Fan QW and Weiss WA PI3K signaling in glioma—animal models and therapeutic challenges. Brain Pathol. 2009; 19; 112-120.

Coldwell MJ, Mitchell SA, Stoneley M, MacFarlane M and Willis AE Initiation of Apaf-1 translation by internal ribosome entry. Oncogene. 2000; 19: 899-905.

Coleman ML, Sahai EA, Yeo M, Bosch M, Dewar A and Olson MF Membrane blebbing during apoptosis results from caspase-mediated activation of ROCK1. Nat Cell Biol. 2001; 3: 339-345.

Costanzo A, Merlo P, Pediconi N, Fulco M, Sartorelli V, Cole PA, Fontemaggi G, Fancuilli M, Schiltz L, Blandino G, Balsano C and Levrero M DNA damage-dependent acetylation of p73 dictates the selective activation of apoptotic target genes. Mol Cell. 2002; 9: 175-186.

Cotran RS, Kumar V and Collins T, eds. *Robbins Pathologic Basis of Disease, Sixth Ed.* Saunders Company, Philadelphia, 1999.

D'Amours D, Sallmann FR, Dixit VM and Poirier GG Gain-of-function of poly(ADP-robose) polymerase-1 upon cleavage by apoptotic proteases: implications for apoptosis. J Cell Sci. 2001; 114: 3771-3778.

Danial NN and Korsmeyer SJ Cell death: critical control points. Cell. 2004; 116: 205-219.

Deming PB, Schafer ZT, Tashker JS, Potts MB, Deshmukh M and Kornbluth S Bcr-Abl-mediated protection from apoptosis downstream of mitochondrial cytochrome c release. Mol Cell Biol. 2004; 24: 10289-10299.

Denault JB, Békés M, Scott FL, Sexton KM, Bogyo M and Salvesen GS Engineered hybrid dimeres: tracking the activation pathway of caspase-7. Mol Cell. 2006; 23: 523-533.

Deshmukh M, Du C, Wang X and Johnson EM Exogenous smac induces competence and permits caspase activation in sympathetic neurons. J Neurosci. 2002; 22: 8018-8027.

Deveraux QL and Reed JC IAP family protein—suppressors of apoptosis. Genes & Development. 1999; 13: 239-252.

Dickerson RE, Takano T, Eisenberg D, Kallai OB Samson L, Cooper A and Margoliash E Ferricytochrome c. I. General features of the horse and bonito proteins at 2.8 Å resolution. J Biol Chem. 1971; 246: 1511-1535.

Diekert K, IPMde Kroon A, Ahting U, Niggemeyer B, Neupert W, de Kruijff B and Lill R Apocytochrome c requires the TOM complex for translocation across the mitochondrial outer membrane. EMBO J. 2001; 20: 5626-5635.

Dihazi GH and Sinz A Mapping low-resolution three-dimensional protein structures using chemical cross-linking and Fourier transform ion-cyclotron resonance mass spectrometry. Rapid Commun Mass Spectrom. 2003; 17; 2005-2014.

Ditzel M, Wilson R, Tenev T, Zachariou A, Paul A, Deas E and Meier P Degradation of DIAP1 by the N-end rule pathway is essential for regulating apoptosis. Nat Cell Biol. 2003; 5: 467-473.

Dix MM, Simon GM and Cravatt BF Global mapping of the tophography and magnitude of proteolytic events in apoptosis. Cell. 2008; 134: 679-691.

Donovan M and Cotter TG Caspase-independent photoreceptor apoptosis in vivo and differential expression of apoptotic protease activating factor-1 and caspase-3 during retinal development. Cell Death Differ. 2002; 9: 1220-1231.

Downward J PI 3-kinase, Akt and cell survival. Semin Cell Dev Biol. 2004; 15; 177-182.

Dumont ME, Cardillo TS, Hayes MK and Sherman F Role of cytochrome c haem lyase in mitochondrial import and accumulation of cytochrome c in S. cerevisiae. Mol Cell Biol. 1991; 11: 5487-5496.

Dumont ME, Ernst JF and Sherman F Coupling of haem attachment to import of cytochrome c into yeast mitochondria. J Biol Chem. 1988; 263: 15928-15937.
Duronio V The life of a cell: apoptosis regulation by the PI3K/PKB pathway. Biochem J. 2008; 415: 333-344.

Earnshaw WC, Martins LM and Kaurmann SH Mammalian caspases: structure, activation, substrates, and functions during apoptosis. Annu Rev Biochem. 1999; 68: 383-424.

Ferby I, Blazquez M, Palmer A, Eritja R and Nebreda AR A novel p34(cdc2)-binding and activating protein that is necessary and sufficient to trigger G(2)/M progression in Xenopus oocytes. Genes Dev. 1999; 13: 2177-2189.

Fischer U, Janssen K and Schulze-Osthoff K Cutting-edge apoptosis-based therapeutics: a panacea for cancer? BioDrugs. 2007; 21: 273-297.

Fleming AB and Saltzman WM Clin Pharmacokinet. 2002; 41: 403-419.

Fortin A, Cregan SP, MacLaurin JG, Kushwaha N, Hickman ES, Thompson CS, Hakim A, Albert PR, Cecconi F, Helin K, Park DS and Slack RS APAF1 is a key transcriptional target for p53 in the regulation of neuronal cell death. J Cell Biol. 2001; 155: 207-216.

Freije WA, Castro-Vargas FE, Fang Z, Horvath S, Cloughesy T, Liau LM, Mischel PS and Nelson SF Gene expression profiling of gliomas strongly predicts survival. Cancer Res. 2004; 64: 6503-6510.

Fuentes-Prior P and Salvesen GS The protein structures that shape caspase activity, specificity, activation and inhibition. Biochem J. 2004; 384: 201-232.

Furukawa Y, Nishimura N, Furukawa Y, Satoh M, Endo H, Iwase S, Yamada H, Matsuda M, Kano Y and Nakamura M Apaf-1 is a mediator of E2F-1-induced apoptosis. J Biol Chem. 2002; 277: 39760-39768.

Galli R, Binda E, Organelli U, Cipelletti B, Gritti A, De Vitis S, Fiocco R, Foroni C, Dimeco F and Vescovi A Isolation and characterization of tumorigenic, stem-like neural precursors from human glioblastoma. Cancer Research. 2004; 64: 7011-7021.

Galluzzi L, Zamzami N, de La Motte RT, Lemaire C, Brenner C, Kroemer G Methods for the assessment of mitochondrial membrane permeabilization in apoptosis. Apoptosis. 2007; 12: 803-813.

Goldstein JC, Waterhouse NJ, Juin P, Evan GI and Green DR The coordinate release of cytochrome c during apoptosis is rapid, complete and kinetically invariant. Nat Cell Biol. 2000; 2: 156-162.

Goodrich LV, Milenković L, Higgins KM and Scott MP Altered neural cell fates and medulloblastoma in mouse patched tumors. Science. 1997; 277: 1109-1113.

Green DR and Amarante-Mendes GP The point of no return: Mitochondria, caspases, and the commitment to cell death. Results Probl Cell Differ. 1998; 24: 45-61.

Green DR and Reed JC Mitochondria and apoptosis. Science. 1998; 281: 1309-12.

Greenwood J and Gautier J XLX is an IAP family member regulated by phosphorylation during meiosis. Cell Death Differ. 2007; 14: 559-567.

Hanahan D and Weinberg RA The hallmarks of cancer. Cell. 2000; 100: 57-70.

Hao Z, Duncan GS, Chang CC, Elia A, Fang M, Wakeham A, Okada H, Calzascia T, Jang Y, You-Ten A, Yeh WC, Ohashi P, Wang X and Mak TW Specific ablation of the apoptotic functions of cytochrome c reveals a differential requirement for cytochrome c and Apaf-1 in apoptosis. Cell. 2005; 121: 579-591.

Harlin H, Reffey SB, Duckett CS, Lindstein T and Thompson CB Characterization of XIAP-deficient mice. Mol Cell Biol. 2001; 21: 3604-3608.

Harris CC p53 tumor suppressor gene: from the basic research laboratory to the clinic—an abridged historical perspective. Carcinogenesis. 1996; 17: 1187-1198.

Hart MG, Grant R, Garside R, Rogers G, Somerville M and Stein K Temozolomide for high grade glioma. Cochrane Database Syst Rev. 2008: CD007415.

Hermanson M, Funa K, Hartman M, Claesson-Welsh L, Heldin CH, Westermark B and Nistér M Platelet-derived growth factor and its receptors in human glioma tissue: expression of messenger RNA and protein suggests the presence of autocrine and paracrine loops. Cancer Res. 1992; 52: 3213-3219.

Hill MM, Adrain C, Duriez PJ, Creagh EM and Martin SJ Analysis of the composition, and activity of native Apaf-1 apoptosomes. EMBO J. 2004; 23: 2134-2145.

Holley CL, Olson MR, Colón-Ramos DA and Kornbluth S Reaper eliminates IAP proteins through stimulated IAP degradation and generalized translational inhibition. Nat Cell Biol. 2002; 6: 439-444.

Hsu SY, Kaipia A, McGee E, Lomeli M and Hsueh AJ Bok is a pro-apoptotic Bcl-2 protein with restricted expression in reproductive tissue and heterodimerizes with selective anti-apoptotic Bcl-2 family members. Proc Natl Acad Sci USA. 1997; 94: 12401-12406.

Hu Y, Ding L, Spencer DM and Núñez G WD-40 repeat region regulates Apaf-1 self-association and procaspase-9 activation. J Biol Chem. 1998. 273: 33489-33494.

Huang Y, Park YC, Rich RL, Segal D, Myszka DG and Wu H Structural basis of caspase inhibition by XIAP: differential roles of the linker versus the BIR domain. Cell. 2001; 104: 781-790.

Humphrey T, Humphrey TC and Brooks G Cell cycle control: mechanisms and protocols. Humana Press, 2005.

Huntly BJ and Gilliland DG Cancer biology: summing up cancer stem cells. Nature. 2005; 435: 1169-1170.

Jiang X, Kim HE, Shu H, Zhao Y, Zhang H, Kofron J, Donnelly J, Burns D, Ng SC, Rosenberg S and Wang X Distinctive roles of PHAP proteins and prothymosin-alpha in a death regulatory pathway. Science. 2003; 299: 223-226.

Jiang X, Kim HE, Shu H, Zhao Y, Zhang H, Kofron J, Donnelly J, Burns D, Ng SC, Rosenberg S and Wang X Distinctive roles of PHAP proteins and prothymosin-alpha in a death regulatory pathway. Science. 2003; 299: 223-226.

Johnson CE, Huang YY, Parrish AB, Smith MI, Vaughn AE, Zhang Q, Wright KM, Van Dyke T, Wechsler-Reya RJ, Kornbluth S and Deshmukh M Differential Apaf-1 levels allow cytochrome c to induce apoptosis in brain tumors but not in normal neural tissues. Proc Natl Acad Sci USA. 2007; 104: 20820-20825.

Johnson CE and Kornbluth S Caspase cleavage is not for everyone. Cell. 2008; 134: 720-721.

Johnstone RW, Ruefli AA and Lowe SW Apoptotis: a link between cancer genetics and chemotherapy. Cell. 2002; 108: 153-164.

Jones CM and Smith JC An overview of Xenopus development. Methods Mol Biol. 2008; 461: 385-394.

Kalkhof S, Ihling C, Mechtler K and Sinz A Chemical cross-linking and high-performance Fourier transform ion cyclotron resonance mass spectrometry for protein interaction analysis: application to a Calmodulin/target peptide complex. Anal Chem. 2005; 77: 495-503.

Kenney AM, Widlund HR and Rowitch DH Hedgehog and PI-3 kinase signaling converge on Nmyc1 to promote cell cycle progression in cerebellar neuronal precursors. Devleopment. 2004: 131: 217-228.

Kerr JF, Wyllie AH and Currie AR Apoptosis: a basic biological phenomenon with wide-ranging implications in tissue kinetics. Br J Cancer. 1972; 26:239-257.

Kim H, Jiang X, Du F and Wang X PHAPI, CAS and Hsp70 promote apoptosome formation by preventing Apaf-1 aggregation and enhancing nucleotide exchange on Apaf-1. Mol Cell. 2008; 30: 239-247.

Kim HE, Du F, Fang M and Wang X Formation of apoptosome is initiated by cytochrome c-induced dATP hydrolysis and subsequent nucleotide exchange on Apaf-1. Proc Natl Acad Sci USA. 2005; 102: 17545-17550.

Kischkel FC, Hellbardt S, Behrmann I, Germer M, Pawlita M, Krammer PH and Peter ME Cytotoxicity-dependent APO-1 (Fas/CD95)-associated proteins form a death-inducing signaling complex (DISC) with the receptor. EMBO J. 1995; 14: 5579-5588.

Kluck RM, Ellerby LM, Ellerby HM, Naiem S, Yaffe MP, Margoliash E, Bredesen D, Mauk AG, Sherman F and Newmeyer DD Determinants of cytochrome *c* pro-apoptotic activity. J Biol Chem. 2000; 275: 16127-16133.

Knobbe CB and Reifenberger G Genetic alterations and aberrant expression of genes related to the phosphatidyl-inositol-3'-kinase/protein kinase B (Akt) signal transduction pathway in glioblastomas. Brain Pathol. 2003; 13: 507-518.

Köhler C, Orrenius S and Zhivotovsky B Evaluation of caspase activity in apoptotic cells. Journal of Immunological Methods. 2002; 265: 97-110.

Kornbluth S and Evans EK analysis of apoptosis using Xenopus egg extracts. 2001; Curr Protoc Cell Biol; Chapter 11: Unit 11.12.

Korsmeyer SJ Chromosomal translocations in lymphoid malignancies reveal novel proto-oncogenes. Annu Rev Immunol. 1992; 10: 785-807.

Kugler W, Buchholz F, Köhler F, Eibl H, Lakomek M and Erdlenbruch B Downregulation of Apaf-1 and caspase-3 by RNA interference in human glioma cells: consequences for erucylphosphocholine-induced apoptosis. Apoptosis. 2005; 10: 1163-1174.

Kuo CT, Mirzadeh Z, Soriano-Navarro M, Rasin M, Wang D, Shen J, Sestan N, Garcia-Verduogo J, Alvarez-Buylla A, Jan LY and Jan YN Postnatal deletion of Numb/Numblike reveals repair and remodeling capacity in the subventricular neurogenic niche. Cell. 2006; 127: 1253-1264.

Kurokawa M, Zhao C, Reya T and Kornbluth S Inhibition of apoptosome formation by suppression of Hsp90beta phosphorylation in tyrosine kinase-induced leukemias. Mol Cell Biol. 2008; 28: 5494-5506.

Landesman Y, Goodenough DA and Paul DL Gap junctional communication in the early Xenopus embryo. J Cell Biol. 2000; 150: 929-936.

LeBlanc HN and Ashkenazi A Apo2L/TRAIL and its death and decoy receptors. Cell Death Differ. 2003; 10: 66-75.

Ledgerwood EC and Morison IM Targeting the apoptosome for cancer therapy. Clin Cancer Res. 2009; 15: 420-424.

Lena A, Rechichi M, Salvetti A, Bartoli B, Vecchio D, Scarcelli V, Amoroso R, Benvenuti L, Gagliardi R, Gremigni V and Rossi L Drugs targeting the mitochondrial pore act as cytotoxic and cytostatic agents in temozolomide-resistant glioma cells. J Transl Med. 2009; 7: 13.

Lesniak MS and Brem H Targeted therapy for brain tumours. Nat Rev Drug Discov. 2004; 3: 499-508.

Levine AJ p53, the cellular gatekeeper for growth and division. Cell. 1997; 88: 323-331.
Li F, Srinivasan A, Wang Y, Armstrong RC, Tomaselli KJ and Fritz LC Cell-specific induction of apoptosis by microinjection of cytochrome c. Bcl-xL has activity independent of cytochrome c release. J Biol Chem. 1997; 272: 30299-30305.

Li H, Zhu H, Xu CJ and Yuan J Cleavage of BID by caspase 8 mediates the mitochondrial damage in the Fas pathway of apoptosis. Cell. 1998; 94: 491-501.

Li MO, Sarkisian MR, Mehal WZ, Rakic P and Flavell RA Phosphatidylserine receptor is required for clearance of apoptotic cells. Science. 2003; 302: 1560-1563.

Li P, Nijhawan D, Budihardjo I, Srinivasula SM, Ahmad M, Alnemri ES, and Wang X Cytochrome c and dATP-dependent formation of Apaf-1/caspase-9 complex initiates an apoptotic protease cascade. Cell. 1997: 91: 479-89.

Liu JR, Opipari AW, Tan L, Jiang Y, Zhang Y, Tang H and Nunez G Dysfunctional apoptosome activation in ovarian cancer: implications for chemoresistance. Cancer Res. 2002; 62: 924-931.

Liu L, Chahroudi A, Silvestri G, Wernett ME, Kaiser WJ, Safrit JT, Komoriva A, Altman JD, Packard BZ and Feinberg MB. Visualization and quantification of T cell-mediated cytotoxicity using cell-permeable fluorogenic caspase substrates. Nature Medicine. 2002; 8: 185-189.

Liu X, Kim CN, Yang J, Jemmerson R and Wang X Induction of apoptotic program in cell-free extracts: requirement for dATP and cytochrome c. Cell. 1996; 86: 147-157.

Liu Z, Lin H, Ye S, Liu Q, Meng Z, Zhang C, Xia Y, Margoliash E, Rao Z and Liu X Remarkably high activities of testicular cytochrome c in destroying reactive oxygen species and in triggering apoptosis. Proc Natl Acad Sci USA. 2006; 103: 8965-8970.

Livak KJ and Schmittgen RD Analysis of relative gene expression data using real-time quantitative PCR and the 2(-Delta Delta C(T)) method. Methods. 2001; 25: 402-408.

Lüthi AU and Martin SJ The CASBAH: a searchable database of caspase substrates. Cell Death Differ. 2007; 14: 641-650.

Madden SD, Donovan M and Cotter TG Key apoptosis regulating proteins are down-regulated during postnatal tissue development. Int J Dev Biol. 2007; 51: 415-423.

Mahrus S, Trinidad JC, Barkan DT, Sali a, Burlingame AL and Wells JA Global sequencing of proteolytic cleavage sites in apoptosis by specific labeling of protein N termini. Cell. 2008; 134: 866-876.

Maller JL The elusive progesterone receptor in Xenopus oocytes. Proc Natl Acad Sci USA. 2001; 98: 8-10.

Martin AG and Fearnhead HO Apocytochrome *c* blocks caspase-9 activation and bax-induced apoptosis. J Biol Chem. 2002; 277: 50834-50841.

Martin AG, Nguyen J, Wells JA and Fearnhead HO Apo cytochrome c inhibits caspases by preventing apoptosome formation. Biochem Biophys Res Commun. 2004; 319: 944-950.

Martin MC, Allan LA, Lickrish M, Sampson C, Morrice N and Clarke PR Protein kinase A regulates caspase-9 activation by Apaf-1 downstream of cytochrome c. J Biol Chem. 2005; 280: 15449-15455.

Martinez F, Rienzi L, Iacobelli M, Ubaldi F, Mendoza C, Greco E and Tesarik J Caspase activity in preimplantation human embryos is not associated with apoptosis. Human Reproduction. 2002; 17: 1584-1590.

Mashima T, Oh-hara T, Sato S, Mochizuki M, Sugimoto Y, Yamazaki K, Hamada J, Tada M, Moriuchi T, Ishikawa Y, Kato Y, Tomoda H, Yamori T and Tsuruo T p53-defective tumors with a functional apoptosome-mediated pathway: a new therapeutic target. J Natl Cancer Inst. 2005; 97: 765-777.

Mauk AG, Mauk MR, Moore GR and Northrup SH Experimental and theoretical analysis of the interaction between cytochrome c and cytochrome b5. J Bioenerg Biomembr. 1995; 27: 311-330.

Mayer A, Neupert W and Lill R Translocation of apocytochrome c across the outer membrane of the mitochondria. J Biol Chem. 1995; 270: 12390-12397.

McCall TD, Pedone CA and Fults DW Apoptosis suppression by somatic cell transfer of Bcl-2 promotes sonic hedgehog-dependent medulloblastoma formation in mice. Cancer Res. 2007; 67: 5179-5185.

Mellinghoff IK, Wang MW, Vivanco I, Haas-Kogan DA, Zhu S, Dia EQ, Lu KV, Yoshimoto K, Huang JH, Chute DJ, Riggs BL, Horvath S, Liau LM, Cavenee WK, Rao PN, Beroukhim R, Peck TC, Lee JC, Seller WR, Stokoe D, Prados M, Cloughesy TF, Sawyer CL and Mischel PS Molecular determinants of the response of glioblastomas to EGFR kinase inhibitors. N Engl J Med. 2005; 353: 2012-2024.

Miller TM and Johnson EM Jr Metabolic and genetic analyses of apoptosis in potassium/serum-deprived rat cerebellar granule cells. J Neurosci. 1996; 16: 7487-7495.

Mirkes PE 2001 Warkany lecture: To die or not to die, the role of apoptosis in normal and abnormal mammalian development. Teratology. 2002; 65: 228-239.

Mitchell SA, Spriggs KA, Coldwell MJ, Jackson RJ and Willis AE The Apaf-1 internal ribosome entry segment attains the correct structural conformation for function via interactions with PTB and unr. Mol Cell. 2003; 11: 757-771.

Molliver DC, Wright DE, Leitner ML, Parsadanian AS, Doster K, Wen D, Yan Q and Snider WD IB4-binding DRG neurons switch from NGF to GDNF dependence in early postnatal life. Neuron. 1997; 19: 849-861.

Moore KD, Dillon-Carter O, Conejero C, Poltorak M, Chedid M, Tornatore C and Freed WJ In vitro properties of a newly established medulloblastoma cell line, MCD-1. Mol Chem Neuropathol. 1996; 29: 107-126.

Morgan MJ and Thorburn A Measurement of caspase activity in individual cells reveals differences in the kinetics of caspase activation between cells. Cell Death Differ. 2001; 8: 38-43.

Morison I, Cramer Borde EM, Cheesman EJ, Cheong PK, Holyoake AJ, Fichelson S, Weeks RJ, Lo A, Davies SMK, Wilbanks SM, Fagerlund RD, Ludgate MW, da Silva Tatley FM, Coker MSA, Bockett NA, Hughes G, Pippig DA, Smith MP, Capron C and Ledgerwood EC A mutation of human cytochrome c enhances the intrinsic apoptotic pathway but causes only thrombocytopenia. Nature Genet. 2008; 40: 387-389.

Moroni MC, Hickman ES, Lazzerini Denchi E, Caprara G, Colli E, Cecconi F, Müller H and Helin K Apaf-1 is a transcriptional target for E2F and p53. Nat Cell Biol. 2001; 3: 552-558.

Moroni MC, Hickman ES, Lazzerini Denchi E, Caprara G, Colli E, Cecconi F, Müller H and Helin K. Apaf-1 is a transcriptional target for E2F and p53. Nat Cell Biol. 2001; 3: 552-558.

Mouhamad S, Galluzzi L, Zermati Y, Castedo M and Kroemer G Apaf-1 deficiency causes chromosomal instability. Cell Cycle. 2007; 6: 3103-3107.

Mrugula MM and Chamberlain MC Mechanisms of disease: temozolomide and glioblastoma—look to the future. Nat Clin Pract Oncol. 2008; 5: 476-486.

Mulhern RK, Merchant TE, Gajjar A, Reddick WE and Kun LE Late neurocognitive sequelae in survivors of brain tumours in childhood. Lancet Oncol. 2004; 5: 399-408.

Muller DR, Schindler P, Towbin H, Wirth U, Voshol H, Hoving S and Steinmetz MO Isotope-tagged cross-linking reagents. A new tool in mass spectrometric protein interaction analysis. Anal Chem. 2001; 73: 1927-1934.

Murray AW Cell cycle extracts. Methods Cell Biol 1991; 36: 581-605.

Nagane M, Levitzki A, Gazit A, Cavenee WK and Huang HJ Drug resistance of human glioblastoma cells conferred by a tumor-specific mutant epidermal growth factor receptor through modulation of Bcl-$X_L$ and caspase-3-like proteases. Proc Natl Acad Sci. 1998; 95: 5724-5729.

Newmeyer DD, Farschon DM and Reed JC Cell-free apoptosis in Xenopus egg extracts: inhibition of Bcl-2 and requirement for an organelle fraction enriched in mitochondria. Cell. 1994; 79: 353-364.

Newton, HB Primary brain tumors: review of etiology, diagnosis and treatment. Am Fam Phyisican. 1994; 49: 787-797.

Nguyen JT and Wells JA Direct activation of the apoptosis machinery as a mechanism to target cancer cells. Proc Natl Acad Sci USA. 2003; 100: 7533-7538.

Norbury CJ and Zhivotovsky B DNA damage-induced apoptosis. Oncogene. 2004; 23: 2797-2808.

Nutt LK, Margolis SS, Jensen M, Herman CE, Dunphy WG, Rathmell JC and Kornbluth S Metabolic regulation of oocyte cell death through the CaMKII-mediated phosphorylation of caspase-2. Cell. 2005; 123: 89-103.

Ohgaki H Epidemiology of brain tumors. Methods Mol Biol. 2009; 472: 323-342.

Oliver TG, Read TA, Kessler JD, Mehmeti A, Wells JF, Huynh TT, Lin SM and Wechsler-Reya RJ Loss of patched and disruption of granule cell development in a pre-neoplastic stage of medulloblastoma. Development. 2005; 132: 2425-2439.

Olson MV, Johnson DG, Jiang H, Xu J, Alonso MM, Aldape KD, Fuller GN, Bekele BN, Yung WK, Gomez-Manzano C and Fueyo J Transgenic E2F1 expression in the mouse brain induces a human-like bimodal pattern of tumors. Cancer Res. 2007; 67: 4005-4009.

Oltersdorf T, Elmore SW, Shoemaker AR, Armstrong RC, Augeri DJ, Belli BA, Bruncko M, Deckwerth TL, Dinges J, Hajduk PJ, Joseph MK, Kitada S, Korsmeyer SJ, Kunzer AR, Letai A, Li C, Mitten MJ, Nettesheim DG, Ng S, Nimmer PM, O'Connor JM, Oleksijew A, Petros AM, Reed JC, Shen W, Tahir SK, Thompson CB, Tomaselli KJ, Wang B, Wendt MD, Zhang H, Fesik SW and Rosenberg SH An inhibitor of Bcl-2 family proteins induces regression of solid tumours. Nature. 2005; 435: 677-681.

Opel D, Westhoff MA, Bender A, Braun V, Debatin KM and Fulda S Phosphatidlyinositol 3-kinase inhibition broadly sensitizes glioblastoma cells to death receptor- and drug-induced apoptosis. Cancer Res. 2008; 68: 6271-6280.

Ow YP, Green DR, Hao Z and Mak TW Cytochrome c: functions beyond respiration. Nat Rev Mol Cell Biol. 2008; 9: 532-542.

Patchell RA, Regine WF, Ashton P, Tibbs PA, Wilson D, Shappley D and Young B A phase I trial of continuously infused intratumoral bleomcyin for the treatment of recurrent glioblastoma multiforme J Neurooncol. 2002; 60: 37-42.

Peltenburg LT, de Bruin EC, Meersma D, Smit NP, Schrier PI and Medema JP Expression and function of the apoptosis effector Apaf-1 in melanoma. Cell Death Differ 2005: 12: 678-679.

Peng X, Chen H, Draney DR, Schutz-Geschwender A and Olive DM A non-fluorescent, broad range quencher dye for FRET assays. Analytical Biochemistry. 2009; doi: 10.1016/j.ab.2009.02.024.

Peter ME and Krammer PH The CD95 (APO-1/Fas) DISC and beyond. Cell Death Differ. 2003; 10: 26-35.

Peter ME, Heufelder AE and Hengartner MO Advances in apoptosis research. Proc Natl Acad Sci USA. 1997; 94:12736-12737.

Phillips HS, Kharbanda S, Chen R, Forrest WF, Soriano RH, Wu TD, Misra A, Nigro JM, Colman H, Soroceanu L, Williams PM, Modrusan Z, Feuertstein BG and Aldape K Molecular subclasses of high-grade glioma predict prognosis, delineate a pattern of disease progression, and resemble stages in neurogenesis. Cancer Cell. 2006; 9: 157-173.

Philpott A and Yew PR The Xenopus cell cycle: an overview. Methods Mol Biol. 2005; 296: 95-112.

Pietsch T, Waha A, Koch A, Kraus J, Albrecht S, Tonn J, Sörensen N, Berthold F, Henk B, Schmandt N, Wolf HK, von Deimling A, Wainwright B, Chenevix-Trench G, Wiestler OD and Wicking C Medulloblastomas of the desmoplastic variant carry mutations of the human homologue of the Drosophila patched. Cancer Res. 1997; 57: 2085-2088.

Pinkse MW, Vitto PM, Hilhorst MJ, Ooms B and Heck AJ. Selective isolation at the femtomole level of phosphopeptides from proteolytic digests using 2D-NanoLC-ESI-MS/MS and titanium oxide precolumns. Anal. Chem. 2004; 76: 3935-3943.

Pitti RM, Marsters SA, Lawrence DA, Roy M, Kischkel FC, Dowd P, Huang A, Donahue CJ, Sherwood SW, Baldwin DT, Godowski PJ, Wood WI, Gurney AL, Hillan KJ, Cohen RL, Goddard AD, Botstein D and Ashkenazi A Genomic amplification of a decoy receptor for Fas ligand in lung and colon cancer. Nature. 1998; 396: 699-703.

Potts PR, Singh S, Knezek M, Thompson CB and Deshmukh M Critical function of endogenous XIAP in regulating caspase activation during sympathetic neuronal apoptosis. J Cell Biol. 2003; 163: 789-799.

Price J Neural stem cells – Where are you? Nature Medicine. 2001; 7: 998-998.

Quinn JA, Jiang SX, Carter J, Reardon DA, Desjardins A, Vredenburgh JJ, Rich JN, Gururangan S, Friedman AH, Bigner DD, Sampson JH, McLendon RE, Herndon II JE, Threatt S and Friedman HS Phase II trial of Gliadel plus O6-Benzylguanine in adults with recurrent glioblastoma multiforme. Clin Cancer Res. 2009; 15: 1064-1068.

Raffel C, Jenkins RB, Frederick L, Hebrink D, Alderete B, Fults DW and James CD Sporadic medulloblastomas contain PTCH mutations. Cancer Res. 1997; 57: 842-845.

Rainov NG, Söling A and Heidecke V Novel therapies for malignant gliomas: a local affair? Neurosurg Focus. 2006; 20: E9.

Rao G, Pedone CA, Del Valle L, Reiss K, Holland EC and Fults DW Sonic hedgehog and insulin-like growth factor synergize to induce medulloblastoma formation from nestin-expressing neural progenitors in mice. Oncogene. 2004; 23: 6156-6162.

Read T, Fogarty, MP, Markant SL, McLendon RE, Wei Z, Ellison DW, Febbo PG and Wechsler-Reya RJ Identification of CD15 as a marker for tumor-propagating cells in a mouse model of medulloblastoma. Cancer Cell. 2009; 15: 135-147.

Rehm M, Dussmann H, Janicke RU, Tavare JM, Kogel D and Prehn JH Single-cell fluorescence resonance energy transfer analysis demonstrates that caspase activation during apoptosis is a rapid process. Role of caspase-3. Journal of Biological Chemistry. 2002; 277: 24506-24514.

Riedl SJ and Salvesen GS The apoptosome: signaling platform of cell death. Nature Reviews. 2007; 9: 405-413.

Riedl SJ, Li W, Chao Y, Schwarzenbacher R and Shi Y Structure of the apoptotic protease-activating factor 1 bound to ADP. Nature. 2005; 434: 926-933.

Riedl SJ, Renatus M, Schwarzenbacher R, Zhou Q, Sun C, Fesik SW, Liddington RC and Salvesen GS Structural basis for the inhibition of caspase-3 by XIAP. Cell. 2001; 104: 791-800.

Rodriguez J and Lazebnik Y Caspase-9 and Apaf-1 form an active holoenzyme. Genes Dev. 1999; 13: 3179-3184.

Ruggiero A, Conter V, Milani M, Biagi E, Lazzareschi I, Sparano P and Riccardi R Intrathecal chemotherapy with antineoplastic agents in children. Paediatr Drugs. 2001; 3: 237-246.

Rutkowski DT and Kaufman RJ A trip to the ER: coping with stress. Trends Cell Biol. 2004; 14: 20-28.

Sagata N, Watanabe N, Vande Woude GF and Ikawa Y The c-mos proto-oncogene product is a cytostatic factor responsible for meiotic arrest in vertebrate eggs. Nature. 1989; 342: 512-518.

Saleh A, Srinivasula SM, Balkir L, Robbins PD and Alnemri ES Negative regulation of the Apaf-1 apoptosome by Hsp70. Nat Cell Biol. 2000; 2: 476-483.

Salvesen GS and Dixit VM Caspase activation: the induced-proximity model. Proc Natl Acad Sci USA. 1999; 96: 10964-10967.

Salvesen GS and Duckett CS IAP proteins: blocking the road to death's door. Mol Cell Biol. 2002; 3: 401-410.

Sanchis D, Mayorga M, Ballester M and Comella JX Lack of Apaf-1 expression confers resistance to cytochrome c-driven apoptosis in cardiomyocytes. Cell Death Differ. 2003; 10: 977-986.

Sandri M and Carraro U Apoptosis of skeletal muscles during development and disease. Int J Biochem Cell Biol. 1999; 31: 1373-1390.

Schafer ZT and Kornbluth S The apoptosome: physiological, developmental, and pathological modes of regulation. Developmental Cell. 2006; 10: 549-561.

Schafer ZT, Parrish AB, Wright KM, Margolis SS, Marks JR, Deshmukh M and Kornbluth S Enhanced sensitivity to cytochrome c-induced apoptosis mediated by PHAP1 in breast cancer cells. Cancer Res. 2006; 66: 2210-2218.

Schüller U, Schober F, Kretzschmar HA and Herms J Bcl-2 expression inversely correlates with tumour cell differentiation in medulloblastomas. Neuropathol Appl Neurobiol. 2004; 30: 513-521.

Schultz, D.R., and Harrington, W.J.Jr. Apoptosis: Programmed cell death at a molecular level. Semin Arthritis Rheum; 2003:32: 345-369.

Shi Y Activation of initiator caspases: history, hypotheses, and perspectives. Journal of Cancer Molecules. 2005; 1: 9-18.

Shi Y Mechanisms of caspase activation and inhibition during apoptosis. Molecular Cell. 2002; 9: 459-470.

Shi, Y Apoptosome assembly. Methods Enzymol. 2008; 442: 141-153.

Shi, Y Mechanical aspects of apoptosome assembly. Current Opinion in Cell Biology. 2006; 18: 677-684.

Shiozaki EN and Shi Y Caspase activation, inhibition, and reactivation: a mechanistic view. Protein Sci. 2004; 13: 1979-1987.

Shiozaki EN, Chai J and Shi Y Oligomerization and activation of caspase-9, induced by Apaf-1 CARD. Proc Natl Acad Sci USA. 2002; 99: 4197-4204.

Singh SK, Clarke ID, Terasaki M, Bonn BE, Hawkins C, Squire J and Dirks PB Identification of a cancer stem cell in human brain tumors. Cancer Research. 2003; 63: 5821-5828.

Sinz A Chemical cross-linking and mass spectrometry for mapping three-dimensional structures of proteins and protein complexes. J Mass Spectrom. 2003; 38: 1225-1237.

Skulachev V Cytochrome c in the apoptotic and antioxidant cascades. FEBS Letters. 1998; 423: 275-280.

Slee EA, Harte MT, Kluck RM, Wolf BB, Casiano CA, Newmeyer DD, Wang H, Reed, JC, Nicholson DW, Alnemri ES, Green DR and Martin SJ Ordering the cytochrome c-initiated caspase cascade: hierarchical activation of caspases-2, -3, -6, -7, -8, -10 in a caspase-9-dependent manner. J Cell Biol. 1999; 144: 281-292.

Soderblom EJ, Bobay BG, Cavanagh J and Goshe MB Tandem mass spectrometry acquisition approaches to enhance identification of protein-protein interactions using

low-energy collision-induced dissociative chemical crosslinking reagents. Rapid Commun Mass Spectrom. 2007; 21: 3395-3408.

Soengas MS, Capodieci P, Polsky D, Mora J, Esteller M, Opitz-Araya X, McCombie R, Herman JG, Gerald WL, Lazebnik YA, Cordón-Caró C and Lowe SW Inactivation of the apoptosis effector Apaf-1 in malignant melanoma. Nature. 2001; 409: 207-211.

Solary E, Giordanetto F and Kroemer G Re-examining the role of cytochrome c in cell death. Nat Genet. 2008; 40: 387-389.

Srinivasula SM and Ashwell JD IAPs: What's in a name? Molecular Cell. 2008; 30: 123-135.

Srinivasula SM, Ahmad M, Fernandes-Alnemri T and Alnemri ES Autoactivation of procaspase-9 by Apaf-1 mediated oligomerization. Mol Cell. 1998; 1: 949-957.

Srinivasula SM, Hedge R, Saleh A, Datta P, Shiozaki E, Chai J, Lee RA, Robbins PD, Fernandes-Alnemri T, Shi Y and Alnemri ES A conserved XIAP-interaction motif in caspase-9 and Smac/DIABLO regulates caspase activity and apoptosis. Nature. 2001; 410: 112-116.

Stegh AH, Kim H, Bachoo RM, Forloney KL, Zhang J, Schulze H, Park K, Hannon GJ, Yuan J, Louis DN, DePinho RA and Chin L Bcl2L12 inhibits post-mitochondrial apoptosis in glioblastoma. Genes Dev. 2007; 21: 98-111.

Stennicke HR, Deveraux QL, Humke EW, Reed JC, Dixit VM and Salvesen GS Caspase-9 can be activated without proteolytic processing. J Biol Chem. 1999; 274: 8359-8362.

Stupp R, Hegi ME, Gilbert MR and Chakravarti A Chemoradiotherapy in malignant glioma: standard of care and future directions. J Clin Oncol. 2007; 25: 4127-4136.

Sun L, Hui AM, Su Q, Vortmeyer A, Kotliarov Y, Pastorino S, Passaniti A, Menon J, Walling J, Bailey R, Rosenblum M, Mikkelsen T and Fine HA Neuronal and glioma-derived stem cell factor induces angiogenesis within the brain. Cancer Cell. 2006; 9: 287-300.

Taieb F, Thibier C and Jessus C On cyclins, oocytes, and eggs. Mol Reprod Dev. 1997; 48: 397-411.

Taskher JS, Olson M and Kornbluth S Post-cytochrome c protection from apoptosis conferred by a MAPK pathway in Xenopus egg extracts. Mol Biol Cell. 2002; 13: 393-401.

Taylor, RC, Cullen SP and Martin SJ Apoptosis: controlled demolition at the cellular level. Nat Rev Mol Cell Biol. 2008; 9: 231-241.

Tong J and Margoliah E Cytochrome c heme lyase activity of yeast mitochondria. J Biol Chem. 1998; 273: 25695-25702.

Tsuchiya Y, Murai S and Yamashita S Apoptosis-inhibiting activities of BIR family proteins in Xenopus egg extracts. FEBS J. 2005; 272: 2237-2250.

Tsuruta F, Masuyama N and Gotoh Y The phosphatidylinositol 3-kinase (PI3K)-Akt pathway suppresses Bax translocation to mitochondria. J Biol Chem. 2002; 277: 14040-14047.

Tung JJ, Hansen DV, Ban KH, Loktev AV, Summers MK, Adler JR 3rd and Jackson PK A role for the anaphase-promoting complex inhibitor Emi2/XErp1, a homolog of early mitotic inhibitor 1, in cytostatic factor arrest of Xenopus eggs. Proc Natl Acad Sci USA. 2005; 102: 4318-4323.

Turley RS, Finger EC, Hempel N, How T, Fields TA and Blobe GC The type III transforming growth factor-beta receptor as a novel tumor suppressor gene in prostate cancer. Cancer Res. 2007; 67: 1090-1098.

Umetani N and Hoon DS Frequent LOH at chromosome 12q22-23 and Apaf-1 inactivation in glioblastoma. Brain Pathol. 2004; 14: 224.

Vaughn AE and Deshmukh M Essential postmitochondrial function of p53 uncovered in DNA damage-induced apoptosis in neurons. Cell Death Differ. 2007; 14: 973-981.

Vaughn AE and Deshmukh M Glucose metabolism inhibits apoptosis in neurons and cancer cells by redox inactivation of cytochrome c. Nat Cell Biol. 2008; 10: 1477-1483.

Vazquez A, Bond EE, Levine AJ and Bond GL The genetics of the p53 pathway, apoptosis and cancer therapy. Nat Rev Drug Discov. 2008; 7: 979-987.

Verma YK, Gangenahalli GU, Singh VK, Gupta P, Chandra R, Sharma RK and Raj HG Cell death regulation by B-cell lymphoma protein. Apoptosis. 2006; 11: 459-471.

Wang S, Yan-Neale Y, Cai R, Alimov I and Cohen D Activation of mitochondrial pathway is crucial for tumor selective induction of apoptosis by LAQ824. Cell Cycle. 2006; 5: 1662-1668.

Watanabe T, Hirota Y, Arakawa Y, Fujisawa H, Tachibana O, Hasegawa M, Yamashita J and Hayashi Y. Frequent LOH at chromosome 12q22-23 and Apaf-1 inactivation in glioblastoma. Brain Pathol. 2003; 13: 431-439.

Wechsler-Reya R and Scott MP The developmental biology of brain tumors. Annu Rev Neurosci. 2001; 24: 385-428.

Weir HK, Thun MJ, Hankey BF, Ries LA, Howe HL, Wingo PA, Jemal A, Ward E, Anderson RN and Edwards BK Annual report to the nation on the status of cancer, 1975-2000, featuring the uses of surveillance data for cancer prevention and control. J Natl Cancer Inst. 2003; 95: 1276-1299.

Westphal M, Hilt DC, Bortev E, Delavault P, Olivares R, Warnke PC, Whittle IR, Jääskeläinen J and Ram Z A phase III trial of local chemotherapy with biodegradable carmustine (BCNU) wafers (Gliadel wafers) in patients with primary malignant glioma. Neuro Oncol. 2003; 5: 79-88.

Wolf BB, Schuler M, Li W, Eggers-Sedlet B, Lee W, Tailor P, Fitzgerald P, Mills GB and Green DR Defective cytochrome c-dependent activation in ovarian cancer cell lines due to diminished or absent apoptotic protease activating factor-1 activity. J Biol Chem. 2001; 276: 34244-34251.

Woo EJ, Kim YG, Kim MS, Han WD, Shin S, Robinson H, Park SY and Oh BH Structural mechanism for inactivation and activation of CAD/DFF40 in the apoptotic pathway. Mol Cell. 2004; 14: 531-539.

Wride MA and Sanders EJ Programmed cell death in development. Int Rev Cytol. 1995; 163: 105-173.

Wright KM, Linhoff MW, Potts PR and Deshmukh M Decreased apoptosome activity with neuronal differentiation sets the threshold for strict IAP regulation of apoptosis. J Cell Biol. 2004; 167: 303-313.

Wright KM, Smith MI, Farrag L and Deshmukh M Chromatin modification of Apaf-1 restricts the apoptotic pathway in mature neurons. J Cell Biol. 2007; 179: 825-832.

Wroble BN and Sible JC Chk2/Cds1 protein kinase blocks apoptosis during early development of Xenopus laevis. Developmental Dynamics. 2005; 233: 1359-1365.

Wu Q, Guo Y, Yamada A, Perry J, Wang M, Araki M, Freel C, Tung J, Tang W, Margolis S and Kornbluth S A role for Cdc2- and PP2A-mediated regulation of Emi2 in the maintenance of CSF arrest. Current Biology. 2007; 17: 213-224.

Xie J, Johnson RL, Zhang X, Bare JW, Waldman FM, Cogen PH, Menon AG, Warren RS, Chen LC, Scott MP and Epstein EH Jr Mutations of the PATCHED gene in several types of sporadic extracutaneous tumors. Cancer Res. 1997; 57: 2369-2372.

Yakovlev AG, Ota K, Wang G, Movsesyan V, Bao WL, Yoshihara K and Faden AI Differential expression of apoptotic protease-activating factor-1 and caspase-3 genes and susceptibility to apoptosis during brain development and after traumatic brain injury. J Neurosci. 2001; 21: 7439-7446.

Ye P, Xing Y, Dai Z and D'Ercole AJ *In vivo* actions of insulin-like growth factor-I (IGF-I) on cerebellum development in transgenic mice: evidence that IGF-I increases proliferation of granule cell progenitors. Brain Res Dev Brain Res. 1996; 95: 44-54.

Yin Q, Park HH, Chung JY, Lin Sc, Lo YC, da Graca LS, Jiang X and Wu H Caspase-9 holoenzyme is a specific and optimal procaspase-3 processing machine. Mol Cell. 2006; 22: 259-268.

Yu T, Wang X, Purring-Koch C, Wei Y and McLendon GL A mutational epitope for cytochrome c binding to the apoptosis protease activation factor-1. J Biol Chem. 2001; 276: 13034-13038.

Yu X, Acehan D, Ménétret J, Booth CR, Ludtke SJ, Riedl SJ, Shi Y, Wang X and Akey C A structure of the human apoptosome at 12.8 Å resolution provides insights into this cell death platform. Structure. 2005; 13: 1725-1735.

Zermati Y, Mouhamad S, Stergiou L, Besse B, Galluzzi L, Boehrer S, Pauleau AL, Rosselli F, D'Amelio M, Amendola R, Castedo M, Hengartner M, Soria JC, Cecconi F and Kroemer G. Nonapoptotic role for Apaf-1 in the DNA damage checkpoint. Mol Cell. 2007; 28: 624-637.

Zhou P, Chou J, Sanchez Olea R, Yuan J and Wagner G Solution structure of Apaf-1 CARD and its interaction with caspase-9 CARD: A structural basis for specific adaptor/caspase interaction. Proc Natl Acad Sci USA. 1999; 96: 11265-11270.

Ziegler DS, Kung AL and Kieran MW Anti-apoptosis mechanisms in malignant glioma. J Clin Oncol. 2008; 26: 493-500.

Zou H., Li Y, Liu X and Wang X An APAF-1-cytochrome c multimeric complex is a functional apoptosome that activates procaspase-9. J Biol Chem. 1999; 274: 11549-11556.

# Biography

## Carrie Elizabeth Johnson

Born to Thomas and Kathleen Johnson on December 16, 1979 in Bethesda, MD.

### Education

M.D., Ph.D. Molecular Cancer Biology, Certificate in Cell and Molecular Biology
Duke University, Durham, NC, May 2010

B.S. Biology with Distinction
Duke University, Durham, NC, May 2001

### Publications

**Johnson CE**, Freel CF and Kornbluth S Features of programmed cell death in intact Xenopus oocytes and early embryos revealed by near-infrared fluorescence and real-time monitoring. In submission, 2009.

Andersen JL, **Johnson CE**, Freel CD, Parrish AB, Day JL, Buchakjian MR, Nutt L, Thompson JW, Moseley MA and Kornbluth S. Mitotic phosphorylation of caspase-2 restrains apoptosis upstream of cytochrome c. In submission, 2009.

**Johnson CE** and Kornbluth S Caspase cleavage is not for everyone. Cell. 2008; 134: 720-721.

**Johnson CE**, Huang YY, Parrish AB, Smith MI, Vaughn AE, Zhang Q, Wright KM, Van Dyke T, Wechsler-Reya RJ, Kornbluth S and Deshmukh M Differential Apaf-1 levels allow cytochrome c to induce apoptosis in brain tumors but not in normal neural tissues. Proc Natl Acad Sci USA. 2007; 104: 20820-20825.

Dissanayake SK, Wade M, **Johnson CE**, O'Connell MP, Leotlela PD, French AD, Shah KV, Hewitt KJ, Rosenthal DT, Indiq FE, Jiang Y, Nickoloff BJ, Taub DD, Trent JM, Moon RT, Bittner M and Weeraratna AT The Wnt5A/protein kinase C pathway mediates motility in melanoma cells via the inhibition of metastasis suppressors and initiation of an epithelial to mesenchymal transition. J Biol Chem. 2007; 282: 17259-17271.

Chi SL, Wahl ML, Mowery YM, Shan S, Mukhopadhyay S, Hilderbrand SC, Kenan DJ, Lipes BD, **Johnson CE**, Marusich MF, Capaldi RA, Dewhirst MW and Pizzo SV

Angiostatin-like activity of a monoclonal antibody to the catalytic subunit of F1F0 ATP synthase. Cancer Res. 2007; 67: 4716-4724.

Gonzalez-Gronow M, Kalfa T, **Johnson CE** and Pizzo SV The voltage-dependent anion channel is a receptor for plasminogen kringle 5 on human endothelial cells. J Biol Chem. 2003; 278: 27312-27318.

Misra UK, Gonzalez-Gronow M, Gawdi G, Hart JP, **Johnson CE** and Pizzo SV The role of Grp 78 in alpha 2-macroglobulin-induced signal transduction. Evidence from RNA interference that the low density lipoprotein receptor-related protein is associated with, but not necessary for, GRP 78-mediated signal transduction. J Biol Chem. 2002; 277: 42082-42087.

## Honors and Awards

2008: **Invited Speaker,** Pediatric Brain Tumor Foundation Institute Conference: Eliminating Brain Tumor Cells through Apoptosome Activation

2007: **Invited Speaker,** Duke Brain Tumor Program Board of Advisors Meeting: Selective Induction of Apoptosis in Brain Tumors

2003-2010: **NIH Medical Scientist Training Program**, Duke University

2002-2003: **NIH Post-baccalaureate Intramural Research Training Award,** National Human Genome Research Institute, Laboratory of Cancer Genetics